UNIVERSITY OF CALIFORNIA SAN DIEGO

The influence of methane seepage on composition and trophic structure of hard substrate macrofauna within the seep and surrounding systems

A Thesis submitted in partial satisfaction of the
requirements for the degree Master of Science

in

Oceanography

by

Olívia Soares Pereira

Committee in Charge:

Professor Lisa A. Levin, Chair
Professor Carolyn Anela Choy
Professor Greg W. Rouse

2020

The Thesis of Olívia Soares Pereira is approved, and it is acceptable in quality and form for publication on microfilm and electronically:

_____

_____

_____
Chair

University of California San Diego

2020

TABLE OF CONTENTS

LIST OF FIGURES

LIST OF TABLES

ACKNOWLEDGMENTS

We are thankful to the Costa Rica Ministerio de Ambiente y Energía (Sistema Nacional de Áreas de Conservación/Comisión Nacional para la Gestióon de la Biodiversidad) for granting collection permits (AT37-13: SINAC-CUS-PI-R-035-2017, AT42-03: SINAC-SE-064-2018). This work was made possible through the efforts of many aboard RV Atlantis legs AT37-13 and AT42-03, including the captains, crew, and pilots and technicians of DSV Alvin. Additionally, the science parties of both cruises assisted with most collection of samples, and especially Lisa Levin and Jennifer Le assisted with at-sea laboratory processing of the hard substrates. Thank you to the chief scientist of leg AT42-03 Erik Cordes for my first Alvin Dive AD4984, a dream for every deep-sea scientist. The project ROC HITS, which this research is part of, was funded by NSF grant OCE 1635219.

Thank you to the members of my thesis committee: Lisa Levin (Chair), Greg Rouse and Anela Choy for generously offering their time, support and guidance. This thesis is a product of my meetings with all of them.

I greatly appreciate Lisa Levin for her academic, professional and emotional support as my advisor. I am indebted to her for her shared expertise and care for me. Thank you for believing in me and giving me the opportunity to work with you, and for the trust you put in me. Hoping for more years working together.

I thank Jennifer Gonzalez for providing help with the processing of stable isotope samples, as well as Greg Rouse, Oliver Ashford, and Guillermo Mendoza, who contributed to the identification of specimens. Maddison McNeil, Jorge Robles, and Connor Coscino contributed post-cruise sorting samples.

I thank the Scripps Institution of Oceanography department, especially Gilbert Bretado, Shelley Weisel and Maureen McGreevy for the support with academic affairs and patience responding to my many questions.

To my American friends, thank you for embracing the Brazilian. Thank you for the academic and emotional support through shared laughs and crisis. Thank you for your friendship, Ariel Pezner, Alaina Smith, Janna Johnson, Kayla Wilson, Kelli Mullane, Zachary Skelton, Samuel Kekuewa, Wiley Wolfe, Rials Christensen, Leah Werner, Cat Briggs, Natalie Posdaljian, Morgan Ziegenhorn. Especially Ariel Pezner, Alaina Smith and Janna Johnson, thank you for sharing a home.

To my Brazilian high school friends – Paula Kairalla, Hisa Videira, Natalia Ferreira, Carla Romani, Beatriz Jatene, Fernanda Console – thank you for listening, offering me advice, and supporting me through this entire process even from far away.

Last, and most importantly, I thank my father, mother and sister for believing in me and supporting me from a continent away. Thank you to my father for the financial support, for which I am in forever debt. I hope you got to live our dream of studying abroad through me, and I hope I made you all proud.

ABSTRACT OF THE THESIS

The influence of methane seepage on composition and trophic structure of hard substrate macrofauna within the seep and surrounding systems

By

Olívia Soares Pereira

Master of Science in Oceanography

University of California San Diego, 2020

Professor Lisa A. Levin, Chair

Methane seepage often generates precipitation of carbonate rocks, which host microbes and a diverse fauna. These rocks may also promote an interaction between seep and background communities that may last for centuries, providing hard substrate even after seepage ceases. I analyzed composition, density, and trophic structure of macrofaunal invertebrates on carbonate rocks at and surrounding Mound 12, a methane seep site off the coast of Costa Rica, to examine how species and trophic diversities respond to changes in seepage activity at different spatial and temporal scales. By sampling *in situ* carbonate rocks at active and transition sites, I observed declining density and a community shift from a gastropod dominance to more annelids and peracarid crustaceans under less seepage, while carbonates promoted an interaction between such communities functioning as hard substrate for attachment. Defaunated carbonates deployed for 7

years at active and transition sites indicated that grazers are amongst the most successful colonizers, although the community and its trophic structure were not able to fully recover. However, both seep and transition communities showed rapid response, persistence and recovery when carbonates were transplanted to sites with lesser/more seepage activity for 17 months. Finally, wood and bone deployed for 7 years at active and transition sites showed shared species indicating potential interaction between whale, wood, and seep ecosystems when in close proximity. This multi-experimental study offers insight on the resilience of macrofaunal communities and helps us predict community responses to disturbances in seepage activity that may result from growing anthropogenic interference on margins.

1 INTRODUCTION

The deep ocean hosts a variety of extreme environments that support unusual forms of life reliant on chemosynthesis rather than photosynthesis (Bernardino et al., 2012). Among these, methane seeps are highly productive ecosystems based on chemosynthetic primary production (Tunnicliffe et al., 2003), which captures energy from the oxidation of sulfide, methane and hydrogen (Dubilier et al., 2008). While fueling ecosystems with increased biomass relative to the surrounding deep sea, oxidation processes alter the overall cycles of sulfur, oxygen and carbon in the oceans. On a global scale, seep roles in biogeochemical cycling, elemental transformation, and contribution to the marine methane budget have been attracting interest (Boetius & Wenzhoefer, 2013). Besides the role in climate regulation and carbon sequestration (regulating services), methane seeps provide provisioning services, such as valuable resources through their interaction with background fauna, and cultural services such as education, which are non-material and non-consumptive outputs that affect people (Levin et al., 2016). More recently, methane seeps have been found to sustain commercially important species, such as tanner and red crabs, that use the seeps for trophic and reproductive support (Seabrook et al., 2019; Turner et al., 2020), and the Pacific Fishery Management Council recognized methane seeps and associated biota as essential fish habitat (NOAA, 2020). This is the world's first incorporation of seeps in a fish management plan.

Although we understand the basics of endosymbiosis and food chains that support this high biomass at methane seeps, we are still learning about the many different ways that animal and microbial life can use methane to generate biomass and provide essential ecosystem services. Because of their location on continental margins and association with energy resources, some

chemosynthetic ecosystems are highly vulnerable to damage (Levin & Sibuet, 2012; Ramirez-Llodra et al., 2011; Baco et al., 2010). Exploitation of biotic and abiotic resources, waste disposal, pollution and debris inputs are a real threat to the deep sea (Ramirez-Llodra et al., 2011; Mengerink et al., 2014), as well as human disturbance such as bottom trawl fisheries, oil and gas extraction and, more recently, seabed mining (Ramirez-Llodra et al., 2010). There is also a concern regarding damage from scientific sampling (Godet et al., 2001). Scientific activity at hydrothermal vents is regulated by a code of conduct (InterRidge, 2006), but it does not include work at methane seeps. Methane seep fauna is also subject to climate change and accompanying loss of oxygen and ocean acidification (IPCC, 2019). With increasing threat, knowledge of communities associated with these ecosystems, with both endemic and background species, takes on greater importance. The research presented here offers information on seep resilience to disturbances and on how life adapts and recovers from such stressors at extreme environments.

Although most of the deep ocean is covered by sediments, methane seeps are frequently associated with hard substrates, with extensive areas of carbonate concretions formed by microbes (Aloisi et al., 2000). Methane seeps are commonly found on continental shelves on both active and passive margins (Ritt et al., 2010) all over the world and at depths from 400 to 7326 m (Fujikura et al., 1999). Ascending fluids are enriched in mainly methane and hydrogen sulfide; both are dissolved reducing gases, creating singular environments that support a community based on anaerobic oxidation of methane (AOM; Boetius et al., 2000) as well as other forms of chemosynthetic production (Boetius & Wenzhofer, 2013; Levin, 2005). Seeps contain abundant methanotrophic archaea (anaerobic methane oxidizing archaea, ANMEs) forming aggregates with sulfate-reducing gama-proteobacteria (SRBs). These aggregates respire the methane released from

the seafloor through the AOM (Reeburg, 2007; Orphan et al., 2002; Boetius et al., 2000), according to the equation (Boetius et al., 2000):

$$CH_4 + SO_4^{2-} \rightarrow HCO_3^- + HS^- + H_2O \quad (1)$$

The hydrogen sulfide produced is aerobically oxidized by bacteria, including by the mat-forming bacteria *Beggiatoa* and *Thioploca*. Much of the methane that is not consumed anaerobically is respired aerobically by free-living and symbiotic bacteria (Thurber et al., 2013) or released to the hydrosphere (Boetius & Wenzhofer, 2013) and consumed by aerobic methane oxidizing bacteria in the water (Hansman et al., 2017; Mau et al., 2014). Anaerobic methane oxidizers and aerobic methane-oxidizing bacteria remove the majority of methane released, and the main sink for methane happens through the "benthic sediment filter" AOM (Boetius & Wenzhoefer, 2013; Sommer et al., 2006; Orphan et al., 2001; Boetius et al., 2000). The increased alkalinity produced by the AOM (equation 1; Bahr et al., 2009) in the sediment combined with high pH leads to precipitation of carbonates, when the bicarbonate produced by AOM combines with dissolved cations (Bahr et al., 2009; Han et al., 2004; Michaelis et al., 2002):

$$Ca^{2+} + 2HCO_3^- \rightarrow CaCO_3 + CO_2 + H_2O \quad (2)$$

These carbonate rocks host a diversity of microorganisms and fauna that use them for attachment, shelter, and access to food (Case et al., 2015; Levin et al., 2015; Marlow et al., 2014a). Given the broad distribution of methane-derived carbonates on seeps, the benthic filter probably represents a previously unrecognized globally relevant sink for methane (Marlow et al., 2014b) due to their anaerobic methanotrophic and AOM activities. However, their contribution to the overall methane consumption is hard to quantify. Although these methanotrophic communities appear to be different along seepage gradients, they sustain a dynamic ecosystem that is able to adapt to changing environmental conditions and methane fluxes (Case et al., 2015; Marlow et al.,

2014b). And when seepage activity ceases, the carbonates remain, attracting background species that feed on remaining debris or use the structures to gain access to particles in the water (Bowden et al., 2013). At a later time, corals and sponges settle on the hard substrate and form habitats that support high biodiversity. Therefore, those carbonates may also promote an interaction between seep and background communities that may last for centuries (Levin et al., 2016, 2009) through provision of hard substrate and reproductive sites, affecting the biogeochemical conditions.

Areas that connect adjacent ecological assemblages where species interact are called ecotones and function as transition zones, often providing enhancement of species richness (Gage, 2004). The knowledge of how seep communities change from active methane seepage to transition settings and how they interact with background assemblages is crucial for understanding the biodiversity of life at seeps as well as for impact assessment, management, valuation, and for predicting consequences of climate change. Seep ecosystems interact with their surroundings by the transfer of organic material, energy and nutrients through horizontal advection of particulate carbon and trophic transfer by mobile predators and scavengers (Levin et al., 2016). These exchanges enhance ecosystem complexity, and ecotones tend to have higher diversity by having a mixture of endemic and non-endemic species (Cordes et al., 2009), providing complex trophic interactions. It is common to find mixotrophic fauna at transition zones, such as maldanid, nereid, and ampharetid polychaetes, peracarid crustaceans and cnidarians, using chemosynthetically and photosynthetically derived organic sources enabling species to endure variation in seepage activity (Levin et al., 2016).

Ecotones can also provide potential connectivity of chemosynthetic ecosystems through transition zones into background communities, as deep-sea dispersal estimates from modeling and population genetic exceed the diameter of the average chemosynthetic site (Levin et al., 2016).

The overlap of species among chemosynthetic ecosystems (Bernardino et al., 2012) suggests the existence of large-scale faunal networks across ocean basins connected by larval dispersal stages (Kiel, 2016). Organic remains such as whale and wood falls create ephemeral chemosynthetic ecosystems that attract species-rich assemblages, and they may function as stepping stones for vent and seep species (Alfaro-Lucas et al., 2018; Levin et al., 2016; Smith et al., 2015; Smith et al., 2014; Baco & Smith, 2003). Chemosynthetic communities are colonized by specialist and generalist organisms with a broad range of nutrition pathways from chemosynthetic to photosynthetic-produced carbon (Bernardino et al., 2010; Levin & Michener, 2002; Desbruyères et al., 2000). Carbonate rocks at transition zones may then promote links among chemosynthetic ecosystems extending the limits of the ecosystem and its methane-derived carbon production.

Trophic linkages are critical to ecosystem functioning as they transfer energy throughout food webs, and they are identified through stable isotope (usually carbon and nitrogen) analyses (Thurber, 2014), by taking advantage of natural variation in stable isotope ratios (Layman et al., 2007). Generally, there is an isotopic change with each successive trophic level, as animals preferentially excrete ^{14}N over ^{15}N and respire ^{12}C over ^{13}C (McCutchan et al., 2003; Peterson & Fry, 1987; Minagawa & Wada, 1974). The carbon isotope shift between a species' diet and its tissue is small (0 to 1‰) but initial fractionation varies substantially among primary producers, and, therefore, $\delta^{13}C$ is an excellent indicator of carbon sources at the base of the food web (Layman et al., 2007; DeNiro & Epstien, 1978). The diet-tissue shift for the nitrogen isotopes, however, is greater and constant among successive trophic levels, and $\delta^{15}N$ often increases by 2‰ to 4‰ with each trophic level, making the nitrogen isotope a useful tool to estimate trophic position (McCutchan et al., 2003; Post, 2002). Initial $\delta^{15}N$ value is influenced by local N_2 fixation, which

can be carried out by benthic deep-sea bacteria in sediments, archaea syntrophic consortia (Dekas et al., 2009) and by chemosynthetic symbionts of invertebrates (Petersen et al., 2016).

An individual stable isotope composition derives then from its food sources, and isotope composition of multiple individuals can be used to depict the trophic role of that species, i.e. its trophic niche. The position of the species in $\delta^{13}C$- $\delta^{15}N$ bi-plots with species (or individuals and populations) is used to infer aspects of the food web structure with more quantitative measures focusing in one consumer of interest. More recently, community-wide metrics were described to help illustrating how individual species' niches and dispersion of those niches drive variation in important aspects of trophic structure (Layman et al., 2007) including at methane seeps (Levin et al., 2015, 2013).

At methane seeps, chemosynthetic production can have isotopic compositions distinct (e.g. light $\delta^{13}C$) from those of photosynthetic production, which normally has heavier $\delta^{13}C$ values (-15‰ to -25‰; Fry & Sherr, 1984). ANME consortia typically have $\delta^{13}C$ values of -30‰ to -100‰ for archaeal cells and -15‰ to -70‰ for associated symbiotic SRB (House et al., 2009; Orphan et al., 2002). These distinct carbon isotopic compositions provide a model system to explore trophic interactions at methane seeps (Thurber et al., 2012; Levin & Michener, 2002), allowing us to examine the dependency of animals on methane-derived carbon. By analyzing animal tissue and carbonate rock isotope values, Levin et al. (2015) compared trophic resource use of whole-assemblages on carbonates from the Costa Rica margin as a function of seepage activity, location and habitat. They observed that the nutritional heterogeneity introduced by carbonates has a substantial contribution to the diversity of macrofauna with a broad range of feeding modes. Grupe (2014) also observed shifts in isotope composition of macrofaunal on carbonates with different

zones of the seep with low mean $\delta^{13}C$ values for macrofaunal from carbonates, which were the lowest at the seep center, and highest for those from sediments.

2 OBJECTIVES

This study examines the dynamics and resilience of macroinvertebrates on carbonate rocks and how species diversity and trophic diversity respond to changes in seepage gradients, which correspond to chemosynthetic production. We analyzed composition, density, and trophic structure of invertebrates on carbonate rocks at a methane seep site off the coast of Coast Rica (Mound 12 at ~1,000 m depth) (i) along natural seepage gradients, (ii) among colonizers of newly placed rocks, and (iii) on transplanted rocks, to test the overarching hypothesis that seepage activity plays a major role in defining the communities and their trophic structure, and to identify the relevant time and space scales of response. The answers to the questions raised here will give us a better understanding of the sphere of influence of the seep on deep-sea background communities, described by Levin et al. (2016).

By conducting one mensurative experiment and three kinds of manipulative experiments we aimed to observe (1) community differences that occur naturally on carbonates under different seepage regimes; (2) the capacity of the animals to colonize defaunated rocks deployed at sites with different seepage activities (rock colonization experiment); (3) the persistence or recruitment of animals when rocks are moved to different seepage activities imitating cessation or increase of seepage (transplant experiment); and (4) the linkage of seeps to other chemosynthetic communities by deploying organic fall mimics (wood and bone as well as rock) within different seepage activities (substrate colonization experiment). Finally, we compared the community described here

to previous research at Mound 12 with natural background rocks (Levin et al., 2015), experimental rocks, bone and wood parcels put out for 10.5 months in Costa Rica (Grupe, 2014), experimental wood put out for 1-year at seeps in the North Atlantic Ocean (Gaudron et al., 2010), and at Hydrate Ridge, Oregon, where a transplant experiment with carbonate rocks was also conducted (Levin et al., 2017).

Specific questions addressed were:

(1) How do invertebrate macrofaunal communities and their trophic structures change across seepage gradients? Is there interannual variability?

Hypothesis: Communities have higher densities and lower diversity at actively seepage sites with lower $\delta^{13}C$ values based on C derived from anaerobic oxidation of methane, but are more diverse at transition sites, where we expect to find animals from both active and inactive sites co-occurring. As fluid flux can last for extended periods of hundreds of years (Levin et al., 2016), we do not expect to see major interannual variabilities in chemosynthetic production.

(2) Can macrofauna colonize hard substrates and fully recover natural patterns of community composition and trophic structure across seepage gradients within 7 years?

Hypothesis: Grupe (2014) observed that the macrofaunal community was able to colonize carbonate rocks and recover density, biomass, and dominant species within one year, but it did not develop species richness and a food web comparable to that on *in situ* carbonate rocks. We hypothesize that 7 years is enough time for the community to fully recover its composition and trophic structure.

(3) Do seep and background invertebrate macrofaunal communities on hard substrate have different responses and persistence under low and high seepage activity? What are the drivers of these responses?

Hypothesis: Seep species rely on methane-derived carbon associated with active seepage. When transplanted to sites with lesser seepage activity, mimicking seepage cessation, they do not persist due to a lack of their food source. Background communities are able to colonize and thrive on transplanted carbonate rocks at lesser seepage activity, using the rocks as a food source or attachment. Background fauna on rocks transplanted to sites with active seepage are hypothesized to face toxic environments and not persist. Thus, fluid flux and food availability are hypothesized to drive macrofaunal responses to changes in seepage activity.

(4) Do methane seeps function as areas of interaction among chemosynthetic ecosystems?

Hypothesis: Seepage activity plays a major role in defining macrofaunal community composition and its trophic structure on different types of hard substrate. Macrofaunal communities on rocks (methane seeps), bones (whale falls) and wood (wood falls) are predicted to be more similar at active sites, where seepage activity plays a major role in defining macrofaunal community composition and its trophic structure on different types of hard substrate. But at transition sites, the decay of bones and wood should dominate, and the macrofaunal community will be more similar of that of organic falls than seep communities.

3 STUDY AREA

The Pacific margin of Costa Rica is an offshore convergent margin exhibiting evidence for subduction and erosion of continental material (Sahling et al., 2008), where the Cocos Plate subducts beneath the Caribbean Plate at a rate of nearly 90 mm/yr (Kimura et al., 1997). Fluid venting has long been documented in the area (McAdoo et al., 1996), and methane is frequently observed migrating from the sediment to the water column (Mau et al., 2007). Later, sites with

chemosynthetic communities and authigenic carbonates, both indicators of seepage of methane-rich fluids, were discovered (Sahling et al., 2008; Sibuet & Olu, 1998) and new sites are continually being discovered (e.g. Jan 2019 FK190106). There is now evidence for more than 100 seep sites along 580 km of the Costa Rica margin (Sahling et al., 2008). Carbonate mounds rise up to 100 m above the seafloor (Sahling et al., 2008), and 85.7% of the mound volume can be comprised of authigenic carbonates (Klaucke et al., 2008). Seeps were found associated with mounds, faults, subduction scars, and landslides, and almost all of the rock samples from previous studies were methane-related authigenic carbonates (Sahling et al., 2008).

Among these seep sites, Mound 12 (8 55.8'N, 84 18.7'W, Figure 1) is located on the Southeast Costa Rica margin at 990-1000 m water depth (Mau et al., 2006), just below the oxygen minimum zone (Levin et al., 2015). It has been described as a mud volcano (Moerz et al., 2005) that is 30 m high with diameters of about 1-1.6 km. Mudflows suggest that it is a frequently active site (Niemann et al., 2013), with a main active area Southwest of the mound (Mau et al., 2006). Slope sediments intercalated with these mudflows indicate an alternation of seepage with low-activity phases (Niemann et al., 2013), as observed by Mau et al. (2007) within a period of 12 months. Previous studies measured high concentrations of methane in the overlaying waters, indicating that a significant portion of seeping methane escapes into the water column (Mau et al., 2006).

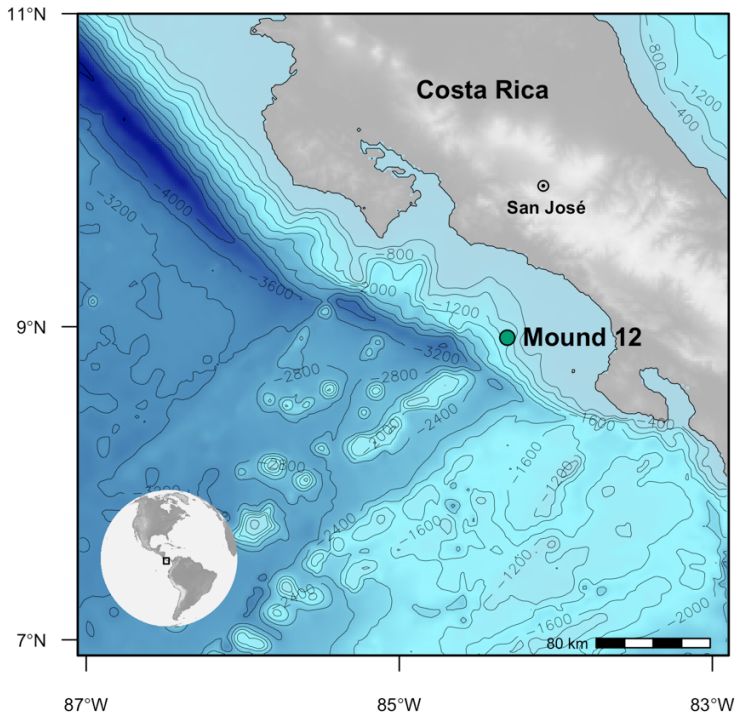

Figure 1: Location of Mound 12, a methane seep off the pacific margin of Costa Rica.

The Mound 12 bottom is characterized by mixed carbonates, hemipelagic sediments and mud extrusions. Carbonate rocks can host annelids, crustaceans, mollusks, and cnidarians, and carbonate assemblages that are different than those in the surrounding sediments (Levin et al. 2015). The macrofaunal community on carbonates varies with seepage activity, showing higher densities and species richness at active sites. Gastropods dominate at active sites, while transition sites are dominated by crustaceans and cnidarians (Levin et al., 2015). Although we have a good understanding of the carbonate rock community composition at Mound 12, questions on seep and background community response to environmental changes (both natural and anthropogenic), and the time and spatial scales to which they react remain unanswered.

4 METHODS

4.1 Sampling

Carbonate rocks were sampled at Mound 12 off the Pacific margin of Costa Rica during two research cruises aboard the RV *Atlantis* (May to June 2017 – AT37-13 – and October 2018 – AT42-03) using the submersible Alvin (Table 1).

Table 1: Summary of average Mound 12 site characteristics and number of rocks collected at Mound 12 on research cruises in 2017 and 2018.

Cruise	Alvin Dives	Dates	Temperature (°C)	Oxygen (µM)	Salinity	No. Rocks*
2017 (AT37-13)	4906, 4907, 4908, 4910, 4917	May 21-23, 25, Jun. 2	4.93	27.01	34.59	17
2018 (AT42-03)	4974, 4975, 4978, 4984, 4985, 4987, 4989	Oct. 20-21, 24, 30-31, Nov. 2, 4	5.23	24.60	34.57	38

* Total number of rocks collected, including experimental rocks.

Unmanipulated samples (*in situ*) were taken at sites with different seepage activity when possible (Table 2). High activity level was defined visually by the presence of microbial mats, methane bubbles or seep megafauna (bathymodiolin mussels, vesicomyd clams, and/or siboglinid tube worms), as previously done by Levin et al. (2015). The rocks were placed into individual containers of Delrin bioboxes on the Alvin basket to avoid cross contamination during recovery, and they were used as control samples for three experiments:

(1) Rock Colonization experiment. To test the dynamics and colonization rate of seep and non-seep communities, defaunated rocks were deployed in active and transition seepage regimes for 7 years.

(2) Transplant experiment (Figure 2). Carbonate rocks were moved by the HOV to different seepage conditions with exposure for 17 months. These experiments addressed the roles of seepage

in determining biological patterns and dynamics of methane seep fauna and the rates and trajectory of community response.

(3) Substrate Colonization experiment. Bone and wood parcels were deployed in active and transition seepage regimes for 7 years to test the interaction between the methane seep and different chemosynthetic ecosystems (whale and wood falls).

Along with the collection of rock samples, the combined use of Alvin, AUV Sentry, and CTD casts provided a three-dimensional picture of oceanographic variables, such as temperature, salinity, dissolved oxygen, and imagery. To characterize particulate organic carbon (POC) stable isotope composition for constraining food webs, surface (0-5 m) and bottom waters (< 15 m above the seafloor) were sampled at each station using 2-4 L of water collected in a Rosette on a CTD.

Table 2: Substrates for which macrofaunal community data were generated at Mound 12, Costa Rica margin. The number of substrates that contributed individuals to isotope analysis is shown in parentheses. The *in situ* carbonates were collected during both 2017 and 2018 cruises. The colonization experiments were deployed for 7 years (deployed in January 2010, recovered in May 2017), and the transplant experiment was conducted for 17 months (start in May 2017, recovered in October 2018). See Appendix 1 for definition of terms.

	Active	**Transition (Inner and Outer)**	**Background**	**Total**
***In situ* carbonate rock**	15	11		26
Colonization Experiment (7 years)				
Carbonate rock	4	4		8
Cow Bone	2	2		4
Wood (Douglas Fir)	4	4		8
Transplant Experiment with carbonate rocks (17 months)				
Active to Inner Transition (A-IT)		6		6
Active to Outer Transition (A-OT)		5		5
Active to Background (A-B)			5	5
Inner Transition to Active (IT-A)	5			5
Inner Transition to Outer Transition (IT-OT)		5		5
Inner Transition to Background (IT-F)			5	5
			TOTAL	**78**

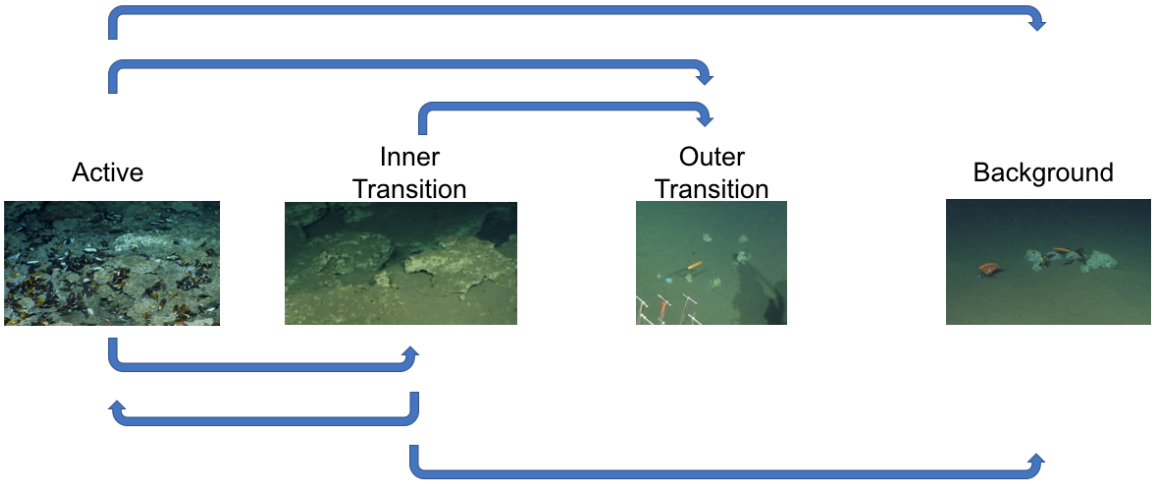

Figure 2: Experimental design of the transplant experiment conducted with carbonate rocks at Mound 12 for 17 months from June 2017 to October 2018.

4.2 Sample processing

4.2.1 Onboard processing

Substrates were photographed intact upon recovery and then were wrapped in aluminum foil to determine the approximate rock surface area later in the laboratory (see section 4.2.2). The associated fauna was removed, and the remaining substrate was placed in cold filtered seawater and left at room temperature overnight for additional infauna to crawl out. These were sieved to 0.3 mm (and 0.042 mm) and preserved in 96% ethanol to be sorted in the laboratory. Subsamples The substrates were then left to dry out. The associated fauna removed upon recovery was sorted to lowest possible taxonomic level using a dissecting microscope and tissue subsamples from three specimens of each species were collected for stable isotope analyses to examine their relative reliance on seep productivity and changes in trophic structure (Levin & Mendoza, 2007). The tissue subsamples were washed in mili-Q water, placed in pre-weighed tin capsules or sterilizes

glass vials (combusted at 500°C for 4 hours) and frozen at -80°C. If large enough, the remaining portion of the animal was frozen as backup and potentially for final identification in the laboratory using morphological and genetic markers. Surface (0-5 m) and bottom waters (< 15 m above the seafloor) were filtered through a glass microfiber filter, and the filter was frozen at -80°C.

4.2.2 On land laboratory processing

In the laboratory at Scripps Institution of Oceanography, the aluminum foil was weighed using a top-loading balance to an accuracy of two decimal places in milligrams. The total weight of the foil was divided by the average weight of a 1 cm^2 piece of foil to determine the approximate rock surface area in cm^2. Samples in jars were resieved using a 0.3-mm mesh, and sorted in freshwater at 12x magnification under a dissecting microscope. The specimens were identified to lowest taxonomic level possible and counted. Individuals in the most common phyla at methane seeps, Annelida and Mollusca, were identified at the family level. Crustaceans were identified at the order or infraorder level, cnidarians at the order level, and echinoderms at the class level. The least abundant groups, Nemertea, Platyhelminthes and Pycnogonida, were identified to phylum. The numbers of animals that were removed at sea upon recovery were added to the laboratory total counts. The specimen tissue subsamples collected for isotope analyses were oven-dried at 60°C overnight, weighed and acidified with 1N phosphoric acid to remove inorganic carbon. Stable isotope measurements ($\delta^{13}C$, $\delta^{15}N$) were made on 0.2-1 mg of dry weight and carried out using a Costech elemental analyzer coupled to a Micromass Isoprime isotope ratio mass spectrometer (EA/IRMS) at Washington State University (WSU). The glass microfiber filters were also sent to WSU for stable isotope measurements of the POC.

4.3 Data syntheses and statistical analyses

Density of the total macrofaunal community and individual species were calculated by dividing the number of animals on each substrate by its surface area and multiplying by 200 to get a density value per 200 cm^2 as in previous literature (Levin et al., 2015). Density data sets were tested for normality and homogeneity of variance. As not all of them showed normal distribution nor homogeneous of variance, non-parametric tests were performed. Wilcox tests were performed to check for variability of densities between seepage activity, years, and experiments for data sets with two factors. For data sets with more than two factors, Kruskal-Wallis tests followed by Dunn's tests using the Benjamini-Hochberg adjustment (Benjamini & Hochberg, 1995) were performed instead.

Community composition was analyzed by percent composition and density per 200 cm^2 by taxonomic group, as percentages do not reflect sample sizes. Community composition data were standardized by the total number of individuals and fourth-root transformed. Multi-dimensional scaling of Bray-Curtis dissimilarities, two-way ANOSIM and two-way SIMPER analyses were performed using Primer7 (Clarke & Gorley, 2015). Taxonomic groups were ranked by abundance to identify similarities in dominant and rare species for *in situ* communities and experimental communities.

Stable isotope statistical analyses were performed using the R software program (R Core Team 2016). Stable isotope data sets were tested for normality and homogeneity of variance. As not all of them showed normal distribution nor homogeneous variance even after log transforming, non-parametric tests were performed. To check for variability of isotope composition between sites, year of collection, and experiments, Wilcox tests were performed for the data sets with two

factors and Kruskal-Wallis test followed by Dunn's test using the Benjamini-Hochberg adjustment (Benjamini & Hochberg, 1995) were performed for data sets with more than two factors.

Community-level isotope metrics (Layman et al., 2007) were generated using Stable Isotope Bayesian Ellipses in R (SIBER) package (Jackson et al., 2011). Standard elliptical area (SEA) and standard elliptical area corrected for sample size (SEAc) were calculated representing relative isotopic niche areas in bivariate $\delta^{13}C$ and $\delta^{15}N$ space. Trophic diversity was calculated as $\delta^{13}C$ and $\delta^{15}N$ ranges and total hull areas (TA). Species packing was determined through measurement of mean distance to centroid (CD) and mean nearest neighbor distance (MNND). Similarities in trophic resource use among communities were determined by computing pairwise ellipse overlaps among seepage activity, substrates and experiments. Bayesian posterior estimates of the ellipses were calculated using 2 chains of 20,000 iterations with a burn-in of 1,000 and thinning of 10. Mean overlap was then expressed as a proportion of the non-overlapping area of the two ellipses (Stewart et al., 2017).

5 RESULTS

5.1 Natural community changes along seepage gradients: *in situ* carbonate rocks

The density of invertebrate macrofauna on *in situ* carbonate rocks (Figure 3) was not significantly different between 2017 and 2018 at active sites (Wilcox test, W = 26, p-value = 0.052) and at transition sites (Kruskal-Wallis, Chi-squared = 3.1182, df = 2, p-value = 0.21), nor among seepage activity in both years (2017: Wilcox test, W = 17, p-value = 0.11; 2018: Kruskal-Wallis, Chi-squared = 3.8182, df = 2, p-value = 0.15). However, while in 2017 the average density was

more than 4 times higher at active sites than at transition sites, in 2018, there was a clear parabolic pattern in average density with increasing distance from the seep (Figure 3).

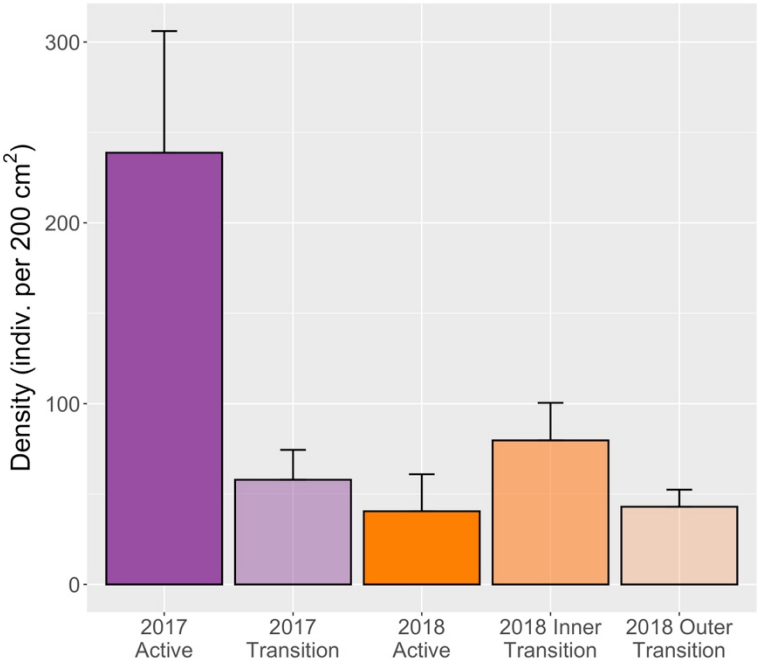

Figure 3: Average ± one standard error density of macrofaunal invertebrate community on *in situ* rocks collected across seepage gradient at Mound 12 in 2017 (purple) and 2018 (orange).

Although density did not differ significantly, the macrofaunal community composition was significantly different between 2017 and 2018 (Two-Way ANOSIM, Global R = 0.339, p-value = 0.001; Figures 3-5), and the groups that contributed to that dissimilarity were more abundant in 2017 (Table 3), they were: Lepetodrilidae (6.93% contribution to dissimilarity), Neolepetopsidae (4.21%), Cataegidae (4.20%), Ophiuroidea (3.91%), Anomura (3.85%), Serpulidae (3.79%), Hesionidae (3.72%), Pyropeltidae (3.69%), Tanaidacea (3.66%), and Amphinomidae (3.64%; SIMPER, average dissimilarity = 67.32; Appendix 3.1).

Seepage activity also significantly affected the whole assemblage composition of the community (Two-Way ANOSIM, Global R = 0.397, p-value = 0.001). In 2017, active sites were dominated by gastropods (51.60% limpets and 36.52% snails). At transition sites, annelids were

the dominant group (43.97%), although their higher percent contribution was a result of a decrease in mollusks, rather than an increase in annelids (Figure 3). Gastropods were the second most abundant group at transition sites with 30.62%, followed by 9.45% peracarids and 6.84% echinoderms. The groups that contributed to the dissimilarity between the communities at active and transition sites were Amphipoda (4.93% contribution to dissimilarity), Tanaidacea (4.17%), Ophiuroidea (4.10%), Serpulidae (3.89%), Chrysopetalidae (3.69%), and Hydroidolina (3.36%) present mainly at transition sites (Table 3A), and the gastropod in the families Neolepetopsidae (4.24%), Provannidae (3.72%), Cataegidae (3.55%), and Anomura (3.31%) present mainly at active sites (SIMPER, average dissimilarity = 68.12; Table 3A, Appendix 3.2).

In 2018, there was a composition change with increasing distance from the active seep from an annelid-gastropod dominated community (53.52% annelids and 22.93% gastropods) to an annelid dominated community at inner transition sites (82.96%; Figure 4), while the annelid composition also changed. Chrysopetalids, syllids, and maldanids were the most abundant annelids at inner transition sites (Table 3B), and they contributed to 14.28% dissimilarity between active and inner transition sites (Appendix 3.3). Hesionids and lacydoniids were the most abundant annelids at active sites (Table 3B), contributing 6.66% of the dissimilarity between active and inner transition (Appendix 3.3). Gastropods mainly present at active sites (Figure 4, Table 3B) also had significant contribution to the dissimilarity between active and inner transition sites (Provannidae: 4.48%, Cataegidae: 3.68%, Neolepetopsidae: 3.50%; SIMPER, average dissimilarity = 68.45; Appendix 3.3). Even further from active seepage (at outer transition sites), the community loses some groups of annelids (e.g. Amphinomidae, Serpulidae, Lacydoniidae, Ampharetidae, Polynoidae, Terebellidae), and the ones present mainly at inner transition sites (Syllidae, Serpulidae, Amphinomidae, and Lacydoniidae; Table 3B) contributed 15.48% of the

dissimilarity between inner transition and outer transition sites. Besides the annelid composition difference, cnidarians and peracarids were better represented at outer than inner transition sites (16.28% and 23.54%, respectively; Figure 4), and, among these, the groups that also contributed to dissimilarity between inner and outer transition sites were Hydroidolina (5.73% contribution to dissimilarity) and Amphipoda (4.44%; SIMPER, average dissimilarity = 63.79%; Appendix 3.4).

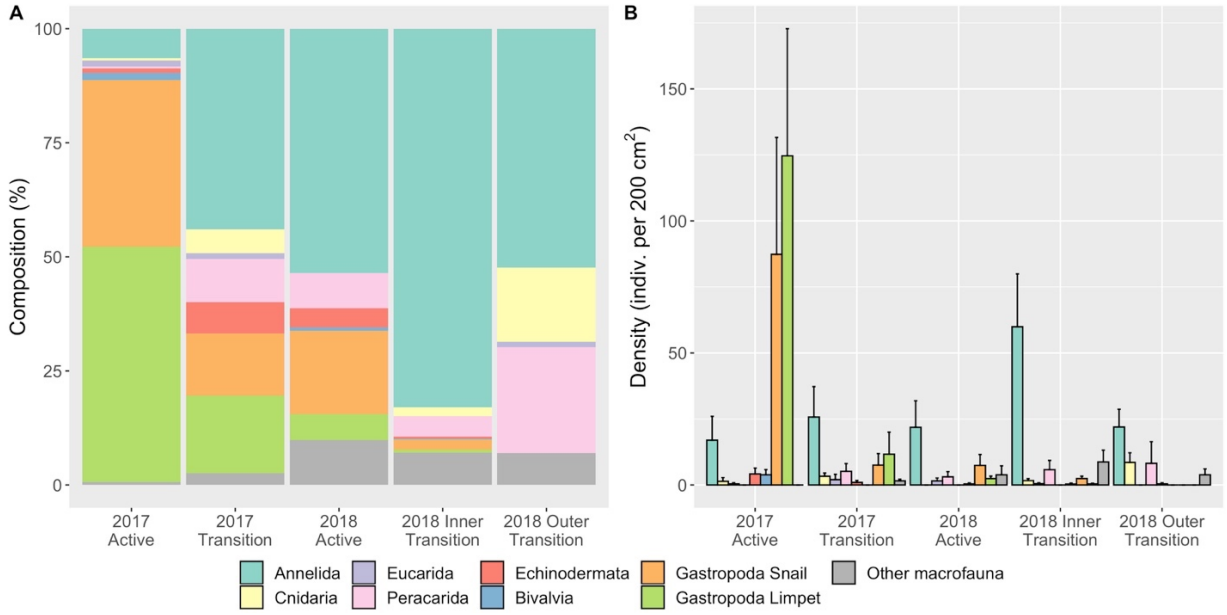

Figure 4: Macroinvertebrate (A) composition and (B) density of individuals by taxon on *in situ* carbonate rocks collected across seepage gradients at Mound 12 in 2017 and 2018.

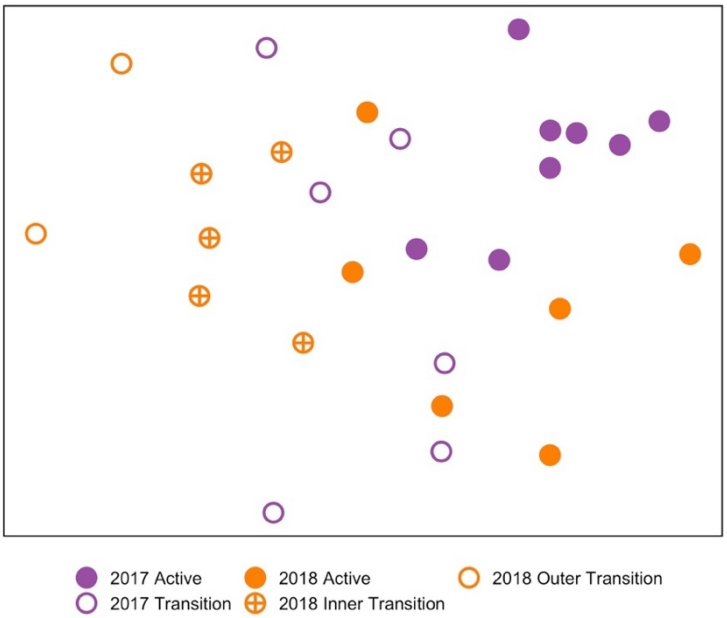

Figure 5: Multi-dimensional scaling analysis of the macrofaunal invertebrate community on *in situ* rocks collected across seepage gradients at Mound 12 in 2017 (purple) and 2018 (orange).

Table 3: Top ten taxa based on densities on *in situ* carbonate rocks collected across seepage gradient at Mound 12 in (A) 2017 and (B) 2018. Raw density data are given in Appendix 2.1.

A. 2017					
Active	**%**	**Transition**	**%**		
Provannidae	30.16	Serpulidae	17.53		
Lepetodrilidae	25.53	Chrysopetalidae	9.74		
Neolepetopsidae	22.14	Neolepetopsidae	9.74		
Skeneidae	5.14	Provannidae	7.79		
Pyropeltidae	3.94	Amphipoda	6.82		
Anomura	1.21	Ophiuroidea	6.82		
Nuculanidae	1.21	Lepetodrilidae	6.82		
Ampharetidae	1.17	Hydroidolina	4.55		
Hesionidae	1.13	Cataegidae	4.22		
Serpulidae	1.05	Hesionidae	3.25		
	92.67		77.27		
B. 2018					
Active	**%**	**Inner transition**	**%**	**Outer transition**	**%**
Cataegidae	11.97	Chrysopetalidae	56.51	Chrysopetalidae	23.64
Lacydoniidae	8.45	Syllidae	6.62	Hydroidolina	21.82
Hesionidae	7.75	Trombidiformes	5.08	Amphipoda	16.36
Tanaidacea	7.04	Maldanidae	3.97	Hesionidae	7.27
Provannidae	4.93	Amphipoda	2.87	Maldanidae	5.45

Table 3 continued.

B. 2018					
Active	**%**	**Inner transition**	**%**	**Outer transition**	**%**
Amphinomidae	4.23	Amphinomidae	2.21	Phyllodocidae	3.64
Dorvilleidae	4.23	Hesionidae	1.77	Syllidae	3.64
Chrysopetalidae	4.23	Hydroidolina	1.77	Ostracoda	3.64
Ophiuroidea	4.23	Lacydoniidae	1.55	Dorvilleidae	1.82
Neolepetopsidae	4.23	Serpulidae	1.10	Flabelligeridae	1.82
	61.27		83.44		89.09

Macrofaunal stable isotope composition of invertebrates on *in situ* rocks varied across seepage gradients and between years (Table 4A, Figure 6). In 2017, mean $\delta^{13}C$ and $\delta^{15}N$ values were significantly lower for macrofauna at active sites ($\delta^{13}C$ = -36.28 ± 1.64, $\delta^{15}N$ = 3.55 ± 1.03), and higher at transition sites ($\delta^{13}C$ = -27.88 ± 2.96, $\delta^{15}N$ = 9.18 ± 1.42) ($\delta^{13}C$: Wilcox test, W = 825, p = 0.005, $\delta^{15}N$: Wilcox test, W = 454.4, p-value < 0.0001). In 2018, the same pattern was observed ($\delta^{13}C$: Kruskal-Wallis, chi-squared = 19.358, df = 2, p-value < 0.0001, $\delta^{15}N$: Kruskal-Wallis, chi-squared = 12.386, df = 2, p-value = 0.002); macrofauna at active sites showed lower $\delta^{13}C$ and $\delta^{15}N$ values ($\delta^{13}C$ = -36.19 ± 1.29, $\delta^{15}N$ = 6.24 ± 0.84) than at inner transition ($\delta^{13}C$ = -33.70 ± 2.72, $\delta^{15}N$ = 7.87 ± 0.64) ($\delta^{13}C$: Dunn's test, z = -2.5219, p-value = 0.005, $\delta^{15}N$: Dunn's test, z = -2.4124, p-value = 0.01), and outer transition ($\delta^{13}C$ = -25.57 ± 0.01, $\delta^{15}N$ = 9.44 ± 0.27) ($\delta^{13}C$: Dunn's test, z = -4.0541, p-value = 0.0001, $\delta^{15}N$: Dunn's test, z = -3.0116, p = 0.004). Carbon isotope composition was also lower at inner transition sites than at outer transition sites ($\delta^{13}C$: Dunn's test, z = -2.6428, p-value = 0.006), but nitrogen isotope composition was not significantly different ($\delta^{15}N$: Dunn's test, z = -1.6858, p-value = 0.05; Table 4A).

At active sites, carbon isotope composition was not significantly different between 2017 and 2018 (Wilcox test, W = 2019.5, p-value = 0.27), but nitrogen was two times higher in 2018 than in 2017 (Wilcox test, W = 1433.5, p-value = 0.0002; Table 4A). The opposite was found at

transition sites, where nitrogen isotope composition was not significantly different between years (Kruskal Wallis, chi-squared = 3.4479, df = 2, p-value = 0.18), but carbon isotope composition was (Kruskal-Wallis, Chi-squared = 8.2972, df = 2, p-value = 0.01), with slightly higher values at outer transition sites in 2018 ($\delta^{13}C$ = -25.6 ± 0.1) than transition sites in 2017 ($\delta^{13}C$ = -27.9 ± 2.9; Dunn's test, z = -2.5519, p-value = 0.008; Table 4A).

Table 4: Mean ± 1 standard error isotope values (‰) of macrofauna on (A) *in situ* carbonate rocks collected across seepage gradients at Mound 12 in 2017 (AT37-13) and 2018 (AT42-03), (B) carbonate rock, bone and wood deployed at active and transition sites for 7 years (2010-2017), and (C) carbonate rocks transplanted across seepage activity for 17 months (2017-2018).

	$\delta^{13}C$ (‰)	**$\delta^{15}N$ (‰)**
A. *In situ* carbonate rock		
2017 Active	-36.3 ± 1.6	3.5 ± 1.0
2017 Transition	-27.9 ± 2.9	9.2 ± 1.1
2018 Active	-36.2 ± 1.3	6.2 ± 0.8
2018 Inner Transition	-33.7 ± 2.7	7.9 ± 0.6
2018 Outer Transition	-25.6 ± 0.1	9.4 ± 0.3
B. Colonization experiment (7 years)		
Carbonate rock Active	-33.4 ± 2.7	1.3 ± 1.0
Carbonate rock Transition	-29.8 ± 1.8	7.4 ± 0.6
Cow Bone Active	-27.1 ± 0.6	4.5 ± 0.3
Cow Bone Transition	-28.3 ± 3.1	6.3 ± 0.5
Wood Active	-35.0 ± 2.2	2.0 ± 0.5
Wood Transition	-26.7 ± 2.2	6.2 ± 0.3
C. Transplant Experiment with carbonate rocks (17 months)		
Active to Inner Transition (A-IT)	-37.0 ± 4.6	6.8 ± 1.6
Active to Outer Transition (A-OT)	-37.7 ± 4.3	8.3 ± 1.0
Active to Background (A-B)	-45.3 ± 9.2	6.2 ± 1.2
Inner Transition to Active (IT-A)	-39.1 ± 3.9	5.9 ± 1.3
Inner Transition to Outer Transition (IT-OT)	-29.4 ± 5.1	9.3 ± 0.8
Inner Transition to Background (IT-B)	-24.2 ± 1.4	9.9 ± 1.4

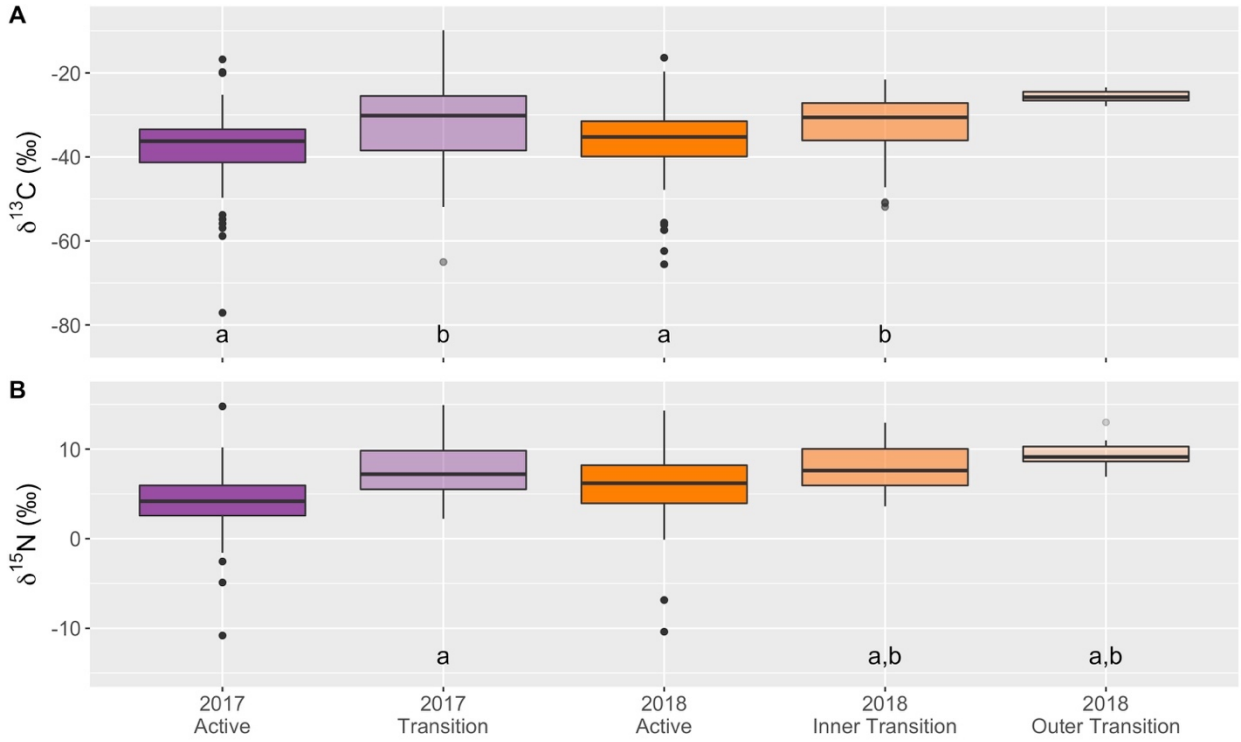

Figure 6: (A) $\delta^{13}C$ and (B) $\delta^{15}N$ values (‰) of macrofaunal invertebrates on *in situ* rocks collected across seepage gradients at Mound 12 in 2017 (purple) and 2018 (orange). Boxplots visualize five summary statistics: the median, two hinges (the 25th and 75th percentiles), and two whiskers (which extend from the hinge to the largest/smallest value at 1.5x the inter-quartile range), as well as outlying points individually. See statistical tests in Appendix 6.1.

Mean $\delta^{13}C$ values were different among taxa (Table 5, Appendix 5.1) in 2017 at active (Kruskal-Wallis, Chi-squared = 24.364, df = 7, p-value < 0.001) and transition sites (Kruskal-Wallis, Chi-squared = 12.322, df = 7, p-value = 0.09), but were not significantly different in 2018 at any site (Active: Kruskal-Wallis, Chi-squared = 11.339, df = 8, p-value = 0.18; Inner transition: Kruskal-Wallis, Chi-squared = 12.745, df = 7, p-value = 0.08; Outer transition: Kruskal-Wallis, Chi-squared = 2.7857, df = 2, p-value = 0.25). While mean $\delta^{15}N$ values were different among taxa at active sites in 2017 (Kruskal-Wallis, Chi-squared = 22.849, df = 7, p-value = 0.002) and 2018 (Kruskal-Wallis, Chi-squared = 17.668 df = 8, p-value = 0.02), they were not significantly different at any transition site (Transition 2017: Kruskal-Wallis, Chi-squared = 11.562, df = 7, p-value = 0.11; Inner transition 2018: Kruskal-Wallis, Chi-squared = 10.432, df = 7, p-value = 0.16; Outer

transition 2018: Kruskal-Wallis, Chi-squared = 4.5, df = 2, p-value = 0.10). Pairwise comparisons are shown in Appendix 6.11.

Mean stable isotope values varied differently across seepage gradients and between years for the different taxa (Table 5A). In 2017 $\delta^{15}N$ values of annelids were twice as low at active than transition sites (Wilcox test, W = 122, p-value < 0.001) and $\delta^{13}C$ values of limpets were 60% lower at active than transition sites (Wilcox test, W = 52, p-value = 0.02), but isotope values did not differ across seepage gradients for the other taxa (Appendix 5.1, statistical tests in Appendix 6.4). In 2018, mean $\delta^{13}C$ and $\delta^{15}N$ values were not significantly different among seepage activities for any taxon (Appendix 5.1, statistical tests in Appendix 6.5).

At active sites, mean $\delta^{13}C$ values were not significantly different between years for the different taxa (Table 5), except for echinoderms, which had values twice as low in 2018 (Wilcox test, W = 3, p-value = 0.50). $\delta^{15}N$ values were 45% and 65% higher in 2018 for annelids (Wilcox, W = 248, p-value = 0.01) and cnidarians (Wilcox, W = 0, p-value = 0.50), respectively, and 1‰ lower in 2018 for echinoderms (Wilcox test, W = 3, p-value = 0.50), but not different for the other taxa (Appendix 5.1). (See Appendix 6.6 for statistical tests).

At transition sites, mean $\delta^{13}C$ and $\delta^{15}N$ values were not significantly different between years for the different taxa (Table 5), except for $\delta^{13}C$ values of cnidarians (Kruskal-Wallis, Chi-squared = 6.5693, df = 2, p-value = 0.03), although no difference was found when looking at pairwise comparisons (Dunn's tests, p-values > 0.025). (See Appendix 6.7 for statistical tests).

Table 5: Mean ± standard error isotope values (‰) by major taxa of the macrofauna community on *in situ* carbonate rocks collected across seepage gradients at Mound 12 in (A) 2017 (AT37-13) and (B) 2018 (AT42-03). Superscripts: Pairs in which there was a significant difference (p-value < 0.05) based on Wilcox tests (p-value < 0.05) or Dunn's test using Benjamini-Hochberg adjustment (p-value < 0.025). See Appendix 6.4-6.7 for statistical tests.

Year/Taxa	**Mean isotope values by seepage activity**					
A. 2017	**Active**		**Transition**			
	$\delta^{13}C$ (‰)	**$\delta^{15}N$ (‰)**	**$\delta^{13}C$ (‰)**	**$\delta^{15}N$ (‰)**		
Annelida	-35.9 ± 1.2	4.6 ± 0.8[1,3]	-36.1 ± 4.2	9.6 ± 0.9[1]		
Cnidaria	-30.3 ± 2.5	3.5 ± 3.3	-29.7 ± 1.5	7.3 ± 1.6		
Eucarida	-28.5 ± 1.2	5.2 ± 0.5	-29.8 ± 4.7	8.9 ± 0.6		
Peracarida	-	-	-29.1 ± 4.7	8.7 ± 0.6		
Echinodermata	-19.8	6.9	-22.1 ± 3.4	3.4 ± 1.6		
Bivalvia	-56.7 ± 20.4	-7.8 ± 2.9	-	-		
Gastropoda:Snail	-38.3 ± 0.8	4.9 ± 0.4	-35.5 ± 3.9	6.2 ± 0.9		
Gastropoda:Limpet	-43.2 ± 2.5[2]	2.7 ± 0.4	-29.9 ± 1.7[2]	4.7 ± 1.3		
Other macrofauna	-36.1 ± 7.9	7.9 ± 1.2	-46.5 ± 3.2	7.4 ± 1.2		
B. 2018	**Active**		**Inner Transition**		**Outer Transition**	
	$\delta^{13}C$ (‰)	**$\delta^{15}N$ (‰)**	**$\delta^{13}C$ (‰)**	**$\delta^{15}N$ (‰)**	**$\delta^{13}C$ (‰)**	**$\delta^{15}N$ (‰)**
Annelida	-36.9 ± 1.9	6.7 ± 0.6[3]	32.0 ± 1.5	8.7 ± 0.7	-26.9 ± 1.0	11.3 ± 1.7
Cnidaria	-30.4	11.5	-28.2 ± 1.1	8.5 ± 0.7	0.8 ± 0.5	8.3 ± 0.5
Eucarida	-21.1	7.5	-	-	-	-
Peracarida	-33.1 ± 6.1	9.4 ± 2.3	-27.4 ± 2.1	6.3 ± 0.8	-24.1	11.0
Echinodermata	-29.2 ± 1.6	5.6 ± 0.8	-33.2 ± 3.4	5.8 ± 0.7	-	-
Bivalvia	-36.8	-10.4	-30.4	10.9	-	-
Gastropoda:Snail	-37.1 ± 1.4	5.7 ± 0.7	-38.2 ± 5.6	7.1 ± 1.1	-	-
Gastropoda:Limpet	-42.1 ± 3.3	2.9 ± 0.9	-33.0 ± 9.4	5.4 ± 1.8	-	-
Other macrofauna	-37.3	4.5	-49.5 ± 2.0	6.3 ± 0.6	-	-

Active sites showed higher ranges of food sources, more trophic levels, and higher trophic diversity than transition sites in both years (Table 6). Within active sites, trophic diversity was higher in 2017 than in 2018 (Figure 7A-B, Table 6). In 2018, community trophic structure was more similar between fauna at active sites and inner transition sites, and less similar between active sites and outer transition sites. In a comparison of 2017 and 2018 data, trophic structure on *in situ* carbonate rocks was also more similar for active sites than transition sites (Figure 8).

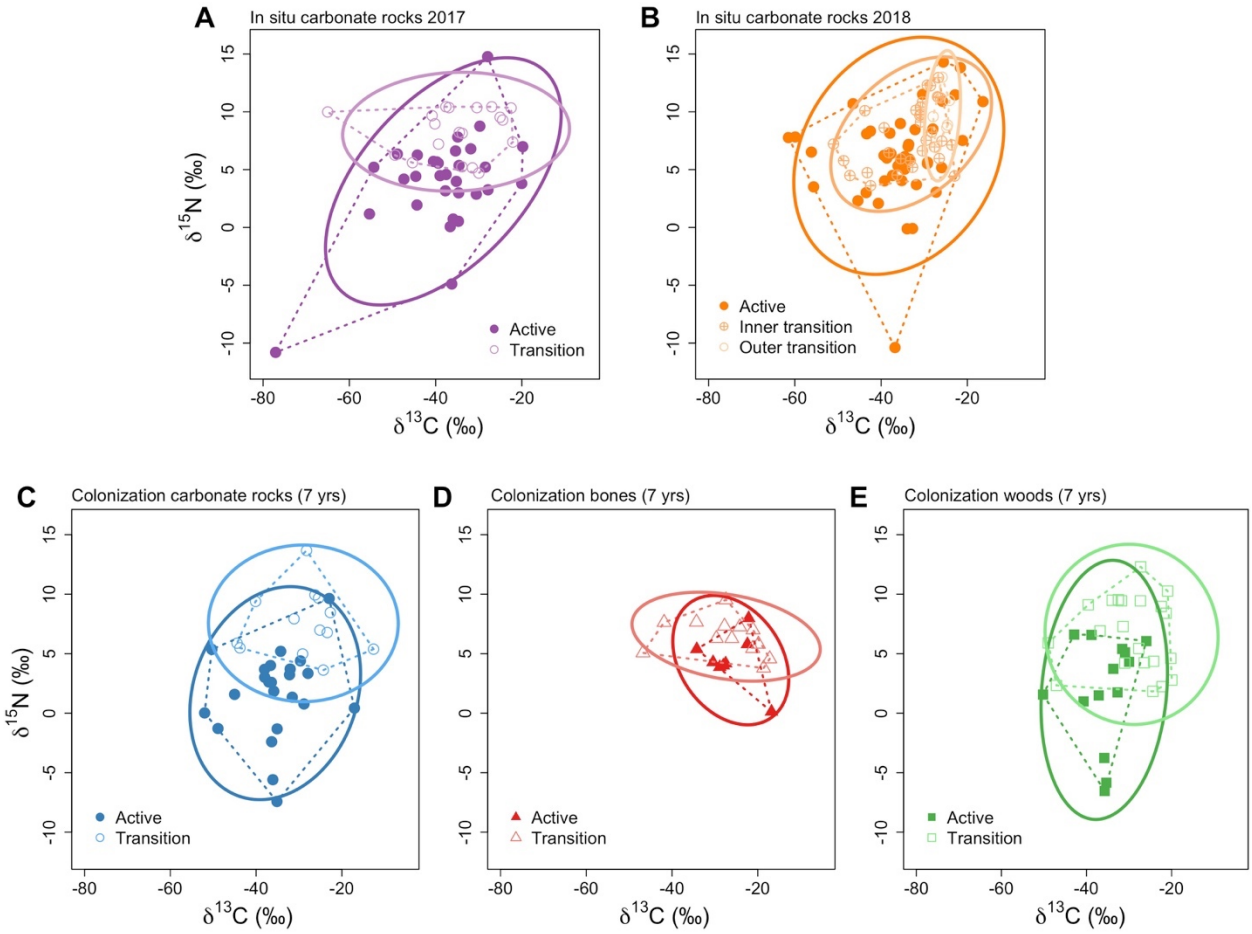

Figure 7: Dual isotope plots of the macrofaunal invertebrate community trophic niche on (A) *in situ* carbonate rocks collected at active and transition sites at Mound 12 in 2017, (B) *in situ* carbonate rocks collected across seepage gradient in 2018, (C) experimental carbonate rocks, (D) cow bones, and (E) wood deployed for 7 years (2010-2017) at active and transition sites at Mound 12. Dashed line: Total hull area Solid line: Corrected standard ellipse area. Raw data in Appendix 7.

Table 6: Average community metrics for the isotopic niche of the macrofauna community on *in situ* carbonate rocks (A) collected across a seepage gradient at Mound 12 in 2017 (AT37-13) and 2018 (AT42-03), (B) on experimental carbonate rocks, cow bones and wood deployed for 7 years (2010-2017) at active and transition sites at Mound 12, and (C) on experimental carbonate rocks transplanted across seepage gradient for 17 months (2017-2018). TA: Total area; CD: Mean distance to centroid; MNND: Mean nearest neighbor distance; SDNND: Standard deviation of nearest neighbor distance; SEA: Standard ellipse area; SEAc: Standard ellipse area corrected for sample size. Raw data in Appendix 7.

	Number of substrates	Range of food sources	Number of trophic levels	Trophic diversity			Species packing		
		$\delta^{13}C$ range	$\delta^{15}N$ range	TA	SEA	SEAc	CD	MNND	SDNND
A. In situ carbonate rocks									
2017 Active	9	57.3	25.6	616.5	124.9	129.2	8.5	2.8	4.2
2017 Transition	5	42.9	5.7	163.4	66.9	70.9	8.1	2.5	3.5
2018 Active	6	45.1	24.7	547.7	124.6	127.7	8.4	2.1	1.9
2018 Inner Transition	5	29.1	9.4	172.2	57.8	59.7	6.7	1.4	0.9
2018 Outer Transition	2	3.8	6.1	13.1	8.3	10.0	2.3	1.8	1.2
B. Colonization experiment (7 years)									
2017 Carbonate Rock Active	4	34.9	17.1	365.0	92.0	96.2	6.9	2.7	2.5
2017 Carbonate Rock Transition	4	31.8	10.1	173.8	76.4	83.4	7.6	3.0	2.7
2017 Cow Bone Active	2	17.4	7.9	54.5	36.9	43.0	4.7	2.5	2.5
2017 Cow Bone Transition		29.6	5.7	99.1	41.3	45.0	7.0	2.6	1.6
2017 Wood Active	2	24.3	13.2	176.6	84.1	91.2	6.5	2.8	2.2
2017 Wood Transition	4	29.0	10.5	215.2	80.7	85.0	7.4	2.3	1.0
C. Transplant experiment with carbonate rocks (17 months)									
Active to Inner Transition	6	46.4	21.1	406.9	135.0	140.9	10.6	2.3	2.2
Active to Outer Transition	5	26.9	8.4	104.0	55.3	62.2	9.5	3.1	1.8
Active to Background	5	51.8	17.2	470.8	250.9	273.7	14.4	5.6	3.4
Inner Transition to Active	5	32.9	8.1	161.3	50.7	53.0	6.7	1.9	1.6
Inner Transition to Outer Transition	5	25.2	8.9	117.4	65.7	73.9	7.5	2.8	1.0
Inner Transition to Background	5	11.5	20.2	108.7	76.0	91.1	5.9	4.5	2.7

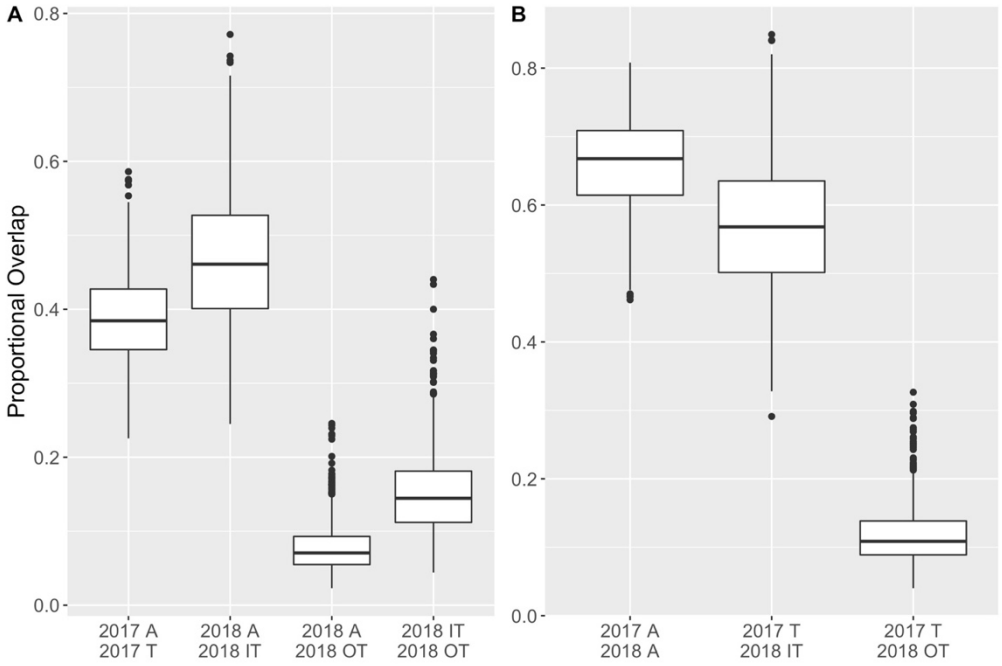

Figure 8: Proportional overlap between isotopic niche areas based on Bayesian estimates of standard ellipse areas corrected for sample size of macrofaunal invertebrates on *in situ* carbonate rocks collected at Mound 12 at active and transition sites in 2017 (AT37-13) and at active, inner transition and outer transition sites in 2018 (AT42-03). (A) Comparisons between seepage activity within year, (B) Comparisons between years within seepage activity. Boxplots visualize five summary statistics: the median, two hinges (the 25th and 75th percentiles), and two whiskers (extend from the hinge to the largest/smallest value at 1.5x the inter-quartile range), as well as outlying points individually.

5.2 Colonization patterns on carbonate rocks: Rock colonization experiment

Defaunated carbonate rocks were deployed at active and transition sites at Mound 12 for 7 years (2010-2017) to test the dynamics and recovery rate of invertebrate macrofaunal communities over periods longer than previously studied at seeps. The density of invertebrate macrofauna on experimental carbonate rocks deployed for 7 years (2010-2017) (610.7 ± 125.4/200 cm^2) was more than twice as high as on *in situ* rocks in 2017 at active sites (238.7 ± 67.3/200 cm^2) (Wilcox test, W = 0, p-value = 0.03), while at transition sites densities on experimental rocks (56.5 ± 25.7/200 cm^2) and *in situ* rocks (57.9 ± 16.5/200 cm^2) were not significantly different (Wilcox test, W = 8, p-value = 1.00; Figure 9). For experimental rocks, density was more than 10 times higher at active than transition sites (Wilcox test, W = 12, p-value = 0.05; Figure 9).

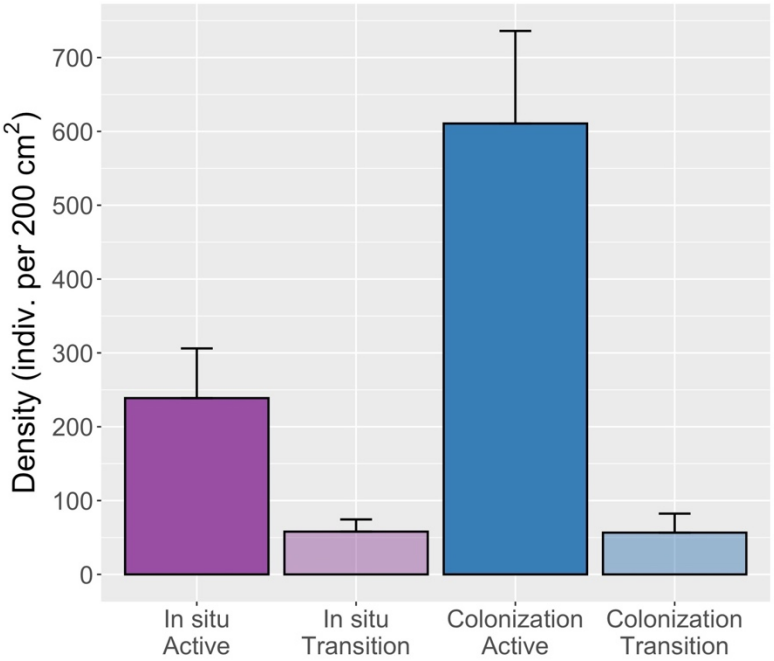

Figure 9: Average ± one standard error density (individuals per 200 cm^2) of macrofaunal invertebrates on *in situ* carbonate rocks (purple) collected across seepage gradient at Mound 12 in 2017 and 2018, and on experimental carbonate rocks (blue) deployed for 7 years (2010-2017).

The taxonomic composition of the carbonate colonizing communities was not significantly different than that of the communities on *in situ* rocks (ANOSIM, Global R = -0.012, p-value = 0.48), although the similarity between 7-year colonization community and the *in situ* community was greater at active sites (SIMPER, average similarity = 46.43) than at transition sites (SIMPER, average similarity = 35.08; Figures 10-11). However, seepage activity had an effect on the composition of the community on colonization rocks (ANOSIM, Global R = 0.464, p-value = 0.004). The community on colonization rocks at active sites was dominated by gastropods (45.04% limpets and 33.70% snails), and was more diverse at transition sites, where annelids were the dominant group (37.89%), followed by limpets (16.77%) and echinoderms (14.29%; Figure 10). Snails were also well represented at transition sites (8.70%; Figure 10), and gastropods overall were the main group contributing to the dissimilarity between communities at active and transition sites (Provannidae = 5.01%, Neolepetopsidae = 4.52%, Lepetodrilidae = 4.47%, Pyropeltidae =

3.18% and Cataegidae = 3.15%; SIMPER, average dissimilarity = 72.38; Appendix 3.5) as they tend to prefer active seepage (Table 7A).

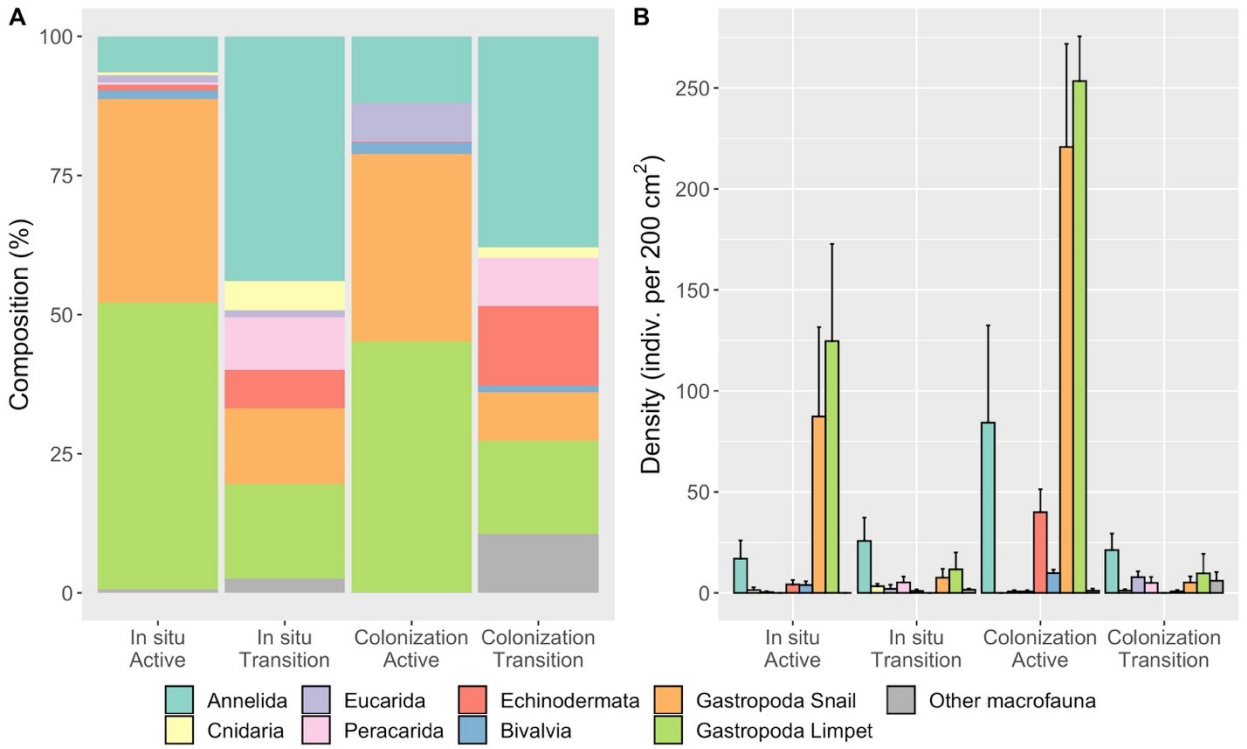

Figure 10: (A) Composition and (B) density (indiv. per 200 cm^2) by taxon of macrofaunal invertebrate community on *in situ* rocks collected at active and transition sites at Mound 12 in 2017 and on experimental carbonate rocks deployed for 7 years (2010-2017).

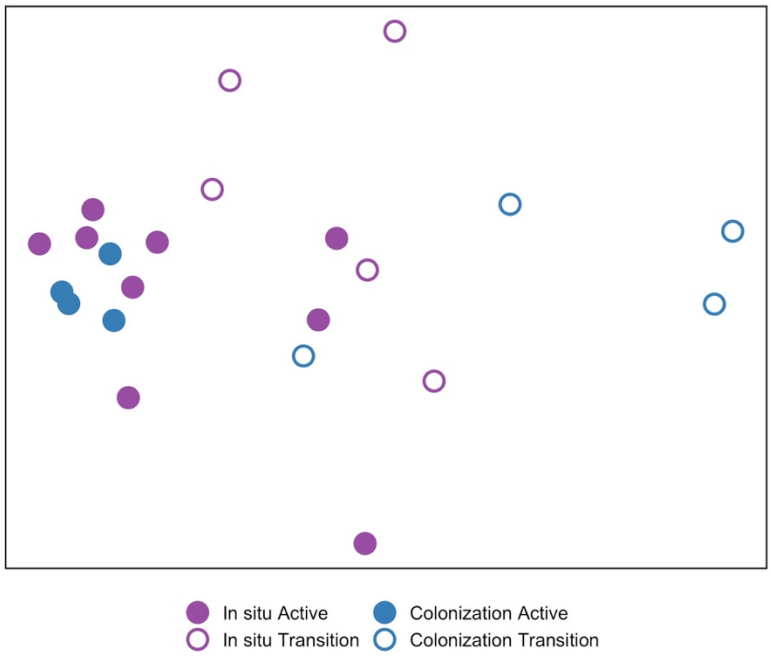

Figure 11: Multi-dimensional analysis of the macrofaunal invertebrate community on *in situ* rocks (purple) collected at active and transition sites at Mound 12 in 2017 and 2018 and on experimental carbonate rocks (blue) deployed for 7 years (2010-2017).

Table 7: Top ten taxa based on densities on *in situ* carbonate rocks collected on experimental (A) carbonate rocks, (B) bones, and (C) wood deployed for 7 years (2010-2017) at active and transition zones at Mound 12. Raw density data in Appendix 2.2.

A. Colonization Carbonate rock			
Active	**%**	**Transition**	**%**
Lepetodrilidae	33.61	Ophiuroidea	14.29
Provannidae	27.58	Neolepetopsidae	11.80
Ampharetidae	8.01	Serpulidae	9.94
Neolepetopsidae	7.89	Amphipoda	6.21
Anomura	6.79	Aplacophora	4.97
Hyalogyniridae	5.99	Phyllodocidae	4.35
Pyropeltidae	3.54	Cataegidae	4.35
Mytilidae	1.69	Lepetodrilidae	4.35
Phyllodocidae	1.31	Hesionidae	3.73
Hesionidae	0.84	Lacydoniidae	3.11
	97.26		67.08

Table 7 continued.

B. Colonization – Cow Bone			
Active	**%**	**Transition**	**%**
Lepetodrilidae	38.67	Hesionidae	22.31
Anomura	20.00	Dorvilleidae	9.92
Pyropeltidae	8.00	Ampharetidae	8.26
Provannidae	6.67	Lacydoniidae	7.44
Neolepetopsidae	6.67	Phyllodocidae	6.61
Ampharetidae	5.33	Tanaidacea	4.96
Dorvilleidae	5.33	Serpulidae	4.13
Cirratulidae	2.67	Capitellidae	4.13
Ophiuroidea	2.67	Provannidae	4.13
Hesionidae	1.33	Amphinomidae	3.31
	97.33		75.21
C. Colonization – Wood			
Active	**%**	**Transition**	**%**
Lepetodrilidae	39.22	Provannidae	38.48
Provannidae	20.04	Hesionidae	18.67
Skeneidae	13.14	Dorvilleidae	4.76
Anomura	10.90	Lepetodrilidae	4.19
Neolepetopsidae	4.85	Neolepetopsidae	4.00
Pyropeltidae	3.38	Ophiuroidea	3.81
Dorvilleidae	3.28	Amphinomidae	2.67
Mytilidae	1.19	Amphipoda	2.48
Ampharetidae	0.90	Skeneidae	2.10
Hyalogyniridae	0.62	Cataegidae	2.10
	97.52		83.24

The macrofaunal community on carbonate rocks deployed for 7 years across seepage gradients showed a high level of recovery regarding their isotopic composition (Figure 12). Animals on colonization rocks recovered the same isotopic pattern as on *in situ* rocks with lower mean carbon and nitrogen isotope values at active sites ($\delta^{13}C = -33.4 \pm 2.7$; $\delta^{15}N = 1.3 \pm 1.0$) than at transition sites ($\delta^{13}C = -29.8 \pm 1.8$; $\delta^{15}N = 7.4 \pm 0.6$; $\delta^{13}C$: Wilcox test, $W = 244$, $p = 0.02$, $\delta^{15}N$: Wilcox test, $W = 79$, $p < 0.0001$). At active sites, mean $\delta^{13}C$ was not significantly different between animals on colonization rocks and on *in situ* rocks (Wilcox test, $W = 1299$, $p = 0.18$; Table 4,

Figure 12A), but mean $\delta^{15}N$ was 3 times higher on *in situ* rocks than on colonization rocks (Wilcox test, W = 2139.5, p = 0.0003; Table 4, Figure 12B) due largely to annelids (Tables 5A, 8A). At transition zones, both carbon and nitrogen isotopes composition were not significantly different between animals on colonization rocks and on *in situ* rocks ($\delta^{13}C$: Wilcox test, W = 268, p = 0.38, $\delta^{15}N$: Wilcox test, W = 343, p = 0.61; Figure 12).

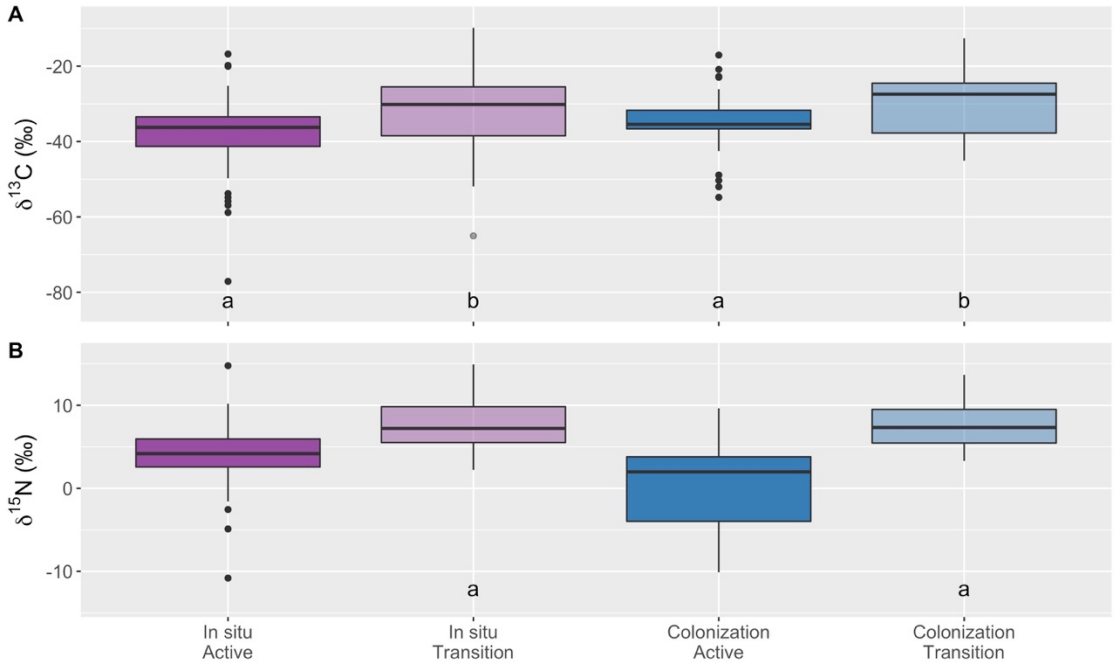

Figure 12: (A) $\delta^{13}C$ and (B) $\delta^{15}N$ values (‰) of macrofaunal invertebrate community on *in situ* carbonate rocks (purple) collected at active and transition zones at Mound 12 in 2017, and on experimental carbonate rocks (blue) deployed for 7 years (2010-2017). Boxplots visualize five summary statistics: the median, two hinges (the 25th and 75th percentiles), and two whiskers (extend from the hinge to the largest/smallest value at 1.5x the inter-quartile range), as well as outlying points individually. See statistical tests in Appendix 6.2.

For the macrofauna on colonization rocks, mean $\delta^{13}C$ and $\delta^{15}N$ values were different among taxa at active sites ($\delta^{13}C$: Kruskal-Wallis, Chi-squared = 11.849, df = 4, p-value = 0.02; $\delta^{15}N$: Kruskal-Wallis, Chi-squared = 22.402, df = 4, p-value < 0.001), but were not significantly different among taxa at transition sites ($\delta^{13}C$: Kruskal-Wallis, Chi-squared = 8.7778, df = 5, p-

value = 0.12; $\delta^{15}N$: Kruskal-Wallis, Chi-squared = 4.2368, df = 5, p-value = 0.51; Table 8A, Appendix 5.2). Pairwise comparisons based on Dunn's tests are shown in Appendix 6.12.

Within colonist groups, seepage activity (active vs transition) had no effect on mean isotopic composition of limpets ($\delta^{13}C$: Wilcox test, W = 0, p-value = 0.12; $\delta^{15}N$: Wilcox test, W = 1, p-value = 0.27) and snails ($\delta^{13}C$: Wilcox test, W = 4, p-value = 1; $\delta^{15}N$: Wilcox test, W = 0, p-value = 0.13), but it did for annelids, which showed three times lower $\delta^{15}N$ values at active sites (Wilcox test, W = 0, p-value < 0.001; Table 8A, Appendix 5.2, statistical tests in Appendix 6.8). Mean isotopic composition of the different macrofaunal groups was not significantly different between colonization rocks and *in situ* rocks at both active and transition sites, except for annelids, which showed 2x lower $\delta^{15}N$ values at active sites on colonization rocks than on *in situ* rocks (Wilcox test, W = 94, p-value = 0.01; Table 8A, statistical tests in Appendix 6.9-6.10).

Table 8: Mean ± standard error isotopic values (‰) by major macrofaunal taxa on experimental (A) carbonate rocks, (B) cow bones, and (C) wood deployed for 7 years (2010-2017) at active and transition zones at Mound 12. *: Significant difference between taxa on colonization rock and on *in situ* rocks based on Wilcox tests (p-value < 0.05). See Appendix 6.8-6.10 for statistical tests.

A. Colonization carbonate rocks	**Active**		**Transition**	
	$\delta^{13}C$ (‰)	**$\delta^{15}N$ (‰)**	**$\delta^{13}C$ (‰)**	**$\delta^{15}N$ (‰)**
Annelida	-35.2 ± 2.2	2.2 ± 0.5*	-35.7 ± 3.9	7.8 ± 1.3
Eucarida	-28.5 ± 1.7	5.3 ± 2,0	NA	NA
Peracarida	NA	NA	-26.9 ± 1.1	8.2 ± 1.6
Echinodermata	NA	NA	-23.4 ± 3.1	6.8 ± 1.4
Bivalvia	-34.4 ± 1.2	-5.4 ± 1.1	NA	NA
Gastropoda:Snail	-36.6 ± 3.0	4.0 ± 1.2[1]	-40.1 ± 0.2	9.4 ± 0.2[1]
Gastropoda:Limpet	-43.8 ± 4.3	1.4 ± 1.7	-18.5 ± 4.3	4.5 ± 0.9
Other macrofauna	NA	NA	-25.1	7.00
B. Colonization bone	**Active**		**Transition**	
	$\delta^{13}C$ (‰)	**$\delta^{15}N$ (‰)**	**$\delta^{13}C$ (‰)**	**$\delta^{15}N$ (‰)**
Annelida	-19.6 ± 2.8	2.9 ± 2.8	-29.9 ± 3.9	6.2 ± 0.6
Cnidaria	NA	NA	-29.7	6.3
Eucarida	-27.5 ± 1.7	4.2 ± 0.2	NA	NA
Peracarida	-22.1	8.00	NA	NA
Echinodermata	-28.0	4.0	-17.2	4.6
Bivalvia	NA	NA	-34.3	7.6

Table 8 continued.

B. Colonization bone	**Active**		**Transition**	
	$\delta^{13}C$ (‰)	**$\delta^{15}N$ (‰)**	**$\delta^{13}C$ (‰)**	**$\delta^{15}N$ (‰)**
Gastropoda:Snail	-30.4 ± 1.1	4.29 ± 0.15	-27.76	7.31
Gastropoda:Limpet	-32.4 ± 2.2	4.88 ± 0.58	-	-
Other macrofauna	NA	-	-24.20 ± 0.50	7.26 ± 5.49
C. Colonization wood	**Active**		**Transition**	
	$\delta^{13}C$ (‰)	**$\delta^{15}N$ (‰)**	**$\delta^{13}C$ (‰)**	**$\delta^{15}N$ (‰)**
Annelida	-34.2 ± 1.2	0.7 ± 2.3	-28.4 ± 1.51=	8.8 ± 0.6
Eucarida	-34.4 ± 5.3	5.5 ± 0.8	-24.4	1.8
Peracarida	NA	NA	-24.2	4.4
Echinodermata	NA	NA	-26.4 ± 1.8	4.2 ± 1.2
Bivalvia	-35.8 ± 0.3	-5.3 ± 0.7	-20.2 ± 0.5	4.6 ± 0.7
Gastropoda:Snail	-34.7 ± 1.7	4.3 ± 0.8	-36.3 ± 7.3	4.6 ± 2.3
Gastropoda:Limpet	-37.2 ± 3.6	3.0 ± 0.8	NA	NA
Other macrofauna	NA	NA	29.2 ± 4.8	8.3 ± 0.9

Trophic structure similarity between active and transition sites was greater for communities on *in situ* rocks (Figure 7A) than on colonization rocks (Figures 7C, 13A), whereas there was an even higher similarity between communities on *in situ* rocks in 2017 and colonization rocks at a given seepage activity (Figure 13B). The community on colonization rocks had greater trophic diversity at active sites than at transition zones, although it was lower than the trophic diversity of the community on *in situ* rocks at active sites in 2017 (Table 6). The opposite trend was observed at transition zones, where the community on colonization rocks showed larger isotopic niche area than on *in situ* rocks in 2017 (Table 6). Proportional niche overlap was similar between *in situ* rocks and within seepage activity (Figure 13).

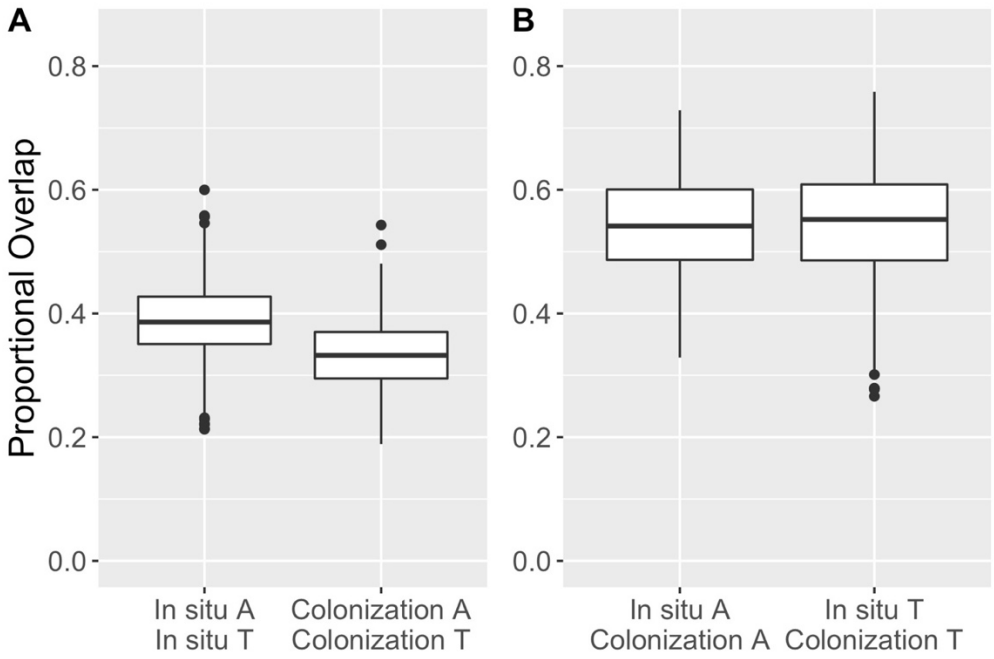

Figure 13: Proportional overlap between isotopic niche areas based on Bayesian estimates of standard ellipse areas corrected for sample size of macrofaunal invertebrates on *in situ* carbonate rocks collected at Mound 12 in 2017 and experimental carbonate rocks deployed for 7 years (2010-2017) at active and transition sites. Overlap was calculated was a proportion of the non-overlapping area of the two ellipses. (A) Comparisons between seepage activity, (B) Comparisons between *in situ* rocks and colonization rocks within seepage activity. A: Active site, T: Transition site. Boxplots visualize five summary statistics: the median, two hinges (the 25th and 75th percentiles), and two whiskers (extend from the hinge to the largest/smallest value at 1.5x the inter-quartile range), as well as outlying points individually.

5.3 Community persistence under changing seepage: Transplant experiment

Carbonate rocks from Mound 12 were transplanted to different seepage conditions for 17 months (2017-2018) to better understand the role of seepage in determining biological patterns and the rates and trajectory of community response and persistence (Figure 2). Densities of invertebrate macrofauna on rocks transplanted from active sites to inner transition sites (A-IT), to outer transition sites (A-OT), or to background sites (A-B) were lower than the average density of communities on *in situ* rocks at active sites collected in 2017 at the start of the experiment (A-IT: Dunn's test, z = 2.262741 p-value = 0.01; A-OT: Dunn's test, z = 2.00126, p-value = 0.02; A-B: Wilcox test, W = 24, p-value = 0.01; Figure 14). For the remaining transplant treatments from

inner transition sites to active sites (IT-A), to outer transition sites (IT-OT) or to background sites (IT-B), densities on the transplanted rocks were not significantly different than densities on *in situ* rocks collected in 2017 at the initial site and in 2018 at the end site of the transplant experiments (IT-A: Kruskal-Wallis, Chi-squared = 3.2176, df = 2, p-value = 0.20; IT-OT: Kruskal-Wallis, Chi-squared = 1.6182, df = 2, p-value = 0.44; IT-B: Wilcox test, W = 15, p-value = 0.28; Figure 14). However, the average density on transplanted rocks tended to increase when the rocks were moved from inner transition sites to active sites (IT-A), and decrease when moved to sites with lesser seepage (IT-OT and IT-B; Figure 14).

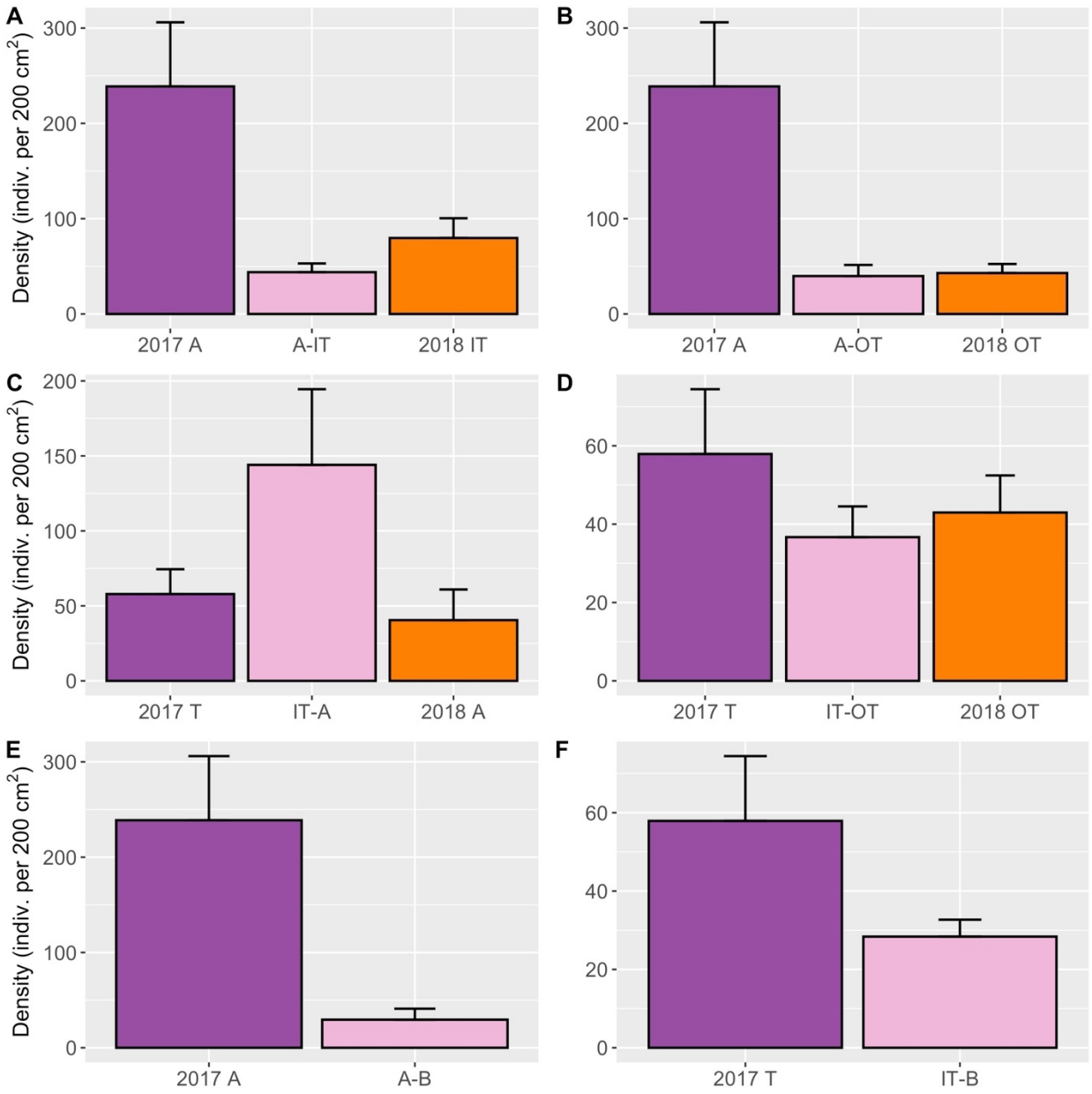

Figure 14: Average ± one standard error density (individuals per 200 cm^2) of macrofaunal invertebrates on experimental rocks transplanted across seepage gradient (pink) for 17 months, and on *in situ* rocks at the initial site collected in 2017 (purple) and at the end site collected in 2018 (orange). Rocks were transplanted from: (A) Active to inner transition, (B) Active to outer transition, (C) Inner transition to active, (D) Inner transition to outer transition, (E) Active to background, and (F) Inner transition to background. A: Active, T: Transition, IT: Inner transition, OT: Outer transition, B: Background.

Community composition on the active to inner transition (A-IT) transplanted rocks was significantly different from the *in situ* communities at the initial active site (ANOSIM, R = 0.438, p-value = 0.003), but it did not differ from the *in situ* communities at the final inner transition site

(ANOSIM, R = 0.084, p-value = 0.18; Global R: 0.45, p-value = 0.001; Figures 15-17A), indicating rapid (17 months) response to change in seepage activity. The groups contributing to the dissimilarity between the communities on active to inner transition transplanted rocks and *in situ* active rocks collected at the start of the experiment were Provannidae (6.14%), Lepetodrilidae (5.66%), Mytilidae (5.47%), Chrysopetalidae (5.42%), Neolepetopsidae (4.96%), Phyllodocidae (3.68%), Ampharetidae (3.45%), Anomura (3.39%), Tanaidacea (3.11%), and Serpulidae (3.01%; SIMPER, Average dissimilarity = 74.22; Appendix 3.6). Among these, gastropods, ampharetids, anomurans, and serpulids were more abundant at active sites in 2017 than on the transplanted rock (Appendix 4.2).

Seepage activity also had an effect on the composition of the community on rocks transplanted from active to outer transition sites (A-OT); by the end of the experiment the transplant composition was significantly different than that of the community on *in situ* active rocks collected in 2017 (ANOSIM, R = 0.767, p-value = 0.001), but did not differ from the community on *in situ* outer transition rocks collected in 2018 (ANOSIM, R = 0.709, p-value = 0.051; Global R = 0.799, p-value = 0.001). The community on *in situ* rocks at the initial active site was dominated by gastropods, and some of the gastropod taxa persisted when rocks were transplanted from active sites to outer transition sites, although the rocks also gained annelids and peracarids (Table 9), causing them to become more similar to the community on *in situ* outer transition rocks collected at the end of the experiment (Figures 15-17B). The groups that contributed the most to the dissimilarity between the active-outer transition transplanted community and the initial *in situ* active community were Provannidae (5.70% contribution to dissimilarity), Lepetodrilidae (5.24%), Neolepetopsidae (4.39%), and Anomura (2.92%), which were more abundant at active sites, and Amphipoda (5.42%), Nereididae (4.30%), Chrysopetalidae

(3.74%) and Polynoidae (3.67%; SIMPER, average dissimilarity = 80.19; Appendix 3.7), which were more abundant on the active to outer transition transplanted rocks (Appendix 4.3).

Community composition on inner transition rocks transplanted to active sites (IT-A) was not significantly different than that of *in situ* transition rocks collected in 2017 or the active rocks collected in 2018 (ANOSIM, Global R = 0.123, p-value = 0.09; Figure 17C). The communities on the transplanted rocks and on 2017 *in situ* transition rocks were dominated by annelids (38.71% and 43.97%, respectively) and limpets (38.57% and 16.94%, respectively; Figure 15-16C, Table 9). Although the community on 2018 *in situ* active rocks was dominated by annelids (53.52%), gastropods were also well represented (18.31% snails and 5.63% limpets). The abundance of annelids did not differ among these three communities, but the higher abundance of gastropods on the transplanted rocks (Figure 15C) accounted for the lower percent composition of annelids (Figure 16C).

For the inner transition to outer transition (IT-OT) transplants, the community composition did not differ from the community on *in situ* outer transition rocks at the end of the experiment in 2018 (ANOSIM, R = 0.382, p-value = 0.09), but there was a significant difference between the inner to outer transition transplanted communities and the *in situ* transition communities from 2017 (ANOSIM, R = 0.432, p-value = 0.008; Global R = 0.412, p-value = 0.004; Figure 17D). The groups contributing the most to the dissimilarity between the transplanted community and the 2017 *in situ* transition community were Isopoda (5.73% contribution to dissimilarity) and Chrysopetalidae (4.48%), which were more abundant on the transplanted rocks (Table 9), and Lepetodrilidae (4.45%), Ophiuroidea (3.96%), Neolepetopsidae (3.89%), Provannidae (3.38%), Serpulidae (3.18%), Cataegidae (3.07%), and Hydroidolina (3.13%; SIMPER, average

dissimilarity = 68.85; Appendix 3.8), which were more abundant on the *in situ* transition rocks (Table 9; Appendix 4.5).

Active rocks transplanted to background sites (A-B) exhibited differences from the community on *in situ* active rocks collected in 2017 (ANOSIM, Global R = 0.643, p-value = 0.0001; Figure 17E). The community on the transplanted rocks had annelids (65.12%), peracarids (10.96%), and bivalves (8.64%) as the dominant taxa, while the community at *in situ* active rocks had a high dominance and density of gastropods (Figures 15-16E). The groups that contributed to dissimilarity and were more abundant at active sites were Provannidae (5.06%), Lepetodrilidae (4.26%), Actiniaria (3.23%), Nuculanidae (3.10%) and Neolepetopsidae (2.96%). Although the density of annelids was not much different between communities on 2017 *in situ* active rocks and active-background transplanted rocks, the annelid composition was different (Appendix 4.6). Within annelids, the families that contributed to dissimilarity between communities were those more abundant on the transplanted rocks: Phyllodocidae (4.17%), Nereididae (3.72%), and Cirratulidae (3.61%), in addition to Amphipoda (4.67%) and Bathymodiolinae (3.14%; SIMPER, average dissimilarity = 72.50; Appendix 3.9).

The same pattern was observed for the inner transition to background (IT-B) transplant treatment; the community on the transplanted rocks was significantly different than the *in situ* community at transition sites in 2017 (ANOSIM, Global R = 0.548, p-value = 0.008; Figure 17F). Both communities were diverse, although annelids showed higher dominance on the transplanted rocks (Figures 15-16F). The main groups contributing to dissimilarity between the communities were Chrysopetalidae (4.72%), Provannidae (4.66%), Cirratulidae (4.34%), Amphipoda (4.12%), Lepetodrilidae (3.82%), Ophiuroidea (3.60%), Aplacophora (3.50%), Neolepetopsidae (3.32%), Amphinomidae (3.26%), and Paraonidae (3.26%; SIMPER, average dissimilarity = 72.71;

Appendix 3.10). Among these, cirratulids, paraonids, and aplacophorans were more abundant on the inner transition to background transplanted rocks than on the 2017 *in situ* transition rocks (Table 9, Appendix 4.7).

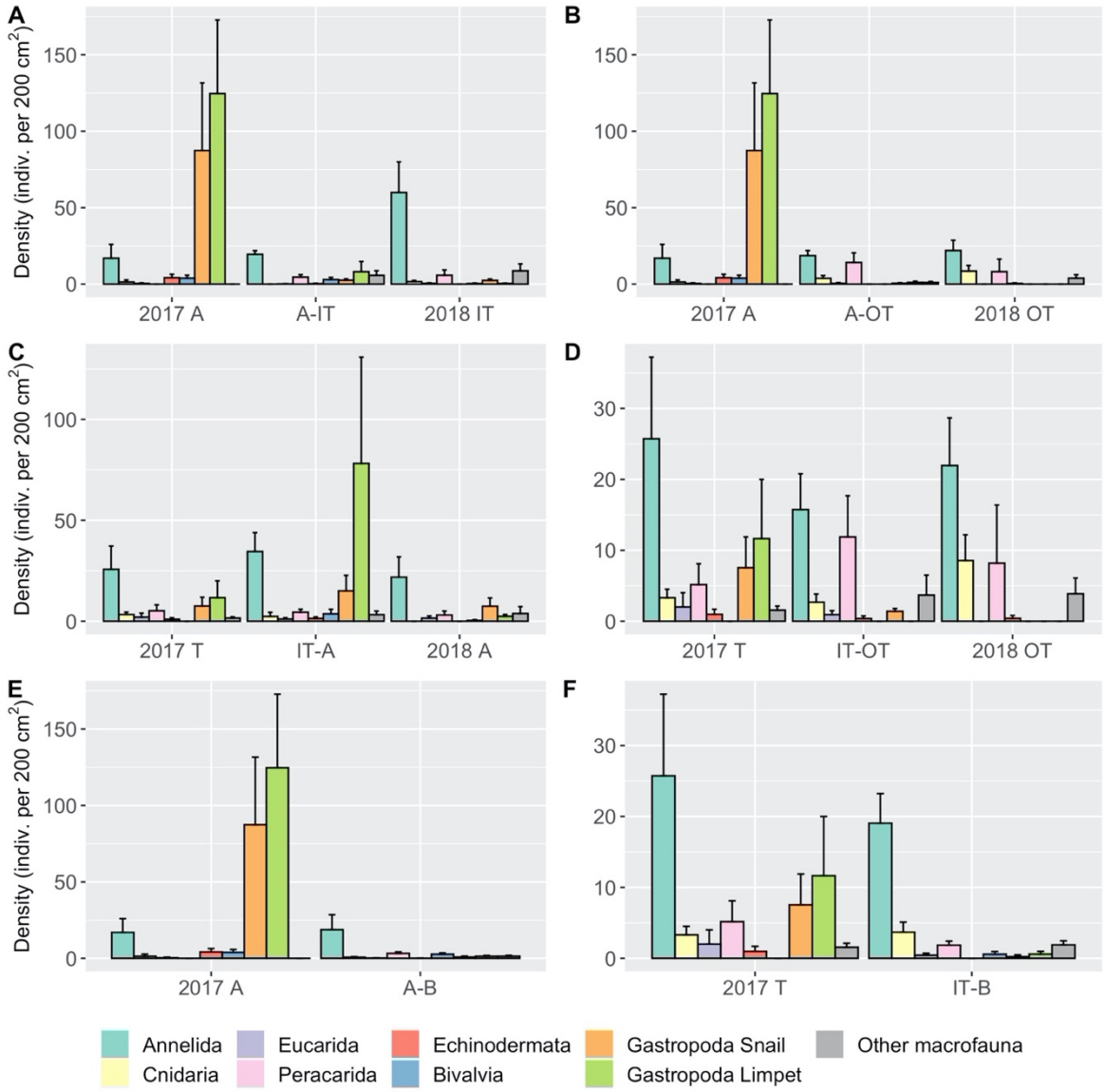

Figure 15: Number of individuals by taxon of macrofauna invertebrates on experimental carbonate rocks transplanted across seepage gradient for 17 months, and on *in situ* carbonate rocks at the initial site collected in and at the end site collected in 2018. Carbonates were transplanted from: (A) Active to inner transition, (B) Active to outer transition, (C) Inner transition to active, (D) Inner transition to outer transition, (E) Active to background, and (F) Inner transition to background. A: Active, T: Transition, IT: Inner transition, OT: Outer transition, B: Background. There were not *in situ* background rocks available for study.

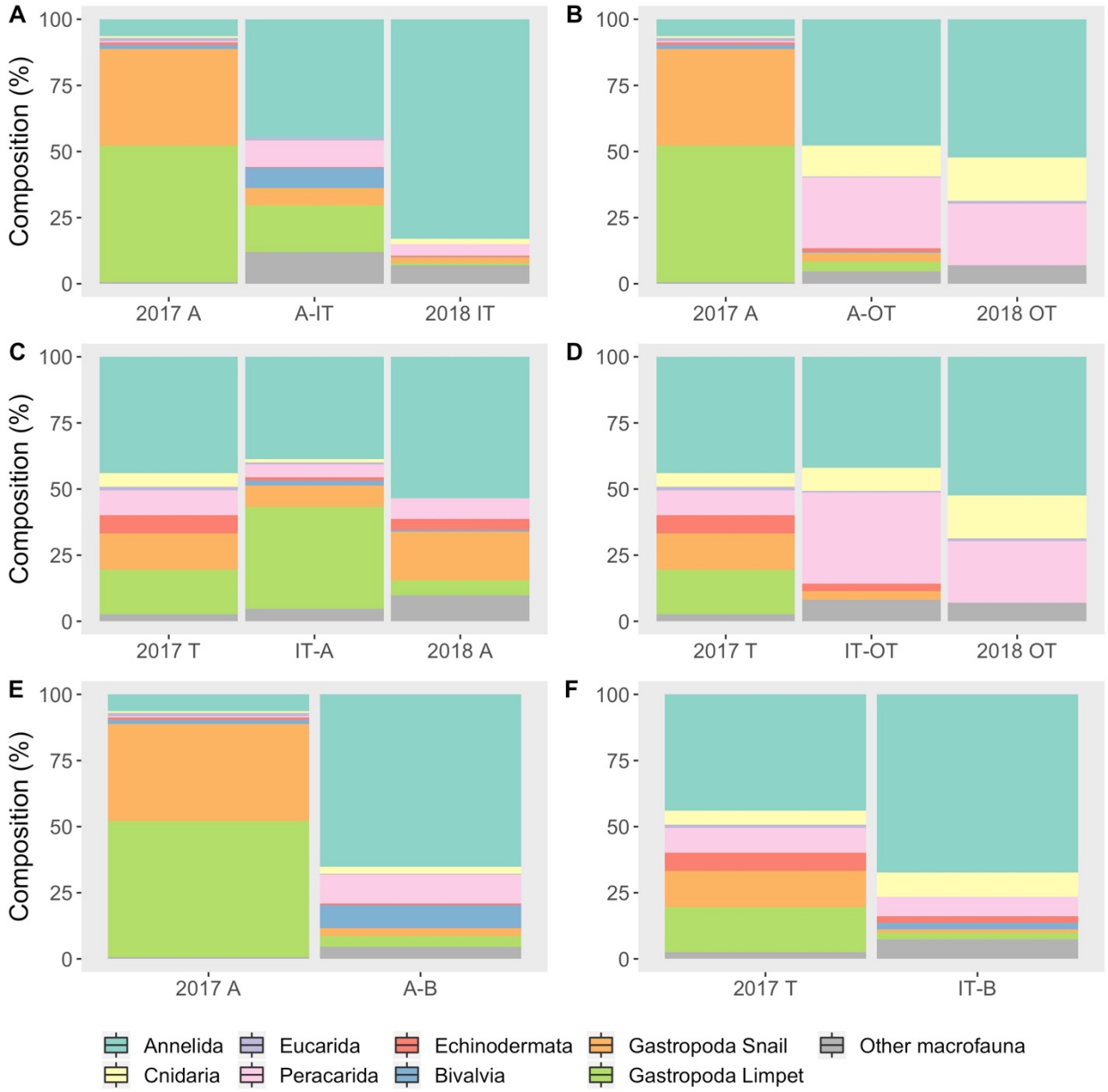

Figure 16: Composition (%) of the macrofaunal invertebrate community on experimental carbonate rocks transplanted across seepage gradient for 17 months, and on *in situ* carbonate rocks at the initial site collected in 2017 and at the end site collected in 2018. Carbonates were transplanted from: (A) Active to inner transition, (B) Active to outer transition, (C) Inner transition to active, (D) Inner transition to outer transition, (E) Active to background, and (F) Inner transition to background. A: Active, T: Transition, IT: Inner transition, OT: Outer transition, B: Background. There were not *in situ* background rocks available for study.

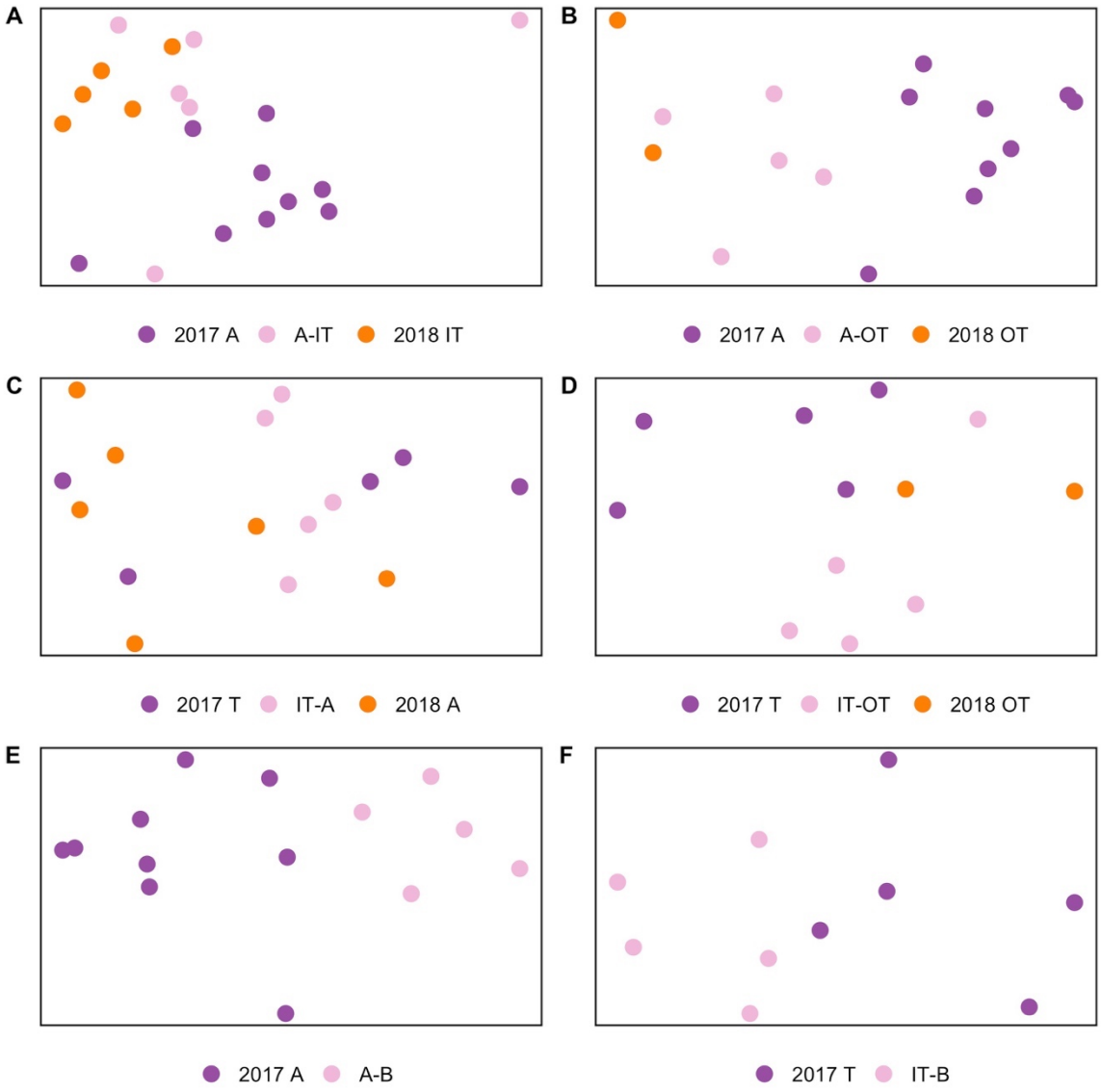

Figure 17: Multi-dimensional analysis of the macrofaunal invertebrate community composition on experimental carbonate rocks transplanted across seepage gradient for 17 months (pink), and on *in situ* carbonate rocks at the initial site collected in 2017 (purple) and at the end site collected in 2018 (orange). Carbonates were transplanted from: (A) Active to inner transition, (B) Active to outer transition, (C) Inner transition to active, (D) Inner transition to outer transition, (E) Active to background, and (F) Inner transition to background. A: Active, T: Transition, IT: Inner transition, OT: Outer transition, B: Background.

Table 9: Top ten taxa based on densities on experimental carbonate rocks transplanted across seepage gradients for 17 months at Mound 12. Carbonates were transplanted from: active to inner transition (A-IT), active to outer transition (A-OT), active to background (A-B), inner transition to active (IT-A), inner transition to outer transition (IT-OT), and inner transition to background (IT-B). Raw density data in Appendix 2.3.

A-IT	**%**	**A-OT**	**%**	**A-B**	**%**
Chrysopetalidae	20.34	Amphipoda	23.85	Phyllodocidae	14.95
Neolepetopsidae	16.90	Chrysopetalidae	11.72	Ampharetidae	12.96
Mytilidae	6.55	Amphinomidae	9.21	Amphipoda	9.30
Trombidiformes	5.17	Actiniaria	8.37	Hesionidae	6.31
Tanaidacea	4.83	Polynoidae	6.28	Amphinomidae	5.65
Cataegidae	4.83	Neolepetopsidae	3.77	Cirratulidae	5.32
Ampharetidae	4.48	Nereididae	3.35	Mytilidae	4.65
Phyllodocidae	3.79	Hydroidolina	3.35	Nereididae	4.32
Amphipoda	3.45	Polyplacophora	2.93	Nuculanidae	3.99
Polyplacophora	3.45	Hesionidae	2.09	Siboglinidae	2.99
	73.79		74.92		70.44
IT-A	**%**	**IT-OT**	**%**	**IT-B**	**%**
Neolepetopsidae	36.12	Isopoda	25.68	Chrysopetalidae	32.10
Chrysopetalidae	21.43	Chrysopetalidae	19.59	Amphinomidae	8.64
Provannidae	4.58	Amphipoda	6.08	Phyllodocidae	8.64
Lacydoniidae	3.77	Hydroidolina	5.41	Hydroidolina	6.79
Tanaidacea	3.64	Amphinomidae	3.38	Cirratulidae	3.70
Hesionidae	3.37	Actiniaria	3.38	Tanaidacea	3.70
Cataegidae	2.70	Polynoidae	2.70	Aplacophora	3.70
Tromidiformes	2.56	Paraonidae	2.70	Polynoidae	2.47
Syllidae	2.43	Tanaidacea	2.70	Ophiuroidea	2.47
Lepetodrilidae	2.29	Ophiuroidea	2.70	Nuculanidae	2.47
	82.89		74.32		74.68

Mean carbon isotope composition of the macrofaunal invertebrate community on the rocks transplanted from active to inner transition sites (A-IT) was not significantly different than the community on active *in situ* rocks at the start (in 2017) (Wilcox test, W = 445, p = 0.35) or from *in situ* inner transition rocks at the end (in 2018) of the experiment (Wilcox test, W = 358, p-value = 0.51) due to the high variability in isotopic composition of the macrofauna on the transplanted rocks, suggesting that they retained "active" trophic composition, as well as gained "transition" trophic composition (Table 4, Figure 18A). However, the community on the A-IT transplanted rocks had mean $\delta^{15}N$ values twice as high as the *in situ* community at active sites in 2017 (Wilcox

test, W = 531, p-value = 0.01; Table 4, Figure 19A). Faunal carbon and nitrogen ranges were greater on the transplanted rocks than those on *in situ* inner transition rocks, the final transplant site (Table 6C). Niche breadth was more diverse on the transplanted rocks than on the *in situ* rocks at initial and end sites and the average degree of trophic diversity was also greater (higher SEAc and CD; Table 6, Figure 20A). Although there was a higher trophic redundancy on the transplanted communities (high MNDD, Table 6), the distribution of trophic niches was more even (low SDNND, Table 6C).

For the community on rocks transplanted from active to outer transition sites (A-OT), mean $\delta^{13}C$ values were not significantly different than for the community on *in situ* rocks at active sites in 2017, the start site of the experiment (Wilcox test, W = 184, p-value = 0.39), and they were 48% lower than $\delta^{13}C$ values of animals on the *in situ* outer transition rocks collected in 2018 (Wilcox test, W = 12.5, p-value = 0.03), suggesting they did not change their food sources and retained their "active" $\delta^{13}C$ values (Table 4, Figure 18B). However, mean community $\delta^{15}N$ values were 20% higher on the transplanted rocks than on the *in situ* rocks at active sites in 2017 (Wilcox test, W = 266, p-value < 0.001) and did not differ from *in situ* rocks at outer transition sites in 2018 (Wilcox test, W = 25, p-value = 0.36; Table 4, Figure 19B), indicating that the community acquired a greater number of taxa with nitrogen isotopic values characteristic of transition zones. The community on the transplanted rocks showed broader niche space than *in situ* rocks at initial and end sites (higher CD, Table 6C), as well as higher diversification at the base of the food web ($\delta^{13}C$ ranges) and possibly more trophic levels ($\delta^{15}N$ ranges) (Table 6C). Trophic diversity was higher on *in situ* rocks at active sites in 2017 (higher TA and SEAc; Table 6C, Figure 20B), but trophic niches were more evenly distributed on the transplanted rocks (lower SDNND; Table 6C).

Carbon isotope composition was not significantly different between the IT-A transplanted communities and both *in situ* rocks at transition sites collected in 2017 (Wilcox test, W = 193, p-value = 0.40) and *in situ* rocks at active sites collected in 2018 (Wilcox test, W = 464, p-value = 0.50; Table 4, Figure 18C). Nitrogen isotope composition did not differ between the transplanted community and the community on *in situ* rocks at active sites in 2018 (Wilcox test, W = 550, p-value = 0.66), but $\delta^{15}N$ values were half the value on the transplanted rocks than on the *in situ* rocks at transition sites in 2017 (Wilcox test, W = 136.5, p-value = 0.02; Table 4, Figure 19C). This suggests that the transplanted community retained "transition" carbon isotope composition, as well as gained "active" carbon isotope composition, but lost niche diversification at the base of the food web and number of trophic levels ($\delta^{13}C$ and $\delta^{15}N$ ranges; Table 6C). Trophic diversity was lower on the transplanted rocks (lower TA and SEAc; Table 6C, Figure 20D) with higher levels of trophic redundancy (lower MNND; Table 6C), although the niches were more evenly distributed (lower SDNND, Table 6C).

Carbon and nitrogen isotope composition did not differ between the communities on rocks transplanted from inner transition to outer transition (IT-OT) and both *in situ* transition rocks collected in 2017 ($\delta^{13}C$: Wilcox test, W = 133, p-value = 0.09, $\delta^{15}N$: Wilcox test, W = 132.5, p-value = 0.09) and *in situ* outer transition rocks collected in 2018 ($\delta^{13}C$: Wilcox test, W = 37, p-value = 0.89, $\delta^{15}N$: Wilcox test, W = 39, p-value = 0.74; Table 4, Figures 18-19D). Carbon and nitrogen ranges were less than for the *in situ* rocks at transition sites in 2017 and higher than on the *in situ* rocks at outer transition rocks in 2018 (Table 6C), suggesting a shift in food sources and number of trophic levels to a less diverse base of the food web. However, average trophic diversity was higher on the transplanted rocks (higher SEAc and CD; Table 6C, Figure 20D) with more

even distribution of trophic niches (lower SDNND; Table 6C), although with more trophic redundancy (lower MNND; Table 6C).

For the transplant treatment active to background (A-B), isotopic composition of the communities on the transplanted rocks was not significantly different from the *in situ* rocks at active sites collected in 2017 ($\delta^{13}C$: Wilcox test, W = 321, p-value = 0.73, $\delta^{15}N$: Wilcox test, W = 291, p-value = 0.37; Table 4, Figures 18-19E), suggesting that the community retained its "active" composition even at non-seepage sites. Although $\delta^{13}C$ and $\delta^{15}N$ ranges and trophic redundancy decreased, trophic diversity increased and trophic niches were more evenly distributed relative to the active in situ rocks (Table 6C, Figure 20E).

For inner transition rocks transplanted to background sites (IT-B), $\delta^{15}N$ values of the community did not differ from those of the community on *in situ* rocks at transition sites collected in 2017 (W = 80.5, p-value = 0.18; Table 4, Figure 19F), but $\delta^{13}C$ values were lower by the end of the experiment on the transplanted rocks (Wilcox test, W = 25, p-value = 0.0003; Table 4, Figure 18F). Niche diversification at the base of the food web decreased, as well as trophic redundancy decreased (lower $\delta^{13}C$ range, higher $\delta^{15}N$ range, higher MNND; Table 6C).

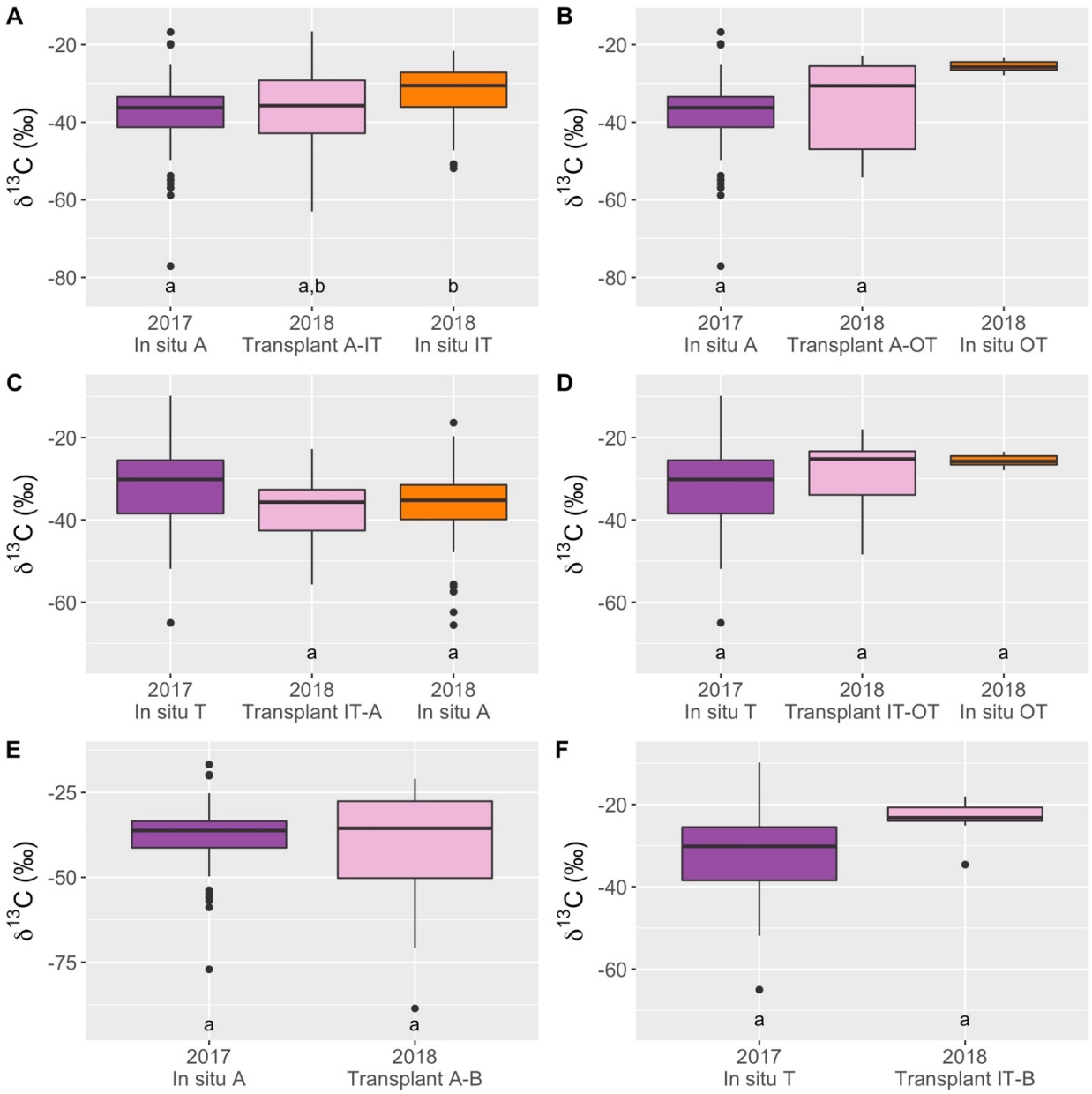

Figure 18: Mean $\delta^{13}C$ values of macrofaunal invertebrates on experimental rocks transplanted across seepage gradient for 17 months (pink), and $\delta^{13}C$ values of macrofaunal invertebrate community on *in situ* rocks at the initial site collected in 2017 (purple) and at the end site collected in 2018 (orange). Rocks were transplanted from: (A) Active to inner transition, (B) Active to outer transition, (C) Inner transition to active, (D) Inner transition to outer transition, (E) Active to background, and (F) Inner transition to background. A: Active, T: Transition, IT: Inner transition, OT: Outer transition, B: Background. Boxplots visualize five summary statistics: the median, two hinges (the 25th and 75th percentiles), and two whiskers (extend from the hinge to the largest/smallest value at 1.5x the inter-quartile range), as well as outlying points individually.

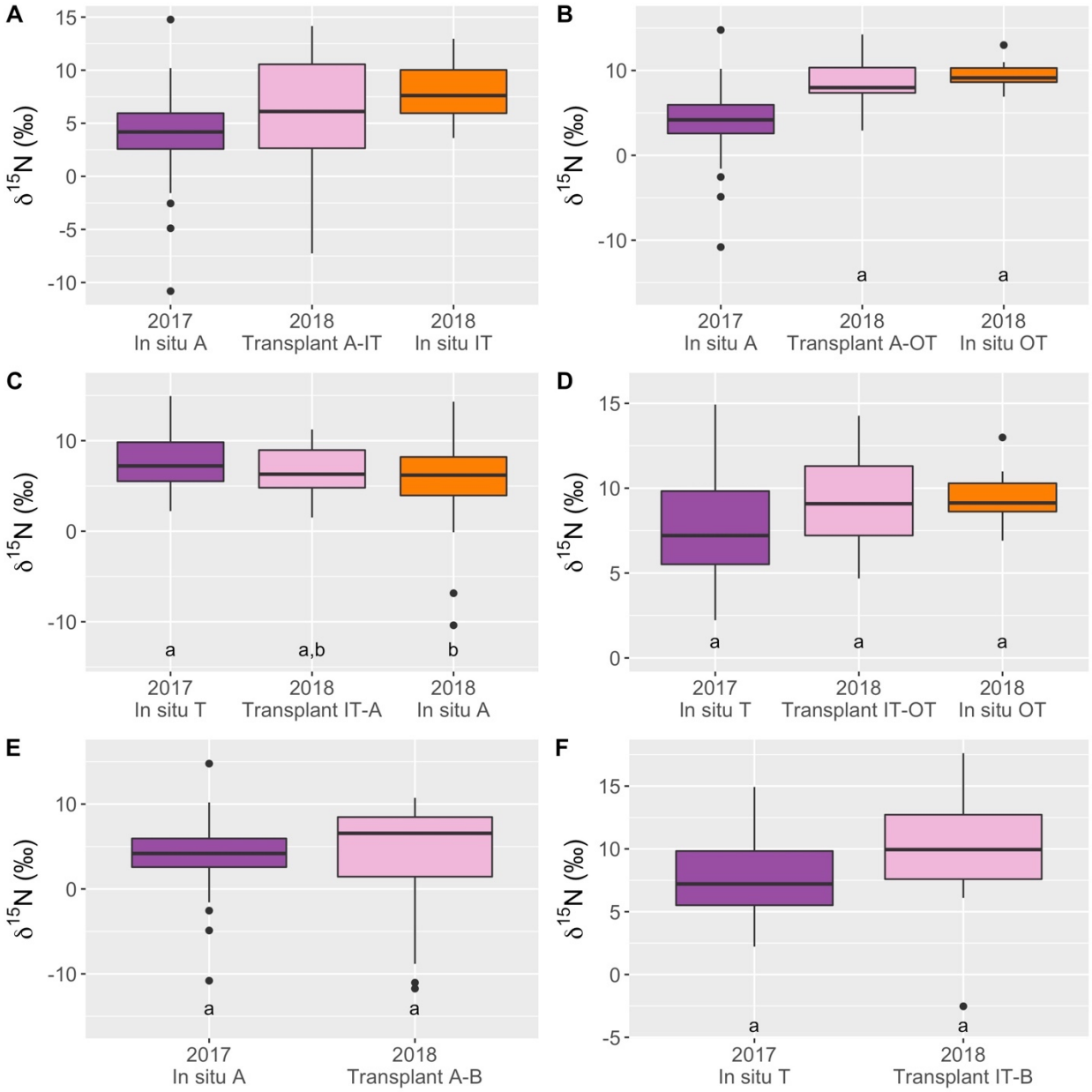

Figure 19: Mean $\delta^{15}N$ values of macrofaunal invertebrates on experimental rocks transplanted across seepage gradient for 17 months (pink), and $\delta^{15}N$ values of macrofaunal invertebrate community on *in situ* rocks at the initial site collected in 2017 (purple) and at the end site collected in 2018 (orange). Rocks were transplanted from: (A) Active to inner transition, (B) Active to outer transition, (C) Inner transition to active, (D) Inner transition to outer transition, (E) Active to background, and (F) Inner transition to background. A: Active, T: Transition, IT: Inner transition, OT: Outer transition, B: Background. Boxplots visualize five summary statistics: the median, two hinges (the 25th and 75th percentiles), and two whiskers (extend from the hinge to the largest/smallest value at 1.5x the inter-quartile range), as well as outlying points individually.

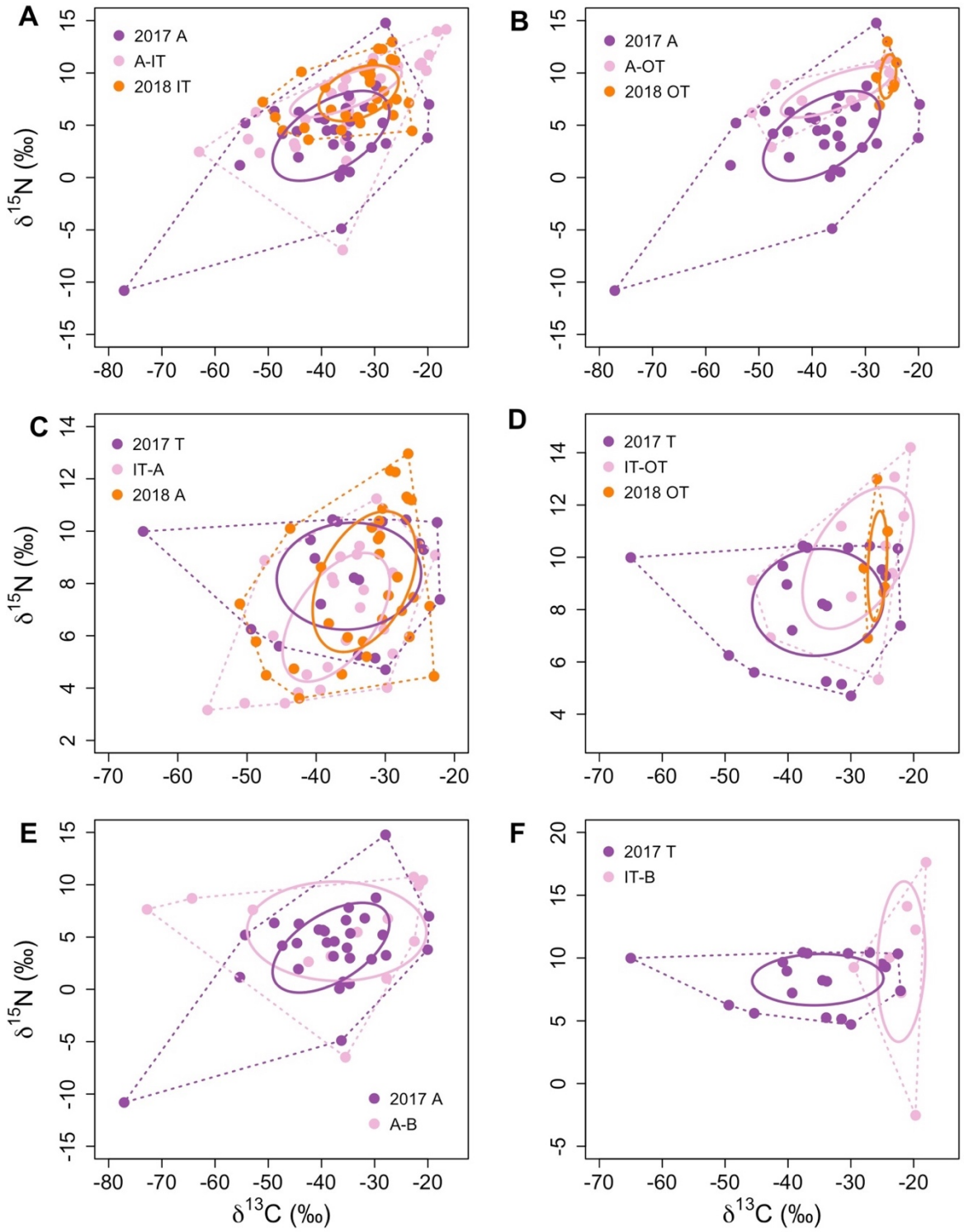

Figure 20: Biplots with total area (dashed line) and corrected standard ellipse area (solid line) of macrofaunal invertebrates on experimental rocks transplanted across seepage gradient for 17 months (pink), and on *in situ* rocks at the initial site collected in 2017 (purple) and at the end site collected in 2018 (orange). Rocks were transplanted from (A) Active to inner transition, (B) Active to outer transition, (C) Inner transition to active, (D) Inner transition to outer transition, (E) Active to background, and (F) Inner transition to background. Dashed line: Total area; Solid line: Corrected standard ellipse area.

Isotopic composition of the different taxa (Table 10) was not significantly different among transplant treatments (see Appendix 6.15 for statistical tests), except for $\delta^{15}N$ values of cnidarians that were 5.6‰ higher on rocks transplanted from active to outer transition sites than on rocks transplanted from inner transition to outer transition sites (Kruskal-Wallis, Chi-squared = 8.725, df = 3, p-value = 0.03) and for $\delta^{15}N$ values of snails that were 0.9‰ lower on rocks transplanted from inner transition to active sites than on rocks transplanted from active to inner transition sites (Wilcox test, W = 30, p-value = 0.05). Cnidarians transplanted from active to outer transition sites showed higher $\delta^{15}N$ values by 2.6‰ than cnidarians on *in situ* rocks at outer transition collected in 2018 (Wilcox test, W = 17, p-value = 0.05), and cnidarians transplanted from inner transition to background sites showed lower $\delta^{13}C$ values by 5.9‰ than cnidarians on *in situ* rocks collected in 2017 at transition sites (Wilcox test, W = 25, p = 0.008). Limpets also changed their $\delta^{15}N$ values when transplanted from active to outer transition sites (Wilcox test, W = 38, p = 0.009), with 6.2‰ higher values than limpets on *in situ* rocks collected in 2017 at active sites. (See Appendix 6.16-6.23 for statistical tests).

Table 10: Mean ± standard error isotope composition by taxa of the macrofauna community on experimental rocks transplanted across seepage gradients for 17 months. Superscript: Pairs in which there was significant difference based on Wilcox tests (p-value < 0.05) or Dunn's test using Benjamini-Hochberg adjustment (p-value < 0.025). See Appendix 5.3-5.10 for comparison among treatments, and Appendix 6.15 for statistical tests.

	Active to Inner Transition (A-IT)		Active to Outer Transition (A-OT)		Active to Background (A-B)	
	$\delta^{13}C$ (‰)	**$\delta^{15}N$ (‰)**	**$\delta^{13}C$ (‰)**	**$\delta^{15}N$ (‰)**	**$\delta^{13}C$ (‰)**	**$\delta^{15}N$ (‰)**
Annelida	-33.8 ± 2.7	6.5 ± 1.1	-40.7 ± 4.4	5.9 ± 1.5	-46.7 ± 6.6	6.5 ± 0.9
Cnidaria	NA	NA	-25.8 ± 1.2	10.9 ± 0.9	NA	NA
Eucarida	NA	NA	-27.3	10.7	-21.0	10.43
Peracarida	-17.4 ±0.8	14.1 ± 0.1	NA	NA	-33.3	5.47
Echinodermata	-21.5	10.8	-24.4 ± 1.6	9.2 ± 1.3	NA	NA
Bivalvia	-32.9 ± 3.1	-3.4 ± 3.4	NA	NA	-35.5 ± 0.2	-6.5 ± 3.1
Gastropoda Snail	-34.2 ± 2.4	8.6 ± 1.0	NA	NA	NA	NA
Gastropoda Limpet	-52.0 ± 2.4	3.5 ± 0.6	-46.9 ± 0.1	8.9 ± 0.1	NA	NA
Other macrfofauna	-41.3 ± 11.0	8.8 ± 2.6	-47.1 ± 4.4	6.5 ± 0.6	-30.6 ± 6.2	6.4 ± 2.1
	Inner Transition to Active (IT-A)		**Inner Transition to Outer Transition (IT-OT)**		**Inner Transition to Background (IT-B)**	
	$\delta^{13}C$ (‰)	**$\delta^{15}N$ (‰)**	**$\delta^{13}C$ (‰)**	**$\delta^{15}N$ (‰)**	**$\delta^{13}C$ (‰)**	**$\delta^{15}N$ (‰)**
Annelida	-35.8 ± 1.4	7.4 ± 0.6	-36.2 ± 6.6	9.0 ± 2.1	-20.4 ± 0.7	13.2 ± 0.9
Cnidaria	-28.9	5.3	-25.6 ± 0.8	5.3 ± 0.5	-23.8 ± 0.3	10.0 ± 1.0
Eucarida	-22.8	9.1	NA	NA	NA	NA
Peracarida	NA	NA	-25.5 ± 3.2	11.9 ± 1.1	-18.0	17.6
Echinodermata	-29.7	4.0	-26.7 ± 3.2	8.9 ± 0.4	NA	NA
Gastropoda: Snail	-39.4 ± 3.7	7.7 ± 1.0	NA	NA	NA	NA
Gastropoda: Limpet	-53.0 ± 2.7	3.3 ± 0.1	NA	NA	NA	NA
Other macrofauna	-40.0 ± 3.7	7.7 ± 1.0	-31.2 ± 6.1	10.6 ± 1.1	-25.2 ± 3.3	5.8 ± 3.1

5.4 Substrate influence on communities: Substrate colonization experiment

In addition to the colonization carbonate rocks mentioned in section 5.2, cow bone and douglas fir wood parcels were deployed in different seepage regimes for 7 years (2010-2017) to test the potential for interaction between methane seeps and organic-fall based chemosynthetic ecosystems, when in close proximity. These experiments were intended to mimic whale falls and wood falls. Macrofaunal densities were not significantly different between active and transition sites for the communities developing on deployed bone (Wilcox test, W = 2, p-value = 1.00) and wood (Wilcox test, W = 15, p-value = 0.06), in contrast to observations for carbonate rock (section 5.2) (Figure 21). Although the average density on carbonate rock was higher than on wood and bone at active sites, and the density on bone was higher than on wood and rock at transition sites (Figure 21), the density values were not significantly different (Active: Kruskal-Wallis, Chi-squared = 5.4, df = 2, p-value = 0.07, Transition: Kruskal-Wallis Chi-squared = 4.0091, df = 2, p-value = 0.13), probably due to the low sample size and great variability within replicates.

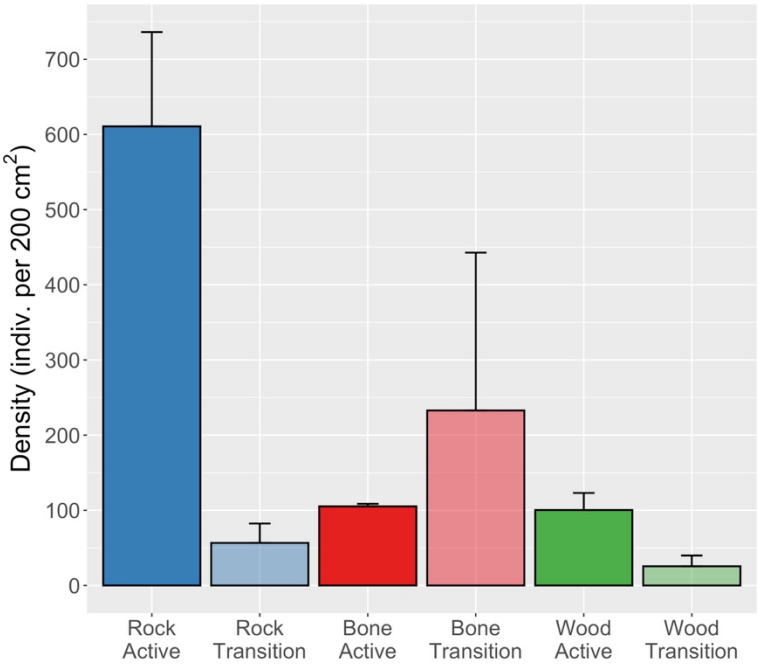

Figure 21: Average ± one standard error density (individuals per cm^2) of the macrofaunal invertebrate community on experimental carbonate rocks (blue), bones (red) and wood (green) deployed for 7 years (2010-2017) at active and transition sites at Mound 12.

Seepage activity significantly affected the assemblage composition of the colonization communities (Two-Way ANOSIM, Global R = 0.81, p-value = 0.001), but substrate type did not (Global R = 0.389, p-value = 1.00; Figures 22-23). Gastropods (snails and limpets) were the most abundant group of colonizers on substrates at active sites (78.74% on rocks, 61.33% on bones, and 81.53% on wood; Figure 22A), including mainly Provannidae, Hyalogyrinidae, Lepetodrilidae, Neolepetopsidae and Pyropeltidae (Table 7). Although the density of gastropods on rocks at active sites was more than 7 times higher than on bone and almost 5 times higher than on wood (Figure 22B), provannids, lepetodrilids, neolepetopsids and pyropeltids showed high rank abundance in all three substrates at active sites, as did anomurans, which were mainly yeti crabs (Table 7, Appendix 4.8). Annelids, mainly ampharetids, dorvilleids and hesionids, were the most abundant group at transition sites (37.89% on rock, 73.55% on bone), except on wood, where snails accounted for 42.43% and annelids, 35.14% of the total macrofauna (Figure 22A). However, there

was no agreement in rank abundances among the substrates at transition sites (Appendix 4.9). The taxa contributing to dissimilarity between colonists of active versus transition sites on all substrates combined were more abundant mainly at active sites (Provannidae = 6.22%, Anomura = 5.45%, Lepetodrilidae = 5.43%, Neolepetopsidae = 3.52%, Pyropeltidae = 3.43%, Mytilidae = 3.41%, and Ampharetidae = 3.37%), but some were more abundant at transition sites (Ophiuroidea = 5.60%, Serpulidae = 4.54%, and Hesionidae = 3.78%; SIMPER, average dissimilarity = 74.84; Appendix 3.11).

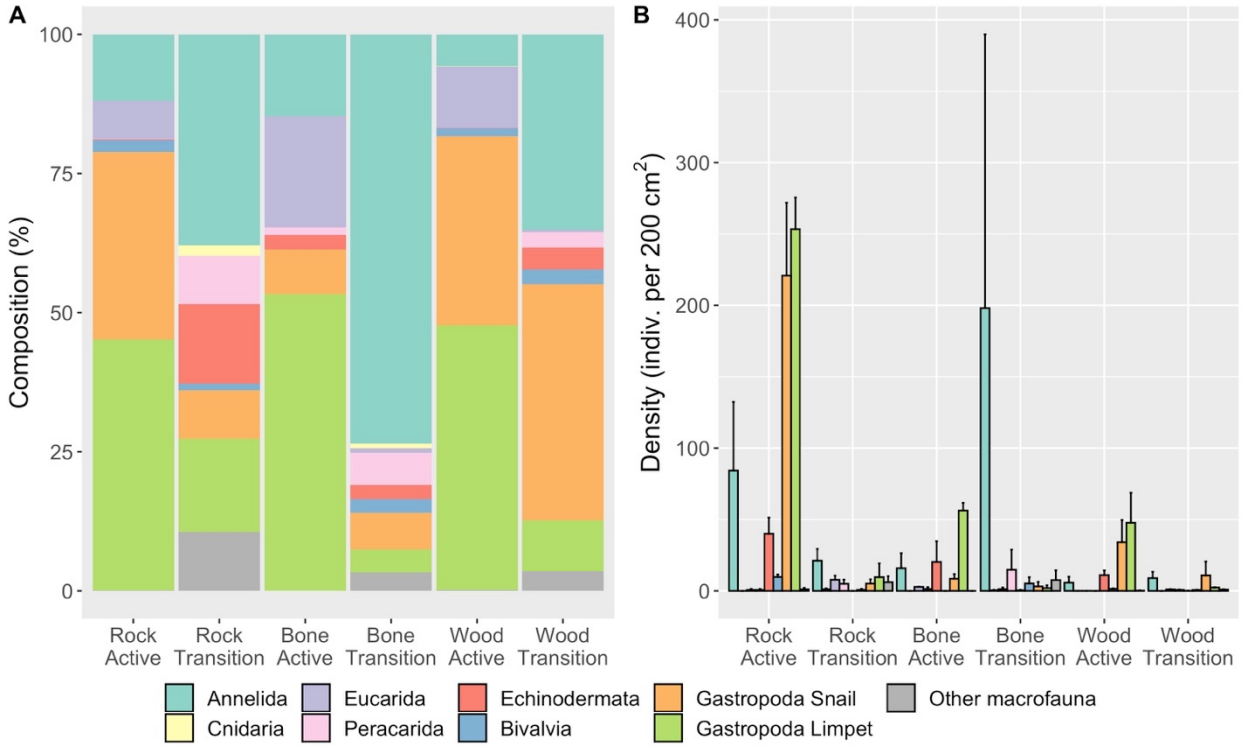

Figure 22: (A) Composition (%) and (B) average density (indiv. per 200 cm^2) of macrofaunal invertebrates on experimental carbonate rock, bone and wood deployed for 7 years (2010-2017) at active and transition sites at Mound 12.

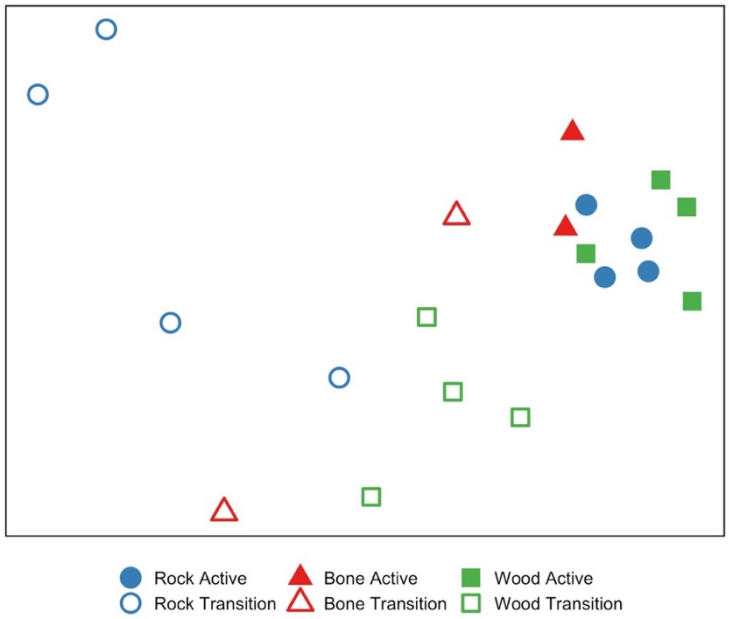

Figure 23: Multi-dimensional scaling analysis of macrofaunal invertebrate community composition on experimental carbonate rock (blue), cow bone (red) and wood (green) deployed for 7 years (2010-2017) at active and transition sites at Mound 12.

The macrofaunal community on experimental hard substrates deployed for 7 years exhibited 3.6‰ and 6.1‰ lower $\delta^{13}C$ and $\delta^{15}N$ values, respectively, at active sites than at transition sites on carbonate rocks ($\delta^{13}C$: Wilcox-test, $W = 244$, $p = 0.02$, $\delta^{15}N$: Wilcox-test, $W = 79$, $p < 0.0001$) and 8.3‰ and 4.2‰ lower $\delta^{13}C$ and $\delta^{15}N$ values, respectively, at active sites than at transition sites on wood ($\delta^{13}C$: Wilcox-test, $W = 240$, $p < 0.0001$, $\delta^{15}N$, Wilcox-test, $W = 226$, $p < 0.0001$; Figure 24). Animals on bone showed 1.8‰ higher $\delta^{15}N$ values at transition sites (Wilcox-test, $W = 41.5$, $p = 0.03$), but no difference was observed for $\delta^{13}C$ values (Wilcox-test, $W = 74$, $p = 0.68$; statistical tests in Appendix 6.3). At active sites, the community isotopic composition varied among different substrates ($\delta^{13}C$: Kruskal-Wallis, chi-squared = 11.3710, df = 2, $p = 0.003$, $\delta^{15}N$: Kruskal-Wallis, chi-squared = 6.2096, df = 2, $p = 0.04$). Animals on bones had higher $\delta^{13}C$ and $\delta^{15}N$ values than on rock ($\delta^{13}C$: Dunn's test, $z = 6.2193$, $p = 0.002$, $\delta^{15}N$: Dunn's test, $z = 2.4563$, $p = 0.007$) and wood ($\delta^{13}C$: Dunn's test, $z = 3.1359$, $p = 0.003$, $\delta^{15}N$: Dunn's test, $z = 2.1756$, $p = 0.01$), but no difference was observed between rock and wood faunal isotope

composition ($\delta^{13}C$: Dunn's test, z = -0.0165, p = 1.00, $\delta^{15}N$: Dunn's test, z = -0.3423, p = 0.37). Mean isotopic composition was not significantly different among the three substrates at transition sites ($\delta^{13}C$: Kruskal-Wallis, chi-squared = 0.7463, df = 2, p = 0.69, $\delta^{15}N$: Kruskal-Wallis, chi-squared = 1.9216, df = 2, p = 0.38).

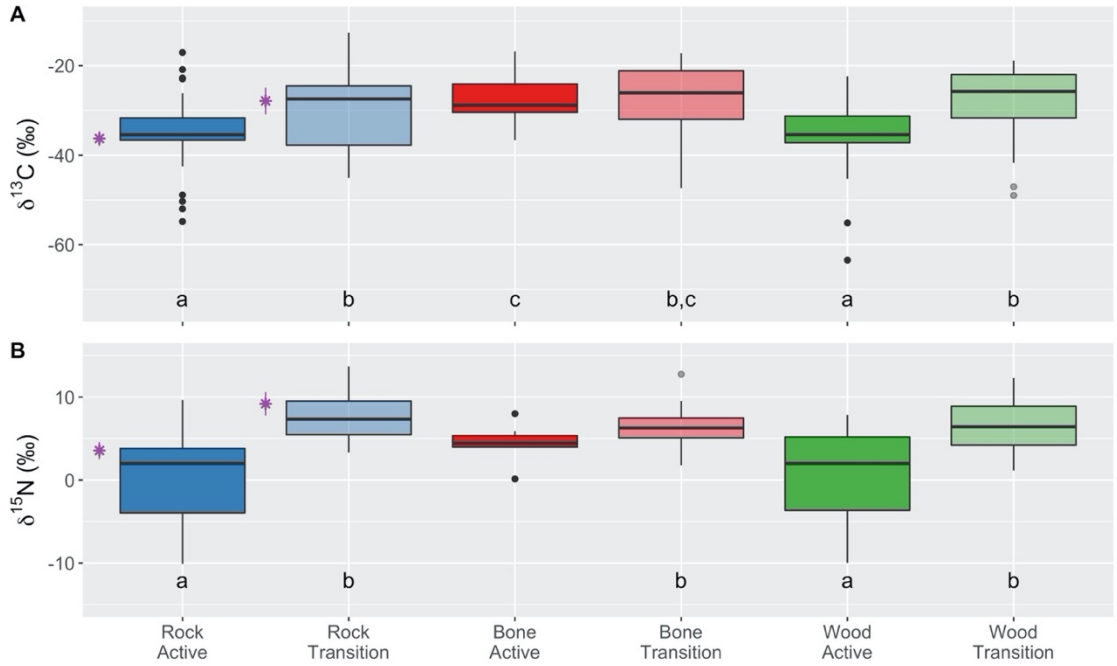

Figure 24: (A) $\delta^{13}C$ and (B) $\delta^{15}N$ values (‰) of macrofauna invertebrates colonizing experimental carbonate rocks (blue), bones (red) and wood (green) deployed for 7 years (2010-2017) at active and transition sites at Mound 12, and mean (± standard deviation) isotopic composition of macrofaunal invertebrate community on *in situ* carbonate rocks (purple) collected in 2017 at active and transition sites. Boxplots visualize five summary statistics: the median, two hinges (the 25th and 75th percentiles), and two whiskers (extend from the hinge to the largest/smallest value at 1.5x the inter-quartile range), as well as outlying points individually. See Appendix 6.3 for statistical tests.

Isotopic compositions of specific taxa were not significantly different among substrates at both active and transition sites, except for annelids that showed 2.7‰ lower $\delta^{15}N$ values on bone than on wood at transition sites (Dunn's test, z = -2.6944, p-value = 0.01; Table 8, statistical tests in Appendix 6.14-6.15).

The macrofaunal community on wood and rock at active sites exhibited greater trophic diversity than at transition sites, while the opposite trend was observed for the community on the

bones (SEAc; Table 6B, Figure 7C-E). The $\delta^{15}N$ range, possibly reflecting the heavy influence by local N fixation, was higher at actives sites for all three substrates, as was niche breadth (and CD; Table 6B). Trophic redundancy was greater at transition sites for rocks and bones, but not for wood (MNND, Table 6B). Within substrates, niche overlap between seepage activity levels was smaller for the community on carbonate rocks than for the communities on wood and bone (Figure 25A).

At active sites, animals on carbonate rock had a higher niche diversification at the base of the food web ($\delta^{13}C$ range) and number of trophic levels or variable N sources ($\delta^{15}N$ range) than those on bone and wood (Table 6B). The same pattern was observed at transition sites. Carbonate rock communities also had the greatest trophic diversity among substrates at active sites, but wood had greater diversity among substrates at transition sites. Animals on bones had lower trophic diversity than those on wood and rock (Figure 7C-E, Table 6B). Niche overlap between substrates was greater at transition sites than at active sites, except between rock and wood (Figure 25).

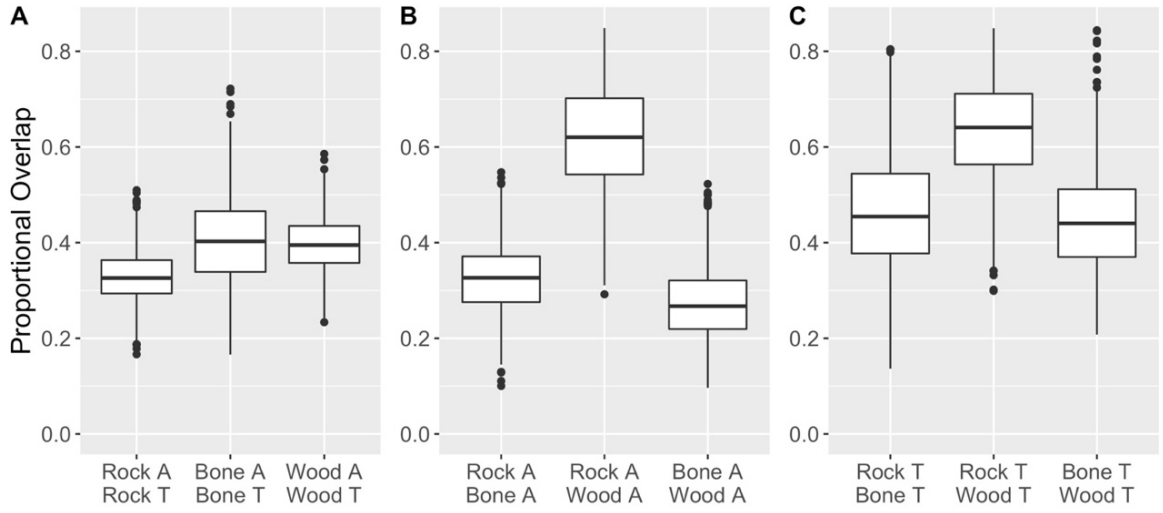

Figure 25: Proportional overlap between carbon and nitrogen isotopic niche areas of macrofaunal invertebrates on experimental carbonate rocks, bone and wood deployed at Mound 12 at active and transition sites for 7 years (2010-2017). (A) Comparisons between seepage activity within substrate, (B) Comparisons among substrates at active sites, (C) Comparisons among substrates at transition sites. A: Active site, T: Transition site. Boxplots visualize five summary statistics: the median, two hinges (the 25th and 75th percentiles), and two whiskers (extend from the hinge to the largest/smallest value at 1.5x the inter-quartile range), as well as outlying points individually.

6 DISCUSSION

6.1 Community changes along seepage gradients

Although most of the deep ocean margin is covered by sediments, methane seeps are frequently associated with carbonate rocks (Aloisi et al., 2000) formed by syntrophic aggregates of methanotrophic archaea (ANMEs) and sulfate-reducing gama-proteobacteria (SRBs; Orphan et al., 2002; Boetius et al., 2000). Marlow et al. (2014a) showed that ANMEs are capable of anaerobic methanotrophy even where seepage seems inactive (no seep megafauna present). As these rocks function as attachment, shelter, and access to food for a variety of microorganisms and fauna (Levin et al., 2015; Marlow et al., 2014a; Levin et al., 2009; Levin, 2005), they can promote an interaction between the seep community (active sites) and the surrounding deep-sea community (transition and background sites; Levin et al., 2016). In this study, active sites at Mound 12 were dominated by neolepetopsid and lepetodrilid limpets and provannid and skeneid snails, while transition sites were dominated by annelids, mainly serpulids and chrysopetalids (Table 3, Figure 4). Levin et al. (2015) reported a shift from a gastropod-dominated community on carbonate rocks at active sites to a community well represented by annelids, crustaceans, and cnidarians at inactive sites at Mound 12 about 8 years earlier. In the present study, the off-seep community at transition sites indeed seems to be intermediate between active and inactive sites, where gastropods are still well-represented as at active sites, as well as peracarid crustaceans, cnidarians and annelids, which were more abundant at inactive sites in Levin et al. (2015). The outer transition community at Mound 12, dominated by annelids, cnidarians and peracarid crustaceans is more similar to the communities at inactive sites reported in Levin et al. (2015). Based on observations of community

composition, it is clear that carbonate rocks are promoting an interaction between seep and background communities.

The typical $\delta^{13}C$ values of ANMEs production are -30‰ to -100‰ for archaeal cells and -15‰ to -70‰ for associated symbiotic SRB (House et al., 2009; Orphan et al., 2002). The influence of ANME are reflected in the carbon isotopic composition of invertebrate macrofauna on carbonate rocks at Mound 12, which differed as a function of seepage, with higher values with increasing distance from active seepage (Table 4A). Active sites also showed a higher range of food sources, potentially more trophic levels, and higher trophic diversity than transition sites in 2017 and 2018 (Table 6A), reflecting more diverse feeding modes at active sites from symbiont-bearers to bacterial grazing, filter feeding, and carnivory (Levin et al., 2015). There was no difference in isotopic composition across seepage gradients for the different macrofaunal groups (except for limpets that showed lower $\delta^{13}C$ values at active sites; Table 5). Thus, the shift to higher isotope values away from active sites is probably caused by the shift in community composition and abundance of certain groups (i.e. the higher proportion of limpets at active sites with lower $\delta^{13}C$ values could lower the average community signature). The low isotope values of animals at transition sites also indicates they are still using methane-derived carbon even at sites with lesser seepage activity, as observed before by Levin et al. (2015) and consistent with microbial studies by Case et al. (2015) and Marlow et al. (2014a). Direct consumption of the carbonate with its microbial associates may be a source of such light organic matter for animals with a radula to scrape rocks, and, as the carbonate may persist for years at lesser seepage (Levin et al., 2016), it supports the hypothesis of ecotone formation. At outer transition zones, where seepage activity is much lower, closer to background conditions, isotopic values were the highest (Table 4A) and

niche breadth was the lowest (Table 6A), indicating that there is a lower diversity of carbon sources and an increased use of photosynthetically-derived carbon away from the seep.

There was noticeable interannual variability between 2017 and 2018, with a higher abundance in 2017 of lepetodrilid and neolepetopsid limpets and anomurans (mainly the yeti crabs *Kiwa puravida*) at active sites and a higher abundance in 2017 of ophiuroids, tanaids, serpulids and hesionids at transition sites (Table 3, Appendix 2.1). Besides the community composition, in 2018, the $\delta^{13}C$ range was lower and $\delta^{15}N$ range was higher (Figure 6), suggesting a lower contribution of chemosynthetic microbial production to the trophic niche of consumers. Neolepetopsid limpets live on hard substrates or upon a variety of hosts such as bivalves and vestimentiferan tubes at hydrothermal vents (Sasaki et al., 2010), and they may feed on small invertebrates (Warén and Bouchet, 2009, 2001; Warén et al., 2006) or graze on authigenic carbonates feeding directly on bacteria on the rocks with their well-develop radula (Zapata-Hérnandez et al., 2013; Sasaki et al., 2010). The yeti crab, *Kiwa puravida*, feeds on epibiotic bacteria farmed on its chelipeds, by waving them in fluid escaping from the seafloor (Thurber et al., 2011). As both these animals feed on microorganisms that are associated with active seepage, their lower abundance in 2018 could indicate that seepage activity declined. Variations of methane concentration within 11-12 months have been reported along the continental slope of Costa Rica due to seismic activity or due to seasonal changes in tides and currents at a local scale (Mau et al., 2007). $\delta^{13}C$ values for the different taxa and for the community were still very low, typical of chemosynthesis, in 2018 and not significantly different than in 2017 (Figure 6, Table 5), suggesting: (1) Seepage activity did not change, and, instead, an increase in non-seep predators, such as fishes and lithodid crabs (megafauna observed during Alvin dives in 2018), could explain the lower abundance of carbonate macrofauna, and an exploitation of organic matter in different

stages of degradation explain the higher $\delta^{15}N$ range (Grémare et al., 1997); or (2) Tissue turnover is slow, and animals retain their isotope composition for one year after a change in seepage activity (see more on tissue turnover in section 6.3).

6.2 Colonization patterns on carbonate rocks

To test the dynamics and colonization rate of seep and non-seep communities, defaunated rocks were deployed in different seepage regime for 7 years (2010-2017). The composition of the carbonate colonizing community was not different than that of the communities on *in situ* carbonates in 2017 (Figures 10-11). Colonizers were gastropod-dominated at active sites and more diverse at transition sites with annelids, peracarid crustaceans, echinoderms and limpets being well-represented (Figure 10). The density of colonists was higher at active than transition sites, as was observed on *in situ* communities, although density was more than two times higher on colonization rocks than on *in situ* rocks at active sites (Figure 9). Provannids, neolepetopsids, lepetodrilids, pyropeltids, ampharetids and anomurans were the most abundant colonists at active sites (Table 7A), and they had similar rank abundances between colonization and *in situ* carbonates (Appendix 4.1), suggesting a mass effect (Leibold et al., 2004), where the frequent movement of nearby animals or localized dispersal allows for these groups to colonize the carbonates (Grupe, 2014). Provannid snails graze on free-living bacteria or get their nutrition from endosymbionts (Smith and Baco, 2003; MacAvoy et al., 2005; Bergquist et al., 2007), while neolepetopsids and lepetodrilids graze on bacteria or feed on small invertebrates (Zapata-Hérnandez et al., 2013; Fox et al., 2002), and ampharetids are generalist deposit feeders (Bergquist et al., 2007). Besides that, although provannids, neolepetopsids, lepetodrilids, pyropeltids, ampharetids and anomurans had

similar rank abundance on colonization rocks and *in situ* rocks (Appendix 4.1), their densities on colonization rocks (Appendix 2.2) were 3-10 times higher than on *in situ* rocks (Appendix 2.1), suggesting they are both good colonizers and great competitors. These feeding strategies might thus represent the most successful feeding modes for colonizing new substrates at active seepage, where seeping fluids allow for microbial communities to flourish on hard substrates (Marlow et al., 2014a; Metaxas and Kelly, 2010). In contrast, the high rank abundance groups on *in situ* carbonates that were absent or not as abundant on colonization rocks, such as skeneid, nuculanid, and cataegid gastropods, and nereidid polychaetes (Appendix 4.1), suggests they are poorer colonizers, either due to competition, lack of their required food or habitat, or poor dispersal ability.

At transition sites, neolepetopsid and lepetodrilid limpets, cataegid snails, serpulid and hesionid polychaetes, and amphipods showed high rank abundance on both colonization rocks and *in situ* rocks (Appendix 4.1), as well as similar densities (Appendix 2.1-2.2), again suggesting a mass effect (Leibold et al., 2004), and potential connection between transition and active sites, as the lepetodrilid limpets are usually grazers of bacteria (Zapata-Hérnandez et al., 2013; Fox et al., 2002) and are more commonly found associated with active seepage. Chrysopetalid polychaetes and provannid snails showed high rank abundance on *in situ* rocks, although they were absent on colonization rocks (Appendix 4.1), suggesting that they are not rapid colonizers at transition sites or were predated.

Mean $\delta^{13}C$ and $\delta^{15}N$ values of the community on colonization rocks at Mound 12 were lower at active sites than at transition sites (Table 4B); the same pattern was observed for the *in situ* carbonate community, which can be explained by the different community composition, as isotopic compositions were not significantly different within taxa (except for annelids) between

seepage activity (Figure 12). Although mean isotope values were not different between colonization rocks and *in situ* rocks, isotope-based trophic diversity and niche breadth were greater on *in situ* rocks than on colonization rocks at both active and transition sites (Table 6, Figure 7A,C). Because the isotopic composition is generated by microbial food, this suggests that the microbial community might not have reached its normal diversity and structure in 7 years, and macrofaunal dietary niche is reduced on the experimental rocks. Because of that, it is possible that animals shift their dietary resources when colonizing a new substrate, which would be reflected on their isotopic composition. For instance, although the isotopic composition of limpets was not significantly different between colonization rocks and *in situ* rocks, they showed higher values on colonization rocks (closer to -20‰; Table 8A), suggesting they are not getting as much of their carbon resource from grazing chemosynthetic bacteria, but from photosynthetically-produced carbon instead. This potential lack of microbial diversity could also explain the absence of Provannidae at transition sites on colonization rocks, as these are grazer snails that potentially did not find their food on the colonization rocks at transition sites, although they showed high rank abundance on *in situ* rocks at transition sites (Appendix 4.1) and, thus, availability of larva should not be an impediment for their colonization.

A previous colonization experiment at methane seeps in Costa Rica for 10.5 months revealed that early successional stages did not have the same trophic structure and community richness, as established communities on *in situ* rocks (Grupe, 2014). Our results show that, within 7 years, the community recovers most of its composition and trophic structure, especially at active sites, although some species-specific trophic niches might still not be fully recovered (e.g. annelids that showed lower $\delta^{15}N$ values on colonization rocks than on *in situ* rocks at active sites; Table 8A, Appendix 5.2). Grupe (2014) observed a dominance in gastropods that could be functioning

as top-down grazers on hard substrates that limit microbial growth. Gastropods were still the dominant groups on colonization rocks after 7 years, with greater densities on colonization rocks than on nearby *in situ* rocks at active and transition sites (Figure 10). This suggest that they are not only successful early colonizers, but they are also able to persist to later successional stages even at transition sites, where they can shift their feeding mode to diets with lesser chemosynthetic content due to lesser seepage activity.

6.3 Community persistence under changing seepage gradients

Carbonate rocks from Mound 12 were transplanted to different seepage condition for 17 months (2017-2018) to better understand the role of seepage in determining the rates and trajectory of community response and persistence as well as trophic patterns (Figure 26). Based on community composition, the communities on carbonate that were transplanted from active sites to inner transition, outer transition or background did not remain as "active communities" (Figure 16). Levin et al. (2017) observed the same pattern on a 13-months transplant experiment at Hydrate Ridge, Oregon, where the transplanted rocks took on the dominant species and rank abundance patterns of their new sites. However, the surviving animals transplanted from active sites to sites with lesser seepage activity in Costa Rica (this study) retained their low $\delta^{13}C$ values characteristic of active seepage but acquired higher $\delta^{15}N$ values (Figures 18-19, 26). It is possible that these results reflect a more rapid turnover of nitrogen than carbon in animal tissues. Although transplant isotopic composition was not significantly different within taxonomic groups among the different treatments with the exception of snails and cnidarians $\delta^{15}N$ values (Table 10), there are interesting patterns that will be discussed below.

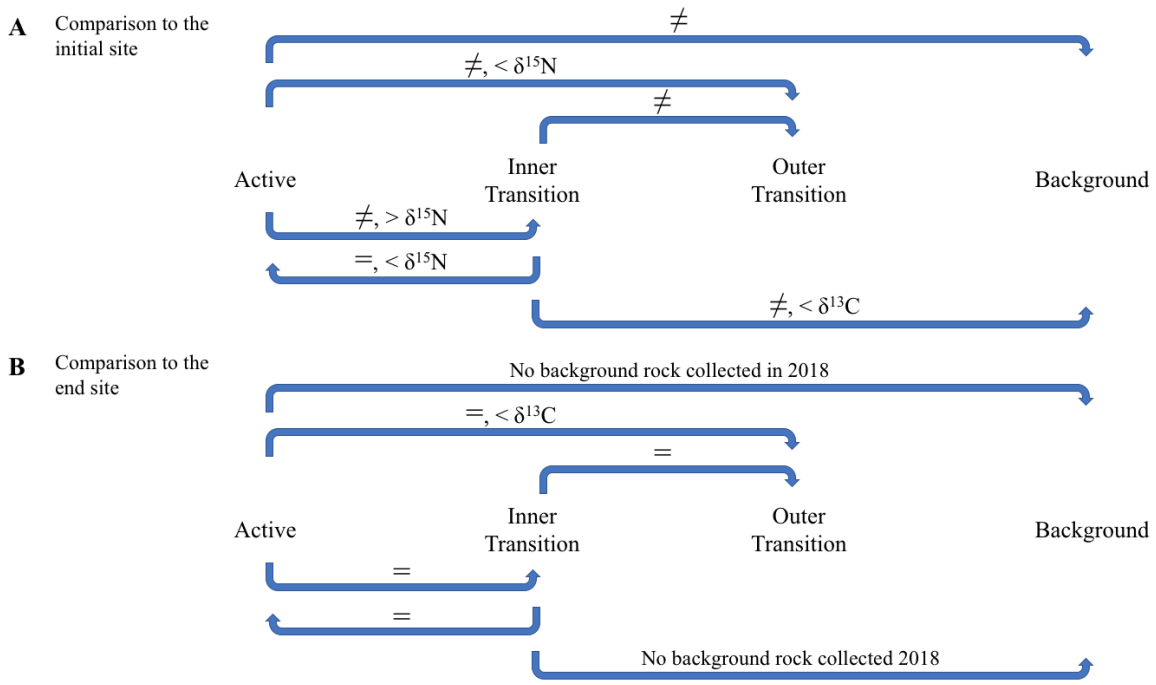

Figure 26: Comparison of community composition (equal and different signs) and stable isotope values (only significantly different pairs are shown) on experimental rocks transplanted across seepage gradient for 17 months (2017-2018) to the communities on *in situ* carbonate rocks collected in 2017 at the initial site (A) and to the communities on *in situ* carbonate rocks collected in 2018 at the end site of the experiment (B) based on ANOSIM analyses for the community data and Wilcox tests for the isotope data.

Although our colonization experiment showed that chrysopetalids, commonly found at transition sites, were not good colonizers of defaunated carbonate rocks at transition sites (Appendix 4.1), they colonized and were amongst the highest ranked abundance on the transplanted carbonates from active sites to lesser seepage activity (Appendix 4.2, 4.3 and 4.6). Chrysopetalids are known to be carnivores or scavengers (Boggeman, 2009) and some might feed on bacterial mats, as observed by Wiklund et al. (2009) around whale falls. Their high abundance may then reflect that transition groups are taking advantage of the transplanted rocks as a food source; perhaps they scavenge some of the active groups that died after being transplanted to lesser seepage (Levin et al, 2017).

Peracarid crustaceans, mainly amphipods and tanaids, were also among the groups with highest rank abundance on the rocks transplanted from active sites to areas with lesser seepage

(Appendix 4.2, 4.3 and 4.6). These crustaceans are usually detritivorous, feeding on phytodetritus (Wurzberg et al., 2011), and are probably not using the rocks as a chemosynthetic food source based on their high isotope values. Peracarid crustaceans provide parental care for their growing offspring after they have left the brood pouch of the female, and, in shallow water, extended parental care is usually seen in tube/burrow-dwelling species (Thiel, 1999; Thiel et al., 1996). Peracarids could then be using old bores in carbonates made by gastropods as reproduction sites to care for their juveniles. Indeed, many adult isopods with juveniles and gravid females were found on the transplanted rocks (Appendix 2.3). Other transition groups such as hydroids and selected annelid families that are not commonly found associated with seepage (Lumbrineridae, Goniadidae, and Cossuridae) colonized the transplanted rocks at lower densities than peracarids (Appendix 2.3). While these annelids are usually burrowers and tubicolous with high motility (Jumars et al., 2015), cossurids are usually deposit feeders (Kędra et al., 2012). Low $\delta^{13}C$ values from a hydrothermal vent in Costa Rica suggest cossurids feed on methanotrophic organic matter (Levin et al., 2012), and Lumbrineridae and Goniadidae are carnivorous or deposit feeders (Jumars et al., 2015, Levin et al., 2015; McLeod et al., 2010; Levin et al., 1999). Thus, they could either be using the carbonates for feeding on dead animals, or as attachment sites.

Seep species such as provannid snails and neolepetopsid limpets are commonly microbial grazers, and it is expected that their response to a transplant to areas with lesser seepage reflects the response of microbes (Levin et al., 2017). Case et al. (2015) observed 30% lower microbial operational taxonomic unit richness (OTU) on rocks transplanted from active to inactive sites at Hydrate Ridge, Oregon, and some new OTUs were acquired. In our transplants from active sites to sites with lesser seepage, most provannids seemed not to survive the transplant to sites with lesser seepage (Appendix 4.2, 4.3 and 4.6). Levin et al. (2017) observed the same pattern and

hypothesized that the lack of *Provanna laevis* (Provannidae) on transplanted rocks from active to inactive sites suggests that they specialize on epsilonproteobacteria that is linked to high fluid flux.

In contrast, neolepetopsids and ampharetids persisted in high rank abundances on our transplanted rocks (Appendix 4.2, 4.3 and 4.6). As mentioned before, neolepetopsid limpets are usually grazers (Zapata-Hérnandez et al., 2013) or they may feed on small invertebrates (Warén and Bouchet, 2001, 2009; Warén et al., 2006). $\delta^{13}C$ values of limpets did not differ on transplanted rocks from *in situ* values, but $\delta^{15}N$ values were higher on rocks transplanted from active to outer transition sites than on *in situ* rocks at active sites (Appendix 5.10). This suggests that limpets could be potentially feeding on the remaining bacteria on the rocks, retaining low $\delta^{13}C$ values, as well as feeding on the small invertebrates that colonized the rock at transition sites, getting higher $\delta^{15}N$ values. Alternatively, the turnover rates of carbon and nitrogen may differ, with the non-seep signature being acquired more quickly for nitrogen than carbon.

Other seep species were also found still alive on some of the transplanted rocks from active sites to sites with lesser seepage activity, such as *Laminatubus* sp. (Serpulidae), *Archinome levinae* (Amphinomidae), *Parougia* sp. (Dorvilleidae), and *Bathymodiolus* sp. (Mytilidae). Only *Bathymodiolus* sp. is known to have symbiotic bacteria (Duperron et al., 2005), although work by Goffredi et al. (in press) suggests that *Laminatubus* sp. farms methanotrophic bacteria in its tentacular crown. For instance, the extremely low $\delta^{15}N$ values of bivalves (mainly Mytilidae) on *in situ* carbonates at active sites (Appendix 5.1) and on transplanted rocks from active sites to inner transition and background sites (Appendix 5.3), suggests that the symbiotic bacteria and, thus, the bivalve are able to persist through a transplant to less seepage activity. Methanotrophic symbioses are limited to environments where there are reducing methane-rich fluids (Petersen & Dubilier, 2009). The persistence of the symbiotic relationship at background sites indicates the possible

presence of methane in the waters, and suggests that influence of the seep can extend further than thought before, reaching sites where no *in situ* carbonate rocks were found. However, mytilid mussels retain a fully formed digestive system and can also feed on phytoplankton-based detritus (Riekenberg et al., 2016) in the form of particulate organic matter (POC). The average POC values at Mound 12 were $\delta^{13}C$ = -25.1‰, $\delta^{15}N$ = 7.34‰ during this study. A slow tissue turnover rate, reported for *Bathymodiolus childressi* as being longer than 1 year (Dattagupta et al., 2004), would bias against seeing a shift in isotopic composition in the transplanted mussels.

The communities that were transplanted from transition sites to outer transition (IT-OT) or background (IT-B) changed their composition and were more similar to communities with lesser seepage activity (Figures 16D, 26). Although there were many groups present on the transplanted rocks that were absent on *in situ* transition and outer transition rocks (e.g. isopods, paraonids, ampharetids, nereidids, and anemones), the high rank abundance and densities of Chrysopetalidae, Hydroidolina and Amphipoda on the transplanted rocks explains this closer similarity to outer transition and background communities than to transition communities (Appendix 4.5). However, mean $\delta^{13}C$ values did not change after transplanting and animals retained low values (Figures 18,26), suggesting that the community was still being supported by chemosynthetic production away from active seepage. As mentioned before, chrysopetalids are carnivores or scavengers (Boggeman, 2009), and they could be feeding on animals that did not survive the transplant to lesser seepage (Levin et al., 2017), which also could explain the higher $\delta^{15}N$ values of the communities on the transplanted rocks from transition sites to outer transition and background sites (Figure 18).

Carbonates transplanted from transition to active sites (IT-A) showed the highest faunal abundance of all transplant treatments (Figure 14). This pattern was also observed by Levin et al.

(2017) at Hydrate Ridge, Oregon. The transplanted community in Costa Rica (this study) retained some of their transition species, especially chrysopetalids, peracarid crustaceans and hydroids, but active seep species were also able to colonize the rocks, and both adults and juveniles of *Archinome levinae* (Amphinomidae), *Provanna laevis* (Provannidae), *Paralepetopsis* sp. (Neolepetopsidae), and *Neolepetopsis* sp. (Neolepetopsidae) were found in high densities on the transplanted rocks (Appendix 2.3). The rapid colonization of these grazers and their slightly lower $\delta^{15}N$ values (Table 10, Figure 26) than of animals on *in situ* rocks at active sites (Table 5) suggest a rapid establishment and growth of a diverse microbial community that provides their food. This is contrast to what was observed with our colonization experiment, where our might suggest that the microbial community did not fully recover in 7 years. In previous studies at Hydrate Ridge, bacterial colonization on carbonates transplanted from inactive to active sites for 13 months was observed in high abundance (Case et al., 2015), allowing for the colonization of provannids (Levin et al., 2017). It was expected that active seepage would create an environment toxic to transition species. However, the presence of such species, especially chrysopetalids, peracarid crustaceans, and hydroids on transplanted rocks from inner transition to active sites suggest that, instead, they can persist under active seepage.

An exception to this was seen with the serpulid worms, mainly *Laminatubus* sp., that showed high rank abundance at transition sites but were not as abundant on the transplanted rocks moved from inner transition to active sites (Appendix 4.4). Previous studies have reported high densities of serpulid aggregations at active sites at Jaco Scar, a hydrothermal seep on the Costa Rica margin (Levin et al., 2012) and massive deposits of fossil serpulid tubes exhibiting various states of authigenic carbonate mineralization related to seepage productivity are reported in Santa Monica Basin (Georgieva et al., 2019). In addition, fossil serpulid tubes from seep deposits in the

Greenland Sea have been reported attached to seep inhabitants such as Mytilidae mussels and Vesicomyidae clams (Vinn et al., 2013, 2014) or be filled by seep carbonate, indicating active seepage after the death of the serpulids (Vinn et al., 2014). Although tube morphology does not show specific adaptations to seep environments (Vinn et al., 2013), the worm itself might farm methanotrophic bacteria as mentioned above (Goffredi et al., in press), allowing serpulids to dominate sites of intense methane seepage. However, in our transplant experiments, serpulids were not as successful when moved to sites with higher seepage activity, possibly due to increased competition for space with gastropods, which are great colonizers as observed in our colonization experiment.

6.4 Interaction of seeps with other chemosynthetic ecosystems

The macrofaunal invertebrate community colonizing experimentally deployed substrates showed similar composition and trophic structure on carbonate rock, wood, and bone deployed for 7 years. The communities on all substrates attained the same level of dissimilarities between active and transition sites observed on *in situ* rocks, with higher carbon and nitrogen stable isotope values at transition sites (Figure 24) and higher abundance of seep species at active sites (Table 7).

At active sites, lepetodrilids, provannids, anomurans (mainly yeti crabs), and neolepetopsids showed high rank abundance on all three substrates (Appendix 4.8), suggesting mass effects (Leibold et al., 2004). Macroinvertebrate communities colonizing transition sites were more dissimilar in composition among substrate types than at active sites (Figure 23), and the lack of correlation between rank abundances of the different substrates (Appendix 4.9) suggest emigration/immigration dynamics (Leibold et al., 2004). At transition sites, the community

composition on wood and bone may not be influenced by seepage activity and is more similar to natural wood- and whale-fall community composition, which rely on decay of the organic substrates.

Grupe (2014) noted a lack of wood-boring taxa on wood deployed for 10.5 months at active and transition sites at Mound 12, and hypothesized that, as succession proceeds, wood and whale-specialists would arrive and cause even more divergence. Gaudron et al. (2010) observed high densities of wood-boring bivalves (*Xylophaga atlantica* and *Xyloredo ingolfa*) in a 1-year colonization experiment at seeps in the North Atlantic. However, in our 7-year experiment, the bone-eating annelid *Osedax*, endemic of whale-falls, was still not found on the bones at transition sites, and only one *Xylophaga* sp. individual was found on one wood piece at transition sites. However, the wood blocks at transition sites were completely burrowed, indicating the presence of *Xylophaga* at earlier successional stages. The burrow presence did not cause major divergence among communities on different substrates. The lack of bone and wood specialist species and of vesicomyid clams such as *Idas* sp, which harbor sulphur-oxidizing symbionts, suggest the end of a sulphophilic stage (Gaudron et al., 2010). The sulphophilic stage in whale- and wood-falls can last for 5-6.8 years, with an apparent colonization of background species (Bernardino et al., 2012). Indeed, seep groups such as neolepetopsids, lepetodrilids, and provannids colonized both wood and bone at transition sites in our 7-year experiment (Appendix 4.9). Although trophic diversity was greater on carbonate rocks than on wood and bone at both active and transition sites (Table 6B, Figure 7C-E), trophic niche overlap was greater among substrates at transition sites (Table 6B), and mean carbon and nitrogen isotopic values were not significantly different among substrates at both active and transition sites (Figure 24).

These observations could indicate that at later successional stages the substrates are used mainly for attachment rather than as food sources and support the idea that hard substrates can function as dispersal stepping stones for chemosynthetic fauna. The ability to colonize and reproduce on different substrates increases the likelihood of a larva finding a settlement site (Vrijenhoek, 2010), and wood (wood falls) and bones (whale-falls) can create ephemeral chemosynthetic habitats that attract a species-rich assemblage with a range of trophic niches, functioning as stepping stones for vent and seep species (Alfaro-Lucas et al., 2018; Kiel, 2016; Smith et al., 2015; Smith et al., 2014; Baco & Smith, 2003). Bernardino et al. (2010) also showed potential habitat heterogeneity of sediment macrofauna created by whale and wood-falls colonized by seep species. This heterogeneity can be exploited by both opportunists and endemic fauna, as observed in this study, sustaining the persistence and evolution of chemosynthesis-dependent species (Bernardino et al., 2010).

7 CONCLUSION

Methane seeps have proven to be common along much of the northeastern Pacific margin (Baumberger et al., 2018) as well as on other margins (Skarker et al., 2014). Understanding the contributions of seep ecosystems to continental margin biodiversity and ecosystem dynamics and functioning advances fundamental science as well as our ability to manage these systems. I analyzed composition, density, diversity and trophic structure of invertebrates on carbonate rocks at a methane seep site off the coast of Coast Rica, Mound 12, along natural seepage gradients, among colonizers of newly placed rocks, and on transplanted rocks to test the overarching hypothesis that seepage activity plays a major role in defining the community composition and

trophic structure, and to identify the relevant time and space scales of community response. The main findings were:

1. Based on community composition and trophic structure, carbonate rocks are promoting an interaction between seep and background communities, forming ecotones where seep and background species coexist.
2. Direct consumption of the microbes on the carbonate itself may be a source of isotopically light ($\delta^{13}C$ and $\delta^{15}N$) organic matter to macrofauna at sites with lesser seepage activity. As the carbonate may persist for years at lesser seepage, they maintain the interaction between seep and the surrounding deep-sea ecosystem.
3. Composition of the macrofauna community on carbonate rocks changed within one year (2017-2018), with a lower abundance of species that feed on chemosynthetic microorganisms associated with active seepage, which could indicate seepage cessation. However, mean $\delta^{13}C$ values were still very low, reflecting chemosynthetic nutritional sources. Thus, there are two possibilities: (1) a higher abundance of non-seep predators and opportunists such as fishes and lithodid crabs could explain the decline of such seep species between; or (2) there was a natural variability in seepage activity due to seismic activity, and macrofauna tissue turnover is slow.
4. The macrofaunal community colonizing bare carbonate rocks recovers most of its composition and trophic structure within 7 years, especially at active sites, although some species-specific trophic niches might still not be fully recovered, potentially due to lack of microbial diversity, as trophic diversity and niche breath were greater on *in situ* rocks than on colonization rocks.
5. Provannids, neolepetopsids, lepetodrilids, pyropeltids, ampharetids and anomurans were the most successful colonizers at active sites, and neolepetopsid and lepetodrilid limpets, serpulid and hesionid polychaetes, amphipods, and cataegid snails, were the most successful colonizers

at seepage transition sites. In both cases, the high abundance of these groups on *in situ* rocks suggest a mass effect, where the frequent movement of nearby animals or localized dispersal allows for these groups to colonize the carbonates.

6. The successful groups of colonizers are mainly grazers on free-living bacteria, get their nutrition from endosymbionts or feed on small invertebrates, and when at lesser seepage they can adapt and shift their diets. Among those, gastropods are not only successful early colonizers but they are also able to persist in high densities at later successional stages even at transition sites, where they can accommodate their diets to sites with lesser chemosynthetic microbial diversity.
7. Skeneid snails, nuculanid bivalves, cataegid snails, and nereidids were the poorest colonizers at active sites, while chrysopetalids and provannids were the poorest colonizers at transition sites, either due to competition or lack of their required food or habitat.
8. The response of seep species to a change in seepage activity when they were transplanted from active sites to sites with lesser seepage, either by adapting their diets or by retaining their symbiotic bacteria, indicates a potential persistence through seepage cessation. The colonization of transition species on these carbonates supports the idea that carbonate rocks promote an interaction between seep and background communities even after seepage cessation.
9. The methane-derived isotopic composition of communities on rocks transplanted from transition to outer transition and background sites indicate that the communities at transition and background sites are still being sustained by chemosynthetic production.
10. The rapid response of grazers on carbonates transplanted from transition sites to active sites indicates a rapid establishment of the chemosynthetic bacterial community and diversity within

17 months. The presence of transition species on these rocks indicate that active seepage is not as toxic for them as hypothesized. Instead, perhaps these species are just not as successful under active seepage as seep endemic species.

11. Seepage activity plays a major role in defining macrofaunal community composition and its trophic structure on different types of hard substrate. However, the presence of seep species on wood and bone deployed for 7 years at both active and transition sites, and the similarity in trophic structure among the communities on different substrates, suggest a potential use of hard substrates of other ephemeral chemosynthetic ecosystems (wood-falls and whale-falls) as attachment, functioning as stepping stones for vent and seep fauna.
12. The multiexperimental design used here allows us to better understand the dynamics of macrofaunal communities on carbonate rocks at methane seeps and their influence on background communities at large spatial and temporal scales. Although the colonization experiment showed that 7 years was not enough for the community to fully recover its composition and trophic diversity, the transplant experiment showed the capacity of the macrofaunal community to persist and adapt to changes in seepage activity within 17 months. Overall, the seep and surrounding assemblages exhibit responses indicative of considerable resilience to variation in seepage. I hypothesize that the key aspect differentiating these experiments is the establishment and recovery of the microbial community and diversity on rocks that sustain the macrofaunal community. While the colonization experiment was performed with defaunated carbonates, the transplant experiment was performed with carbonates hosting microbes and animals. Microbial diversity might take longer than 7 years to develop, but once it is established, the macrofaunal community can recover quickly and persist even under declining seepage. This observation is crucial to predict community

responses to disturbances either in seepage activity or through anthropogenic activity. As human activities such as bottom fishing, or oil and mineral extractions increase on continental margins (Van Dover et al., 2012), if such interferences deeply impact the microbial community on both active seepage and within the sphere of influence of methane seeps, the response of the macrofaunal community will be affected. Such information can aid spatial planning for deep-sea biodiversity maintenance and the designation of protected areas.

APPENDIX

Appendix 1: Terminology

Site	Seep location, Mound 12
Seepage activity	Also referred to as seepage zone or habitat
Active	Defined visually by the presence of microbial mats, methane bubbles or seep megafauna (bathymodiolin mussels, vesicomyd clams, and/or siboglinid tube worms)
Transition	Areas with moderate seepage activity where seep species interact with background species (ecotones)
Inner Transition	Areas with moderate seepage activity where seep species interact with background species (ecotones) with a higher influence from the seep.
Outer Transition	Areas with moderate seepage activity where seep species interact with background species (ecotones) with a higher influence from the background deep sea.
Background	Non-seepage activity
In situ rocks	Unmanipulated, non-experimental carbonate rocks in any zone
Colonization rocks	Experimental defaunated rocks deployed in different seepage zones for 7 years (deployed in January 2010 and recovered in October 2017) or 17 months (from June 2017 to October 2018)
Transplant rocks	Experimental carbonate rocks moved to different seepage zones with exposure for 17 months (deployed in June 2017 and recovered in October 2018). For example, for the transplant treatment active to inner transition (A-IT), experimental carbonate rocks were moved from an active site in 2017 to an inner transition site, from where they were recovered in 2018.

APPENDIX 2: Average densities of invertebrate macrofauna on hard substrates across seepage gradients at Mound 12 collected in 2017 and 2018.

Appendix 2.1: Average densities (number per 200 cm^2) of invertebrate macrofaunal on *in situ* carbonate rocks collected across seepage gradients at Mound 12 in 2017 and 2018.

***In situ* carbonate rocks**					
Cruise	**2017**	**2017**	**2018**	**2018**	**2018**
Seepage activity	**Active**	**Transition**	**Active**	**Inner Transition**	**Outer Transition**
Surface Area (cm^2)	**237.56**	**290.70**	**102.11**	**224.10**	**187.71**
Oligochaeta	NA	NA	NA	0.1 ± 0.3	NA
Serpulidae	2.1 ± 3.2	11.6 ± 22.2	1.3 ± 1.8	1.8 ± 2.2	NA
Polynoidae	0.9 ± 2.0	0.5 ± 0.5	1.0 ± 1.8	1.3 ± 2.0	NA
Hesionidae	1.1 ± 1.4	2.5 ± 4.4	2.9 ± 4.7	1.0 ± 1.1	1.6 ± 2.3
Amphinomidae	0.8 ± 0.8	0.2 ± 0.4	1.8 ± 1.9	2.8 ± 2.9	NA
Ampharetidae	5.2 ± 10.8	NA	0.9 ± 2.1	1.4 ± 3.2	NA
Sabellidae	0.2 ± 0.5	NA	0.2 ± 0.6	0.4 ± 0.6	NA
Dorvilleidae	NA	0.4 ± 0.9	1.8 ± 2.2	0.3 ± 0.6	0.4 ± 0.6
Lumbrineridae	NA	NA	NA	0.4 ± 0.8	NA
Phyllodocidae	1.4 ± 3.1	0.9 ± 0.8	0.9 ± 2.1	0.5 ± 0.8	0.8 ± 1.2
Chrysopetalidae	0.3 ± 0.4	6.0 ± 8.4	1.7 ± 3.5	34.3 ± 46.9	7.8 ± 4.1
Cirratulidae	0.7 ± 1.6	NA	0.2 ± 0.6	0.8 ± 1.0	NA
Trichobranchidae	NA	0.2 ± 0.4	NA	NA	NA
Paraonidae	NA	NA	0.3 ± 0.7	0.1 ± 0.3	NA
Lacydoniidae	1.2 ± 1.9	0.7 ± 1.5	3.7 ± 5.7	1.6 ± 1.7	NA
Maldanidae	NA	0.7 ± 0.8	1.3 ± 1.8	3.6 ± 4.6	2.3 ± 3.2
Flabelligeridae	NA	0.3 ± 0.4	NA	1.1 ± 1.4	0.4 ± 0.6
Syllidae	0.1 ± 0.3	1.2 ± 1.8	0.2 ± 0.6	4.6 ± 3.4	0.8 ± 1.2
Spionidae	NA	0.2 ± 0.4	0.7 ± 1.2	0.5 ± 0.8	NA
Pisionidae	NA	0.2 ± 0.4	NA	NA	NA
Nereididae	2.4 ± 5.5	NA	0.6 ± 1.4	0.3 ± 0.8	NA
Capitellidae	NA	NA	NA	2.3 ± 4.2	0.4 ± 0.6
Pilargiidae	NA	NA	NA	0.1 ± 0.3	NA
Terebellidae	0.3 ± 0.5	NA	1.4 ± 2.2	0.6 ± 0.7	NA
Onuphidae	NA	NA	0.4 ± 0.9	NA	0.4 ± 0.6
Eunicidae	0.2 ± 0.5	NA	0.5 ± 1.2	NA	NA
Actiniaria	1.4 ± 3.1	NA	NA	0.1 ± 0.3	NA
Hydroidolina	NA	2.9 ± 2.5	NA	1.5 ± 1.7	7.7 ± 6.3
Alcyonacea	NA	0.4 ± 0.5	NA	NA	NA
Trombidiformes	NA	0.7 ± 0.8	1.4 ± 2.8	7.1 ± 9.6	0.8 ± 1.1
Amphipoda	NA	4.2 ± 6.4	0.1 ± 0.3	4.1 ± 8.6	3.7 ± 5.2

Appendix 2.1 continued.

***In situ* carbonate rocks**					
Cruise	**2017**	**2017**	**2018**	**2018**	**2018**
Seepage activity	**Active**	**Transition**	**Active**	**Inner Transition**	**Outer Transition**
Surface Area (cm^2)	**237.56**	**290.70**	**102.11**	**224.10**	**187.71**
Anomura	4.0 ± 5.0	0.7 ± 1.5	NA	NA	NA
Brachyura	0.1 ± 0.3	NA	NA	NA	0.4 ± 0.6
Cumacea	NA	NA	NA	0.1 ± 0.3	NA
Isopoda	NA	NA	NA	0.2 ± 0.6	NA
Tanaidacea	NA	0.9 ± 0.8	2.9 ± 4.8	1.2 ± 2.0	NA
Ostracoda	NA	NA	0.3 ± 0.7	0.3 ± 0.4	1.2 ± 0.4
Caridea	NA	0.2 ± 0.4	NA	NA	NA
Ophiuroidea	0.3 ± 0.6	2.0 ± 4.0	1.5 ± 2.7	0.5 ± 0.8	NA
Holothuroidea	0.1 ± 0.3	NA	NA	NA	NA
Aplacophora	NA	NA	0.6 ± 1.4	0.1 ± 0.3	0.8 ± 1.1
Nuculanidae	3.5 ± 4.6	NA	0.4 ± 0.9	NA	NA
Cuspidariidae	NA	NA	NA	0.3 ± 0.8	NA
Mytilidae	0.3 ± 0.5	NA	NA	NA	NA
Pyramidellidae	NA	NA	NA	0.2 ± 0.3	NA
Seguenziidae	NA	0.2 ± 0.4	NA	0.1 ± 0.3	NA
Skeneidae	11.1 ± 22.6	1.3 ± 2.5	0.5 ± 1.2	NA	NA
Cataegidae	3.5 ± 3.9	2.1 ± 2.9	4.9 ± 9.5	1.4 ± 1.5	NA
Hyalogyniridae	0.9 ± 1.4	NA	NA	0.1 ± 0.3	NA
Provannidae	71.8 ± 82.2	4.2 ± 7.3	2.0 ± 1.0	0.6 ± 1.0	NA
Lepetodrilidae	42.3 ± 41.2	4.5 ± 4.5	NA	0.1 ± 0.3	NA
Neolepetopsidae	73.7 ± 68.3	7.1 ± 12.7	1.8 ± 2.0	0.3 ± 0.4	NA
Pyropeltidae	8.6 ± 11.2	NA	0.6 ± 1.1	NA	NA
Polyplacophora	NA	0.9 ± 1.5	1.6 ± 3.5	1.0 ± 1.2	0.8 ± 1.1
Nemertea	NA	NA	NA	0.1 ± 0.3	NA

Appendix 2.2: Average densities (number per 200 cm^2) of invertebrate macrofauna on experimental carbonate rock, bone and wood deployed at active and transition sites for 7 years (2010-2017) at Mound 12.

Colonization experiment						
Substrate	**Carbonate Rock**	**Carbonate Rock**	**Bone**	**Bone**	**Wood**	**Wood**
Habitat	**Active**	**Transition**	**Active**	**Transition**	**Active**	**Transition**
Surface area (cm^2)	**187.60**	**156.95**	**71.41**	**147.97**	**1,047.06**	**1,047.06**
Siboglinidae	3.8 ± 6.7	NA	NA	NA	0.5 ± 1.0	NA
Serpulidae	0.5 ± 0.9	4.9 ± 2.5	NA	10.0 ± 13.0	0.1 ± 0.1	0.1 ± 0.3
Polynoidae	NA	NA	NA	NA	0.3 ± 0.6	0.1 ± 0.2
Hesionidae	7.7 ± 12.7	2.2 ± 2.5	1.5 ± 2.1	65.0 ± 91.9	0.4 ± 0.7	4.7 ± 6.3
Amphinomidae	0.7 ± 1.2	1.1 ± 2.1	NA	1.6 ± 2.2	0.1 ± 0.1	0.7 ± 0.6
Ampharetidae	55.6 ± 66.0	NA	5.9 ± 8.3	22.0 ± 30.1	0.9 ± 0.8	0.1 ± 0.1
Sabellidae	NA	1.0 ± 1.4	NA	0.4 ± 0.5	NA	0.2 ± 0.5
Dorvilleidae	4.0 ± 5.0	0.4 ± 0.7	5.7 ± 4.3	28.9 ± 40.8	3.3 ± 6.3	1.2 ± 1.7
Lumbrineridae	NA	0.4 ± 0.7	NA	NA	NA	NA
Phyllodocidae	8.5 ± 14.7	2.5 ± 3.4	NA	19.2 ± 27.2	NA	0.1 ± 0.3
Chrysopetalidae	0.3 ± 0.5	NA	NA	NA	NA	0.2 ± 0.2
Cirratulidae	NA	1.0 ± 1.4	2.8 ± 0.2	NA	NA	0.1 ± 0.2
Trichobranchidae	NA	0.4 ± 0.7	NA	0.4 ± 0.5	NA	NA
Lacydoniidae	0.3 ± 0.6	1.8 ± 2.7	NA	21.6 ± 30.6	0.1 ± 0.1	0.4 ± 0.7
Maldanidae	0.3 ± 0.5	NA	NA	2.4 ± 3.4	NA	0.1 ± 0.2
Flabelligeridae	1.1 ± 1.8	1.4 ± 2.0	NA	NA	NA	0.2 ± 0.3
Syllidae	NA	1.8 ± 2.8	NA	7.2 ± 10.2	NA	NA
Nereididae	NA	0.4 ± 0.7	NA	2.4 ± 3.4	NA	NA
Capitellidae	NA	NA	NA	12.0 ± 17.0	NA	NA
Pilargiidae	NA	0.4 ± 0.7	NA	NA	NA	NA
Terebellidae	1.4 ± 1.6	NA	NA	4.8 ± 6.8	0.1 ± 0.1	0.1 ± 0.1
Onuphidae	NA	1.5 ± 3.0	NA	NA	NA	NA
Eunicidae	NA	NA	NA	NA	NA	0.1 ± 0.1
Sigalionidae	NA	NA	NA	NA	0.1 ± 0.1	NA
Opheliidae	NA	NA	NA	NA	NA	0.1 ± 0.1
Nephtyidae	NA	NA	NA	NA	NA	0.1 ± 0.1
Actiniaria	NA	0.4 ± 0.7	NA	NA	0.1 ± 0.1	NA
Hydroidolina	NA	0.4 ± 0.7	NA	0.4 ± 0.5	NA	NA
Alcyonacea	NA	0.4 ± 0.7	NA	NA	NA	NA
Trombidiformes	NA	1.1 ± 2.2	NA	NA	NA	0.1 ± 0.1
Amphipoda	0.7 ± 1.2	3.6 ± 4.3	1.3 ± 1.9	2.4 ± 3.4	NA	0.6 ± 0.5
Anomura	40.0 ± 19.6	NA	20.3 ± 20.5	0.4 ± 0.5	10.9 ± 6.4	0.1 ± 0.1

Brachyura	NA	NA	NA	NA	NA	0.1 ± 0.1

Appendix 2.2 continued.

Colonization experiment						
Substrate	**Carbonate Rock**	**Carbonate Rock**	**Bone**	**Bone**	**Wood**	**Wood**
Habitat	**Active**	**Transition**	**Active**	**Transition**	**Active**	**Transition**
Surface area (cm^2)	**187.60**	**156.95**	**71.41**	**147.97**	**1,047.06**	**1,047.06**
Isopoda	NA	0.3 ± 0.5	NA	NA	NA	NA
Tanaidacea	NA	1.1 ± 2.1	NA	12.4 ± 16.5	NA	0.1 ± 0.2
Ostracoda	NA	1.4 ± 2.9	NA	NA	NA	0.1 ± 0.1
Caridea	NA	NA	NA	NA	0.1 ± 0.2	NA
Asteroidea	NA	NA	NA	NA	NA	0.1 ± 0.1
Ophiuroidea	0.7 ± 1.2	7.8 ± 5.7	2.8 ± 0.2	1.2 ± 1.7	0.1 ± 0.1	0.9 ± 0.5
Aplacophora	NA	2.9 ± 5.7	NA	7.2 ± 10.2	0.2 ± 0.4	0.2 ± 0.4
Nuculanidae	0.5 ± 0.9	0.7 ± 1.4	NA	NA	0.2 ± 0.5	0.1 ± 0.1
Juvenile	0.8 ± 1.4	NA	NA	4.8 ± 6.8	NA	0.1 ± 0.2
Xylophagaidae	NA	NA	NA	NA	NA	0.1 ± 0.2
Mytilidae	8.4 ± 0.6	NA	NA	NA	1.2 ± 0.8	NA
Teredinidae	NA	NA	NA	NA	NA	0.3 ± 0.2
Vesicomyidae	NA	NA	NA	0.4 ± 0.5	NA	NA
Pyramidellidae	NA	0.4 ± 0.7	NA	NA	NA	NA
Skeneidae	NA	0.7 ± 1.5	NA	NA	13.2 ± 26.4	0.5 ± 0.9
Cataegidae	0.7 ± 1.2	2.7 ± 3.0	NA	0.8 ± 1.1	0.2 ± 0.3	0.5 ± 0.9
Hyalogyniridae	39.9 ± 52.1	1.4 ± 2.0	1.5 ± 2.1	0.4 ± 0.5	0.6 ± 0.8	0.1 ± 0.2
Provannidae	180.3 ± 48.8	NA	7.1 ± 2.4	12.0 ± 2.8	20.1 ± 6.7	9.6 ± 18.8
Lepetodrilidae	170.8 ± 58.0	2.5 ± 5.0	40.5 ± 3.3	0.8 ± 1.1	39.3 ± 34.2	1.0 ± 0.3
Cocculinidae	NA	NA	NA	NA	0.1 ± 0.1	0.1 ± 0.1
Neolepetopsidae	62.8 ± 28.7	6.8 ± 13.6	7.3 ± 10.4	0.4 ± 0.5	4.9 ± 5.4	1.0 ± 0.8
Pyropeltidae	19.8 ± 13.2	0.4 ± 0.7	8.4 ± 0.5	0.8 ± 1.1	3.4 ± 3.1	0.2 ± 0.4
Polyplacophora	1.1 ± 1.8	0.4 ± 0.7	NA	0.4 ± 0.5	NA	0.3 ± 0.4
Nemertea	NA	0.3 ± 0.5	NA	NA	NA	0.1 ± 0.1
Platyhelminthes	NA	NA	NA	NA	NA	0.1 ± 0.1

Appendix 2.3: Average densities (number per 200 cm^2) of invertebrate macrofauna on experimental rocks transplanted across seepage gradient for 17 months. Rocks were transplanted from: active to inner transition (A-IT), active to outer transition (A-OT), inner transition to active (IT-A), inner transition to outer transition (IT-OT), active to background (A-B), and inner transition to background (IT-B).

Transplant experiment with carbonate rocks						
Treatment	**A-IT**	**A-OT**	**IT-A**	**IT-OT**	**A-B**	**IT-B**
Surface area (cm^2)	**265.74**	**227.29**	**281.89**	**193.40**	**381.30**	**242.51**
Siboglinidae	NA	0.3 ± 0.3	NA	NA	0.8 ± 1.5	NA
Serpulidae	0.6 ± 0.6	0.3 ± 0.6	0.2 ± 0.4	0.1 ± 0.2	0.3 ± 0.4	NA
Polynoidae	0.2 ± 0.4	3.5 ± 2.8	0.4 ± 0.6	1.1 ± 1.9	0.3 ± 0.8	0.6 ± 0.8
Hesionidae	0.9 ± 1.0	0.9 ± 1.0	4.3 ± 3.4	0.9 ± 0.9	1.7 ± 1.7	0.5 ± 1.0
Amphinomidae	1.2 ± 1.2	1.2 ± 1.8	1.7 ± 1.4	1.1 ± 1.4	1.7 ± 1.6	2.5 ± 3.8
Ampharetidae	2.2 ± 3.7	0.3 ± 0.3	1.0 ± 0.8	0.1 ± 0.2	3.5 ± 6.7	0.4 ± 1.0
Sabellidae	NA	NA	0.2 ± 0.3	NA	NA	NA
Dorvilleidae	0.5 ± 1.0	0.5 ± 0.8	0.4 ± 0.5	0.2 ± 0.5	0.2 ± 0.4	NA
Lumbrineridae	0.2 ± 0.4	0.9 ± 1.7	NA	0.3 ± 0.6	0.3 ± 0.6	0.2 ± 0.5
Phyllodocidae	1.9 ± 0.8	0.1 ± 0.2	0.5 ± 0.6	0.6 ± 0.9	4.1 ± 7.1	2.7 ± 4.2
Chrysopetalidae	9.0 ± 5.2	5.5 ± 6.6	19.1 ± 19.0	7.6 ± 7.8	0.2 ± 0.2	8.2 ± 7.5
Cirratulidae	0.2 ± 0.4	NA	0.3 ± 0.6	0.9 ± 1.3	1.8 ± 1.8	1.3 ± 1.0
Trichobranchidae	0.1 ± 0.2	NA	NA	NA	NA	NA
Paraonidae	0.1 ± 0.3	0.2 ± 0.5	NA	1.1 ± 1.8	0.4 ± 0.6	0.9 ± 1.1
Lacydoniidae	0.8 ± 0.8	0.2 ± 0.3	3.5 ± 3.5	NA	NA	NA
Maldanidae	NA	NA	0.3 ± 0.6		0.1 ± 0.3	NA
Flabelligeridae	0.1 ± 0.3	1.4 ± 1.6	NA	0.1 ± 0.2	0.3 ± 0.4	0.2 ± 0.5
Syllidae	1.06 ± 1.4	0.1 ± 0.2	1.8 ± 2.2	NA	0.2 ± 0.4	0.1 ± 0.3
Spionidae	NA	0.1 ± 0.2	0.2 ± 0.2	NA	0.1 ± 0.2	NA
Cossuridae	NA	NA	NA	NA	0.2 ± 0.4	0.1 ± 0.2
Pisionidae	NA	NA	NA	0.2 ± 0.5	NA	NA
Nereididae	0.2 ± 0.4	2.3 ± 1.4	0.1 ± 0.3	0.7 ± 0.7	1.3 ± 0.8	0.2 ± 0.5
Capitellidae	NA	0.2 ± 0.5	0.2 ± 0.4	0.1 ± 0.2	0.4 ± 0.4	0.1 ± 0.2
Terebellidae	0.2 ± 0.4	NA	1.3 ± 1.9	NA	NA	0.2 ± 0.5
Onuphidae	NA	NA	NA	NA	NA	0.1 ± 0.2
Eunicidae	NA	NA	NA	0.2 ± 0.5	0.1± 0.2	0.1 ± 0.3
Chaetopteridae	NA	NA	NA	NA	0.2 ± 0.3	NA
Arenicolidae	NA	NA	NA	NA	0.4 ± 0.6	NA
Goniadidae	NA	NA	NA	NA	0.2 ± 0.4	NA
Iphitimidae	NA	NA	NA	NA	NA	0.2 ± 0.4
Nephtyidae	NA	0.2 ± 0.3	NA	0.4 ± 0.8	NA	NA
Actiniaria	NA	1.7 ± 1.5	0.5 ± 0.7	1.4 ± 2.3	0.7 ± 0.6	0.4 ± 1.0

Appendix 2.3 continued.

Transplant experiment with carbonate rocks						
Treatment	**A-IT**	**A-OT**	**IT-A**	**IT-OT**	**A-B**	**IT-B**
Surface area (cm^2)	**265.74**	**227.29**	**281.89**	**193.40**	**381.30**	**242.51**
Hydroidolina	NA	2.0 ± 2.4	1.3 ± 2.7	1.3 ± 0.9	0.1 ± 0.2	2.6 ± 1.9
Alcyonacea	NA	NA	0.6 ± 1.3	NA	NA	0.6 ± 1.2
Trombidiformes	2.2 ± 2.6	NA	1.7 ± 2.7	0.4 ± 0.8	NA	0.3 ± 0.4
Amphipoda	1.8 ± 2.2	12.0 ± 12.4	1.4 ± 1.9	1.9 ± 1.2	2.8 ± 1.8	0.3 ± 0.7
Anomura	0.2 ± 0.4	NA	NA	NA	0.1 ± 0.2	NA
Brachyura	NA	NA	0.4 ± 0.9	NA	NA	NA
Isopoda	0.9 ± 1.0	0.3 ± 0.6	0.1 ± 0.2	9.1 ± 14.5	0.4 ± 0.4	0.6 ± 1.0
Tanaidacea	1.8 ± 1.3	0.4 ± 0.9	3.2 ± 3.5	0.8 ± 0.8	0.1 ± 0.1	0.9 ± 0.9
Ostracoda	1.5 ± 3.0	NA	0.1 ± 0.2	1.1 ± 2.5	0.3 ± 0.3	0.2 ± 0.4
Caridea	0.1 ± 0.2	NA	1.0 ± 0.8	0.4 ± 0.8	NA	NA
Sessilia	NA	NA	NA	NA	0.6 ± 0.9	0.2 ± 0.4
Mysidacea	NA	1.3 ± 1.7	NA	NA	NA	NA
Ophiuroidea	0.1 ± 0.3	0.3 ± 0.6	1.1 ± 1.3	0.9 ± 1.2	0.2 ± 0.3	0.4 ± 0.6
Holothuroidea	NA	0.2 ± 0.3	NA	NA	NA	NA
Aplacophora	0.3 ± 0.7	NA	0.2 ± 0.3	0.4 ± 0.8	NA	1.1 ± 1.2
Nuculanidae	0.1 ± 0.3	NA	0.9 ± 0.9	NA	1.2 ± 0.6	0.6 ± 0.8
Mytilidae	1.3 ± 3.0	NA	2.7 ± 4.4	NA	1.5 ± 1.4	NA
Solemyidae	0.1 ± 0.3	NA	0.1 ± 0.2	NA	NA	NA
Pyramidellidae	NA	0.2 ± 0.3	NA	NA	NA	0.2 ± 0.5
Skeneidae	NA	NA	0.3 ± 0.8	NA	0.6 ± 1.3	NA
Cataegidae	1.8 ± 1.6	0.3 ± 0.3	2.9 ± 1.6	NA	NA	NA
Hyalogyniridae	0.2 ± 0.5	0.1 ± 0.2	0.6 ± 1.3	0.5 ± 0.7	NA	NA
Provannidae	0.6 ± 1.0	NA	11.2 ± 16.7	0.9 ± 0.8	0.3 ± 0.6	NA
Lepetodrilidae	0.1 ± 0.2	NA	5.2 ± 6.8	NA	0.2 ± 0.3	0.2 ± 0.5
Cocculinidae	0.1 ± 0.3	NA	0.4 ± 0.9	NA	0.1 ± 0.2	NA
Neolepetopsidae	7.9 ± 14.9	1.1 ± 1.5	71.9 ± 112.7	NA	1.1 ± 0.8	0.3 ± 0.5
Pyropeltidae	NA	NA	0.7 ± 1.0	NA	NA	NA
Polyplacophora	1.5 ± 1.9	0.6 ± 0.8	1.1 ± 1.2	1.2 ± 2.5	0.4 ± 0.5	0.1 ± 0.3
Nemertea	0.2 ± 0.4	0.2 ± 0.3	0.1 ± 0.2	0.6 ± 0.6	0.2 ± 0.4	0.1 ± 0.2
Pycnogonida	NA	0.3 ± 0.6	NA	NA	NA	NA

APPENDIX 3: Results of SIMPER analyses based on community composition of macrofaunal invertebrates on hard substrates across seepage gradients at Mound 12 collected in 2017 and 2018.

Appendix 3.1: Taxa contributing most to dissimilarity among macrofaunal invertebrates on *in situ* carbonate rocks collected at Mound 12 in 2017 and 2018. Displayed are the average taxa dissimilarity (Av.Diss), standard deviation of taxa average dissimilarity (Diss/SD), taxon percent contribution to total dissimilarity (Contrib.%), and cumulative contribution to total dissimilarity (Cum.%), based on SIMPER analysis (Primer7).

Groups 2017 and 2018				
Average dissimilarity = 67.82				
Species	**Av.Diss**	**Diss/SD**	**Contrib.%**	**Cum.%**
Lepetodrilidae	4.67	2.14	6.93	6.93
Neolepetopsidae	2.83	1.13	4.21	11.15
Cataegidae	2.83	1.44	4.20	15.35
Ophiuroidea	2.63	1.05	3.91	19.25
Anomura	2.59	1.61	3.85	23.11
Serpulidae	2.55	1.24	3.79	26.90
Hesionidae	2.51	1.29	3.72	30.62
Pyropeltidae	2.49	1.16	3.69	34.31
Tanaidacea	2.46	0.96	3.66	37.98
Amphinomidae	2.45	1.26	3.64	41.61
Maldanidae	2.42	1.02	3.60	45.21
Lacydoniidae	2.34	1.10	3.48	48.69
Dorvilleidae	2.25	0.93	3.34	52.03
Ampharetidae	1.99	1.01	2.95	54.98
Terebellidae	1.93	1.32	2.87	57.86
Provannidae	1.90	1.36	2.82	60.67
Polyplacophora	1.83	0.82	2.71	63.38
Nuculanidae	1.77	0.92	2.63	66.02
Polynoidae	1.73	1.03	2.56	68.58

Appendix 3.2: Taxa contributing most to dissimilarity among macrofaunal invertebrates on *in situ* carbonate rocks collected at active and transition sites at Mound 12 in 2017. Displayed are the average taxa dissimilarity (Av.Diss), standard deviation of taxa average dissimilarity (Diss/SD), taxon percent contribution to total dissimilarity (Contrib.%), and cumulative contribution to total dissimilarity (Cum.%), based on SIMPER analysis (Primer7).

Groups 2017 Transition and 2017 Active				
Average dissimilarity = 68.12				
Species	**Av.Diss**	**Diss/SD**	**Contrib.%**	**Cum.%**
Amphipoda	3.36	2.82	4.93	4.93
Neolepetopsidae	2.89	1.37	4.24	9.18
Tanaidacea	2.84	1.61	4.17	13.35
Ophiuroidea	2.80	0.91	4.10	17.45
Serpulidae	2.65	1.23	3.89	21.35
Provannidae	2.54	1.26	3.72	25.07
Chrysopetalidae	2.51	1.12	3.69	28.76
Cataegidae	2.42	1.31	3.55	32.31
Hydroidolina	2.29	1.15	3.36	35.67
Anomura	2.25	1.47	3.31	38.98
Lepetodrilidae	2.24	1.08	3.28	42.26
Hesionidae	2.17	1.38	3.19	45.45
Flabelligeridae	1.97	1.16	2.89	48.34
Maldanidae	1.95	1.16	2.87	51.20
Pyropeltidae	1.93	1.07	2.83	54.03
Ampharetidae	1.89	1.04	2.77	56.80
Polyplacophora	1.87	0.94	2.75	59.55
Phyllodocidae	1.71	1.19	2.51	62.06
Skeneidae	1.64	0.80	2.40	64.46
Amphinomidae	1.63	1.12	2.40	66.86
Lacydoniidae	1.63	1.06	2.40	69.26

Appendix 3.3: Taxa contributing most to dissimilarity among macrofaunal invertebrates on *in situ* carbonate rocks collected at active and inner transition sites at Mound 12 in 2018. Displayed are the average taxa dissimilarity (Av.Diss), standard deviation of taxa average dissimilarity (Diss/SD), taxon percent contribution to total dissimilarity (Contrib.%), and cumulative contribution to total dissimilarity (Cum.%), based on SIMPER analysis (Primer7).

Groups 2018 Active and 2018 Inner Transition				
Average dissimilarity = 68.45				
Species	**Av.Diss**	**Diss/SD**	**Contrib.%**	**Cum.%**
Chrysopetalidae	4.60	1.82	6.72	6.72
Provannidae	3.07	1.86	4.48	11.20
Trombidiformes	3.00	1.42	4.38	15.58
Syllidae	2.91	1.49	4.26	19.84
Cataegidae	2.52	1.45	3.68	23.51
Neolepetopsidae	2.40	1.25	3.50	27.01
Hesionidae	2.29	1.31	3.35	30.36
Lacydoniidae	2.27	1.45	3.31	33.67
Maldanidae	2.26	1.22	3.30	36.98
Tanaidacea	2.23	1.29	3.26	40.23
Serpulidae	2.15	1.22	3.14	43.37
Flabelligeridae	2.13	1.72	3.11	46.48
Ophiuroidea	2.06	1.16	3.01	49.49
Polyplacophora	2.06	1.20	3.01	52.50
Dorvilleidae	2.00	0.97	2.92	55.42
Amphinomidae	1.99	1.19	2.91	58.33
Polynoidae	1.92	1.13	2.80	61.13
Cirratulidae	1.80	1.15	2.63	63.76
Spionidae	1.79	0.96	2.62	66.38
Hydroidolina	1.77	1.17	2.59	68.97

Appendix 3.4: Taxa contributing most to dissimilarity among macrofaunal invertebrates on *in situ* carbonate rocks collected at inner transition and outer transition sites at Mound 12 in 2018. Displayed are the average taxa dissimilarity (Av.Diss), standard deviation of taxa average dissimilarity (Diss/SD), taxon percent contribution to total dissimilarity (Contrib.%), and cumulative contribution to total dissimilarity (Cum.%), based on SIMPER analysis (Primer7).

Groups 2018 Inner transition and 2018 Outer transition				
Average dissimilarity = 63.79				
Species	**Av.Diss**	**Diss/SD**	**Contrib.%**	**Cum.%**
Hydroidolina	3.66	1.56	5.73	5.73
Amphipoda	2.83	1.07	4.44	10.17
Amphinomidae	2.75	1.60	4.31	14.47
Lacydoniidae	2.61	1.63	4.09	18.56
Ostracoda	2.52	1.64	3.96	22.52
Maldanidae	2.40	1.17	3.77	26.29
Syllidae	2.39	1.05	3.74	30.03
Hesionidae	2.27	1.33	3.56	33.60
Trombidiformes	2.27	1.24	3.55	37.15
Serpulidae	2.13	1.10	3.34	40.49
Aplacophora	2.00	1.01	3.13	43.62
Capitellidae	1.94	0.99	3.03	46.65
Cirratulidae	1.92	1.13	3.01	49.67
Polynoidae	1.92	1.02	3.01	52.68
Polyplacophora	1.90	1.15	2.97	55.65
Tanaidacea	1.88	1.01	2.94	58.59
Cataegidae	1.87	1.09	2.93	61.52
Phyllodocidae	1.86	1.13	2.92	64.45

Appendix 3.5: Taxa contributing most to dissimilarity among macrofaunal invertebrates on experimental carbonate rocks deployed for 7 years (2010-2017) at active and transition sites at Mound 12. Displayed are the average taxa dissimilarity (Av.Diss), standard deviation of taxa average dissimilarity (Diss/SD), taxon percent contribution to total dissimilarity (Contrib.%), and cumulative contribution to total dissimilarity (Cum.%), based on SIMPER analysis (Primer7).

Groups Rock Colonization Active and Rock Colonization Transition				
Average dissimilarity = 72.38				
Species	**Av.Diss**	**Diss/SD**	**Contrib.%**	**Cum.%**
Provannidae	3.63	1.33	5.01	5.01
Ophiuroidea	3.56	1.10	4.92	9.93
Serpulidae	3.46	1.19	4.78	14.71
Neolepetopsidae	3.27	1.41	4.52	19.23
Lepetodrilidae	3.24	1.10	4.47	23.70
Amphipoda	2.98	2.05	4.12	27.82
Anomura	2.87	1.59	3.96	31.78
Pyropeltidae	2.30	1.17	3.18	34.96
Tanaidacea	2.28	1.20	3.15	38.11
Cataegidae	2.28	1.32	3.15	41.26
Ampharetidae	2.25	1.10	3.11	44.37
Hesionidae	2.14	1.36	2.96	47.34
Phyllodocidae	1.98	1.13	2.74	50.07
Chrysopetalidae	1.96	0.90	2.70	52.78
Hydroidolina	1.85	0.95	2.56	55.33
Flabelligeridae	1.84	1.14	2.54	57.88
Dorvilleidae	1.62	0.94	2.24	60.12
Polyplacophora	1.62	0.87	2.24	62.36
Lacydoniidae	1.61	1.08	2.22	64.59
Mytilidae	1.58	1.05	2.18	66.77
Maldanidae	1.54	0.94	2.13	68.90
Amphinomidae	1.51	1.03	2.08	70.98
Terebellidae	1.49	1.11	2.06	73.04

Appendix 3.6: Taxa contributing most to dissimilarity among macrofaunal invertebrates on experimental carbonate rocks transplanted from active to inner transition sites (A-IT) at Mound 12 for 17 months (2017-2018) and on *in situ* carbonate rocks collected at active sites in 2017. Displayed are the average taxa dissimilarity (Av.Diss), standard deviation of taxa average dissimilarity (Diss/SD), taxon percent contribution to total dissimilarity (Contrib.%), and cumulative contribution to total dissimilarity (Cum.%), based on SIMPER analysis (Primer7).

Groups 2017 Active and A-IT				
Average dissimilarity = 74.22				
Species	**Av.Diss**	**Diss/SD**	**Contrib.%**	**Cum.%**
Provannidae	4.56	1.33	6.14	6.14
Lepetodrilidae	4.20	1.41	5.66	11.80
Mytilidae	4.06	0.89	5.47	17.26
Chrysopetalidae	4.02	2.12	5.42	22.69
Neolepetopsidae	3.68	1.10	4.96	27.65
Phyllodocidae	2.73	1.41	3.68	31.33
Ampharetidae	2.56	1.03	3.45	34.78
Anomura	2.51	1.30	3.39	38.16
Tanaidacea	2.31	1.30	3.11	41.27
Serpulidae	2.23	1.05	3.01	44.28
Cataegidae	2.23	1.16	3.01	47.29
Hesionidae	2.23	1.11	3.00	50.29
Pyropeltidae	2.12	0.94	2.86	53.15
Polyplacophora	2.06	0.98	2.78	55.93
Trombidiformes	2.02	0.95	2.72	58.65
Amphinomidae	1.98	1.14	2.66	61.31
Amphipoda	1.91	0.98	2.57	63.88
Terebellidae	1.85	1.15	2.49	66.37
Ophiuroidea	1.80	0.68	2.42	68.79
Isopoda	1.74	0.99	2.35	71.14
Syllidae	1.72	1.06	2.32	73.46
Nuculanidae	1.69	0.91	2.27	75.73

Appendix 3.7: Taxa contributing most to dissimilarity among macrofaunal invertebrates on experimental carbonate rocks transplanted from active to outer transition sites (A-OT) at Mound 12 for 17 months (2017-2018) and on *in situ* carbonate rocks collected at active sites in 2017. Displayed are the average taxa dissimilarity (Av.Diss), standard deviation of taxa average dissimilarity (Diss/SD), taxon percent contribution to total dissimilarity (Contrib.%), and cumulative contribution to total dissimilarity (Cum.%), based on SIMPER analysis (Primer7).

Groups 2017 Active and A-OT				
Average dissimilarity = 80.19				
Species	**Av.Diss**	**Diss/SD**	**Contrib.%**	**Cum.%**
Provannidae	4.57	1.98	5.70	5.70
Amphipoda	4.35	1.72	5.42	11.12
Lepetodrilidae	4.20	2.13	5.24	16.36
Neolepetopsidae	3.52	1.41	4.39	20.75
Nereididae	3.45	2.11	4.30	25.05
Chrysopetalidae	3.00	1.53	3.74	28.79
Polynoidae	2.94	1.73	3.67	32.46
Actiniaria	2.90	1.49	3.62	36.08
Anomura	2.34	1.60	2.92	39.00
Amphinomidae	2.28	1.43	2.85	41.85
Flabelligeridae	2.17	1.07	2.70	44.55
Hesionidae	2.15	1.33	2.68	47.23
Polyplacophora	2.13	1.11	2.65	49.89
Serpulidae	1.97	1.14	2.45	52.34
Mysidacea	1.96	0.80	2.45	54.79
Dorvilleidae	1.93	1.08	2.40	57.19
Pyropeltidae	1.83	1.00	2.28	59.47
Cataegidae	1.76	1.20	2.19	61.67
Ampharetidae	1.73	1.09	2.16	63.82
Hydroidolina	1.71	0.78	2.14	65.96
Ophiuroidea	1.62	0.74	2.02	67.98
Lumbrineridae	1.60	0.70	1.99	69.97
Terebellidae	1.54	1.17	1.92	71.89
Siboglinidae	1.45	1.19	1.80	73.69
Nuculanidae	1.33	0.82	1.66	75.34
Skeneidae	1.29	0.65	1.61	76.96
Isopoda	1.29	0.86	1.61	78.57
Phyllodocidae	1.29	0.89	1.61	80.18
Tanaidacea	1.18	0.59	1.47	81.64

Appendix 3.8: Taxa contributing most to dissimilarity among macrofaunal invertebrates on experimental carbonate rocks transplanted from inner transition to outer transition sites (IT-OT) at Mound 12 for 17 months (2017-2018) and on *in situ* carbonate rocks collected at transition sites in 2017. Displayed are the average taxa dissimilarity (Av.Diss), standard deviation of taxa average dissimilarity (Diss/SD), taxon percent contribution to total dissimilarity (Contrib.%), and cumulative contribution to total dissimilarity (Cum.%), based on SIMPER analysis (Primer7).

Groups 2017 Transition and IT-OT				
Average dissimilarity = 68.85				
Species	**Av.Diss**	**Diss/SD**	**Contrib.%**	**Cum.%**
Isopoda	3.95	1.58	5.73	5.73
Chrysopetalidae	3.08	1.38	4.48	10.21
Lepetodrilidae	3.07	1.79	4.45	14.66
Ophiuroidea	2.72	1.16	3.96	18.62
Neolepetopsidae	2.68	1.15	3.89	22.51
Provannidae	2.32	1.34	3.38	25.89
Serpulidae	2.19	0.85	3.18	29.07
Hydroidolina	2.16	1.17	3.13	32.20
Nereididae	2.15	1.18	3.12	35.32
Cataegidae	2.12	0.79	3.07	38.40
Polyplacophora	2.08	1.05	3.02	41.42
Hesionidae	2.01	1.22	2.92	44.33
Tanaidacea	1.97	1.16	2.86	47.19
Amphinomidae	1.96	1.14	2.85	50.04
Maldanidae	1.94	1.11	2.82	52.85
Flabelligeridae	1.89	1.14	2.74	55.59
Polynoidae	1.83	1.19	2.66	58.26
Actiniaria	1.78	0.75	2.58	60.84
Phyllodocidae	1.72	1.18	2.50	63.34
Paraonidae	1.70	0.76	2.47	65.81
Amphipoda	1.61	1.31	2.34	68.15
Dorvilleidae	1.61	0.89	2.34	70.49

Appendix 3.9: Taxa contributing most to dissimilarity among macrofaunal invertebrates on experimental carbonate rocks transplanted from active to background sites (A-B) at Mound 12 for 17 months (2017-2018) and on *in situ* carbonate rocks collected at active sites in 2017. Displayed are the average taxa dissimilarity (Av.Diss), standard deviation of taxa average dissimilarity (Diss/SD), taxon percent contribution to total dissimilarity (Contrib.%), and cumulative contribution to total dissimilarity (Cum.%), based on SIMPER analysis (Primer7).

Groups 2017 Active and A-B				
Average dissimilarity = 72.50				
Species	**Av.Diss**	**Diss/SD**	**Contrib.%**	**Cum.%**
Provannidae	3.67	1.69	5.06	5.06
Amphipoda	3.38	1.72	4.67	9.72
Lepetodrilidae	3.09	1.58	4.26	13.98
Phyllodocidae	3.02	2.08	4.17	18.15
Nereididae	2.70	1.54	3.72	21.87
Cirratulidae	2.62	1.54	3.61	25.49
Actiniaria	2.34	1.70	3.23	28.71
Mytilidae	2.27	1.33	3.14	31.85
Nuculanidae	2.25	1.65	3.10	34.95
Neolepetopsidae	2.15	1.10	2.96	37.91
Hesionidae	2.08	1.33	2.88	40.79
Amphinomidae	2.07	1.32	2.86	43.65
Ampharetidae	2.07	1.29	2.85	46.50
Anomura	1.98	1.45	2.74	49.24
Serpulidae	1.87	1.22	2.58	51.81
Capitellidae	1.86	1.19	2.56	54.37
Cataegidae	1.75	1.16	2.42	56.79
Polyplacophora	1.73	0.91	2.39	59.18
Ophiuroidea	1.69	0.89	2.32	61.51
Pyropeltidae	1.68	1.01	2.32	63.83
Isopoda	1.66	1.19	2.29	66.12
Ostracoda	1.58	1.08	2.18	68.30
Sessilia	1.51	0.80	2.09	70.38
Terebellidae	1.42	1.18	1.96	72.34
Skeneidae	1.38	0.79	1.91	74.25

Appendix 3.10: Taxa contributing most to dissimilarity among macrofaunal invertebrates on experimental carbonate rocks transplanted from inner transition to background sites (IT-B) at Mound 12 for 17 months (2017-2018) and on *in situ* carbonate rocks collected at transition sites in 2017. Displayed are the average taxa dissimilarity (Av.Diss), standard deviation of taxa average dissimilarity (Diss/SD), taxon percent contribution to total dissimilarity (Contrib.%), and cumulative contribution to total dissimilarity (Cum.%), based on SIMPER analysis (Primer7).

Groups 2017 Transition and IT-B				
Average dissimilarity = 72.71				
Species	**Av.Diss**	**Diss/SD**	**Contrib.%**	**Cum.%**
Chrysopetalidae	3.43	1.23	4.72	4.72
Provannidae	3.39	1.66	4.66	9.38
Cirratulidae	3.16	1.68	4.34	13.72
Amphipoda	3.00	2.09	4.12	17.84
Lepetodrilidae	2.78	1.47	3.82	21.66
Ophiuroidea	2.62	0.93	3.60	25.27
Aplacophora	2.55	1.11	3.50	28.77
Neolepetopsidae	2.41	1.10	3.32	32.09
Amphinomidae	2.37	1.26	3.26	35.35
Paraonidae	2.37	1.08	3.26	38.61
Phyllodocidae	2.30	1.37	3.16	41.77
Hydroidolina	2.29	1.07	3.15	44.92
Cataegidae	2.12	0.78	2.91	47.83
Tanaidacea	2.10	1.12	2.89	50.72
Serpulidae	2.02	0.73	2.78	53.50
Maldanidae	1.94	1.10	2.66	56.16
Flabelligeridae	1.84	1.09	2.54	58.70
Polynoidae	1.84	1.21	2.54	61.24
Alcyonacea	1.84	0.99	2.53	63.77
Hesionidae	1.77	1.03	2.43	66.20
Polyplacophora	1.67	0.86	2.30	68.50
Dorvilleidae	1.66	0.88	2.29	70.79
Nuculanidae	1.55	0.79	2.13	72.92

Appendix 3.11: Taxa contributing most to dissimilarity among macrofaunal invertebrates on experimental carbonate rock, bone and wood deployed for 7 years (2010-2017) at active and transition sites at Mound 12. Displayed are the average taxa dissimilarity (Av.Diss), standard deviation of taxa average dissimilarity (Diss/SD), taxon percent contribution to total dissimilarity (Contrib.%), and cumulative contribution to total dissimilarity (Cum.%), based on SIMPER analysis (Primer7).

Groups Colonization Active and Colonization Transition				
Average dissimilarity = 74.84				
Species	**Av.Diss**	**Diss/SD**	**Contrib.%**	**Cum.%**
Provannidae	4.66	1.73	6.22	6.22
Ophiuroidea	4.19	1.72	5.60	11.83
Anomura	4.08	2.90	5.45	17.28
Lepetodrilidae	4.06	1.32	5.43	22.71
Serpulidae	3.40	1.01	4.54	27.25
Hesionidae	2.83	1.52	3.78	31.03
Neolepetopsidae	2.63	1.07	3.52	34.55
Pyropeltidae	2.57	1.34	3.43	37.98
Mytilidae	2.55	2.00	3.41	41.38
Ampharetidae	2.52	1.31	3.37	44.75
Amphipoda	2.37	1.70	3.17	47.92
Dorvilleidae	2.00	1.31	2.67	50.59
Amphinomidae	1.94	1.23	2.59	53.18
Hyalogyniridae	1.87	1.00	2.50	55.68
Cataegidae	1.84	1.15	2.46	58.14
Cirratulidae	1.79	0.84	2.39	60.53
Phyllodocidae	1.73	0.82	2.32	62.85
Lacydoniidae	1.70	1.04	2.27	65.12
Sabellidae	1.54	0.69	2.06	67.18
Polyplacophora	1.28	0.86	1.71	68.89
Skeneidae	1.28	0.76	1.70	70.60
Terebellidae	1.27	1.07	1.70	72.30
Teredinidae	1.22	0.83	1.64	73.93
Flabelligeridae	1.21	0.93	1.61	75.54

APPENDIX 4: Rank abundance plots of invertebrate macrofaunal communities at Mound 12

Appendix 4.1: Comparison of rank abundances of macrofaunal invertebrate taxa on *in situ* carbonate rocks collected at active and transition sites at Mound 12 in 2017 and on experimental carbonate rocks deployed for 7 years (2010-2017). X and Y axis values are ranks.

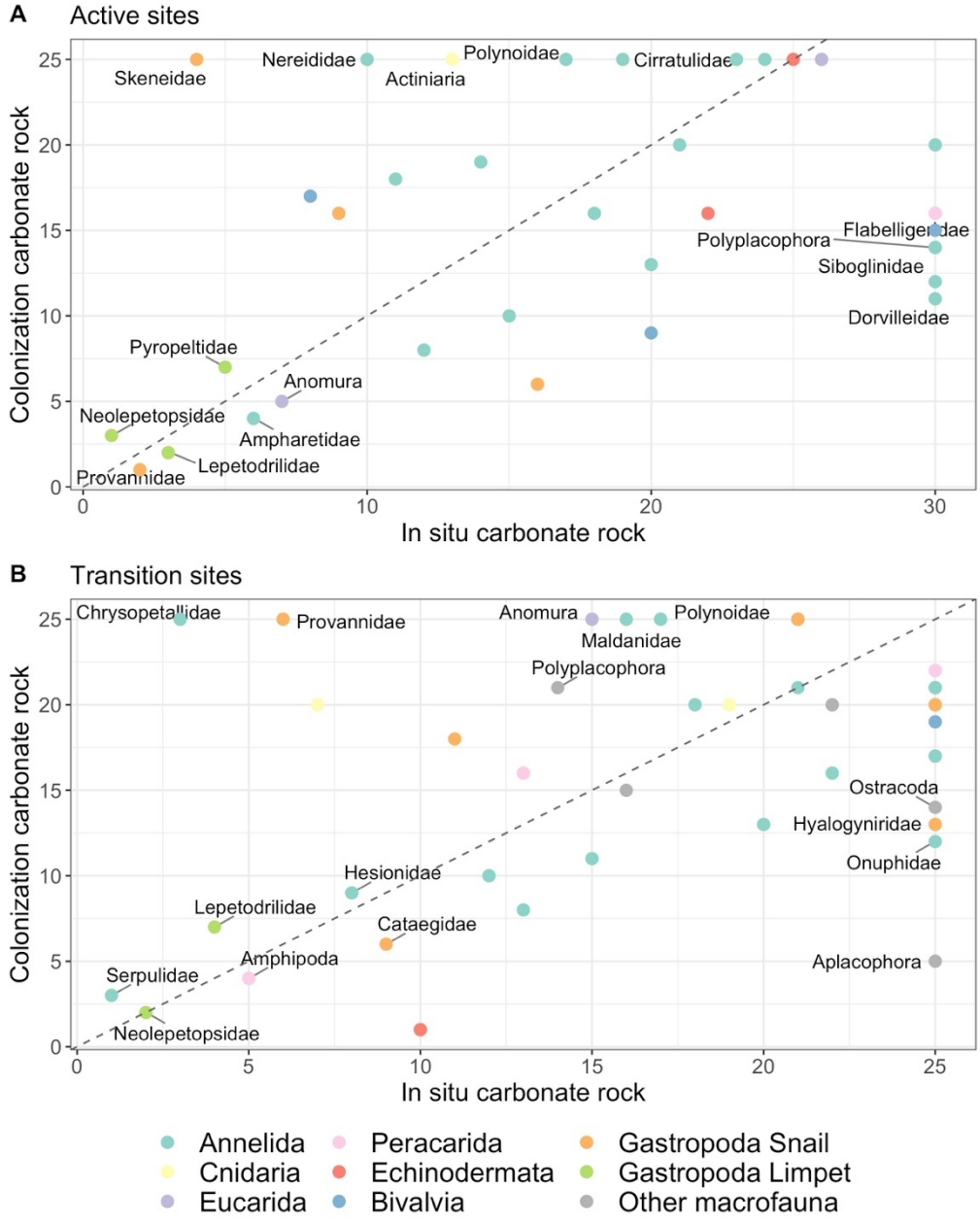

Appendix 4.2: Comparison of rank abundances macrofaunal invertebrates on experimental carbonate rocks transplanted from active sites to inner transition sites for 17 months, and on *in situ* carbonate rocks (A) at active sites collected in 2017 and (B) at inner transition sites collected in 2018.

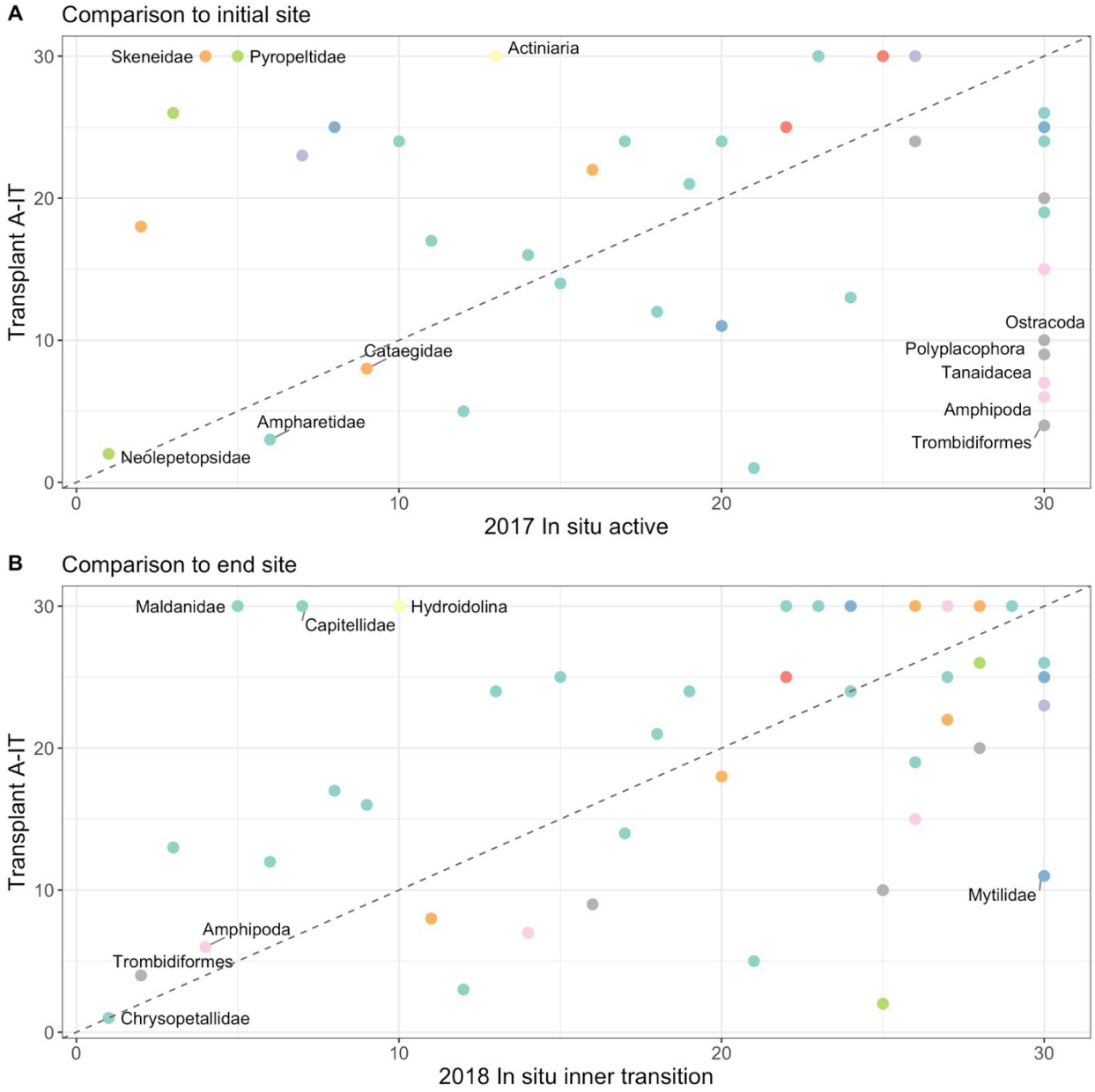

Appendix 4.3: Comparison of rank abundance of macrofaunal invertebrates on experimental carbonate rocks transplanted from active sites to outer transition sites for 17 months, and on *in situ* carbonate rocks (A) at the active sites collected in 2017 and (B) at outer transition sites collected in 2018

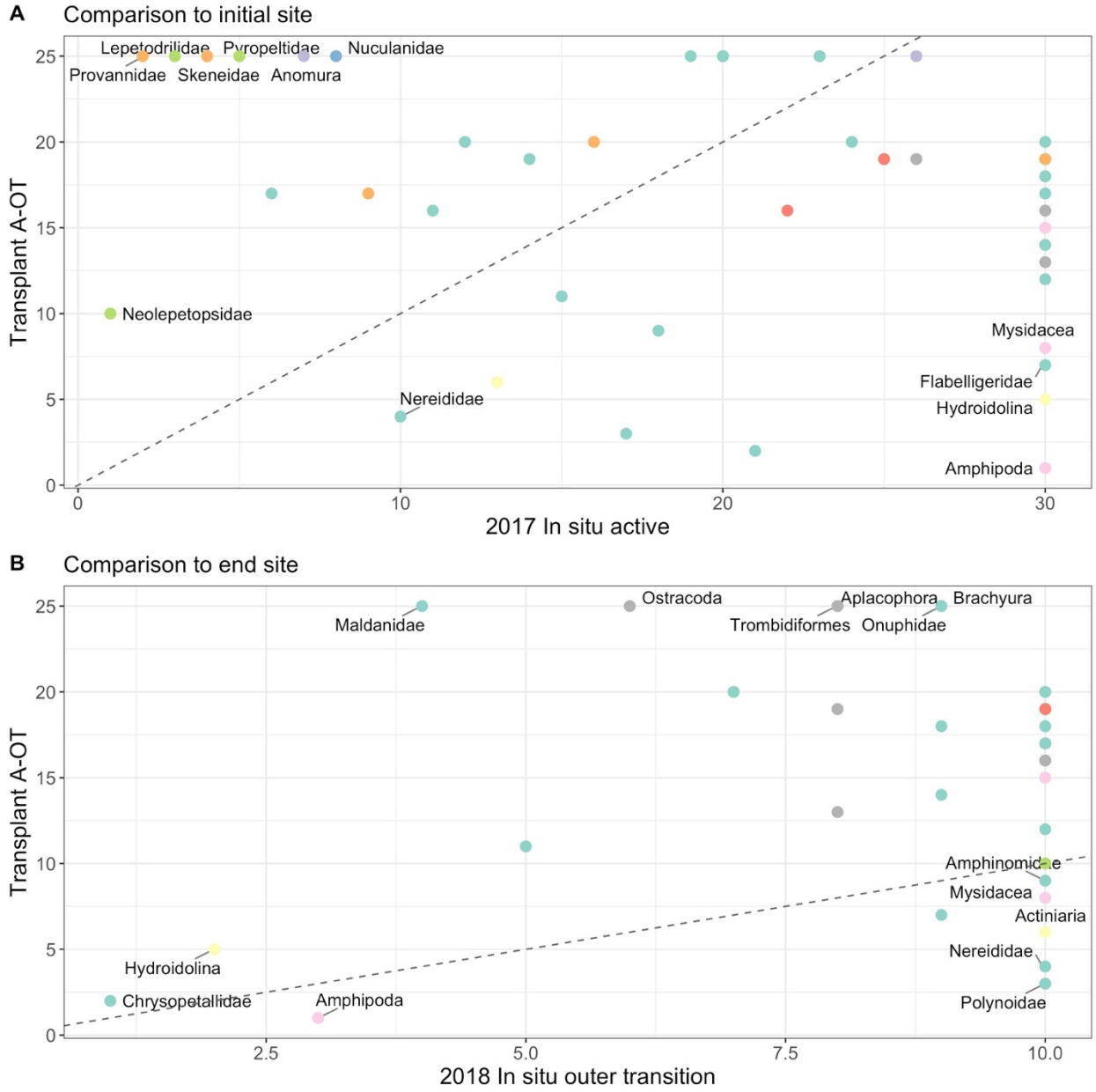

.

Appendix 4.4: Comparison of rank abundance of macrofaunal invertebrates on experimental carbonate rocks transplanted from inner transition sites to active sites for 17 months, and on *in situ*

carbonate rocks (A) at the transition sites collected in 2017 and (B) at active sites collected in 2018.

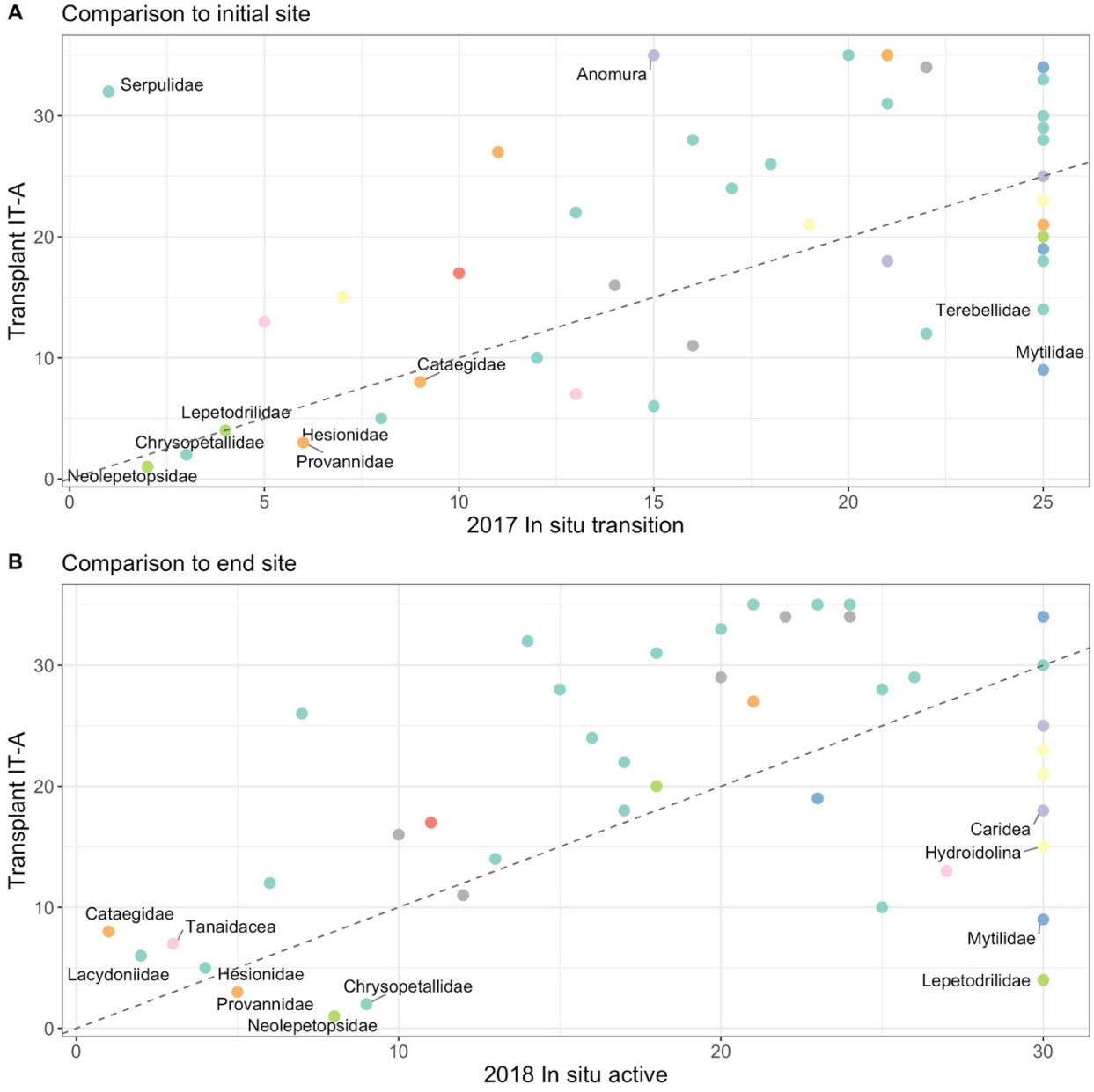

Appendix 4.5: Comparison of rank abundances of macrofaunal invertebrates on experimental carbonate rocks transplanted from inner transition sites to outer transition sites for 17 months, and on *in situ* carbonate rocks (A) at transition sites collected in 2017 and (B) at outer transition sites collected in 2018.

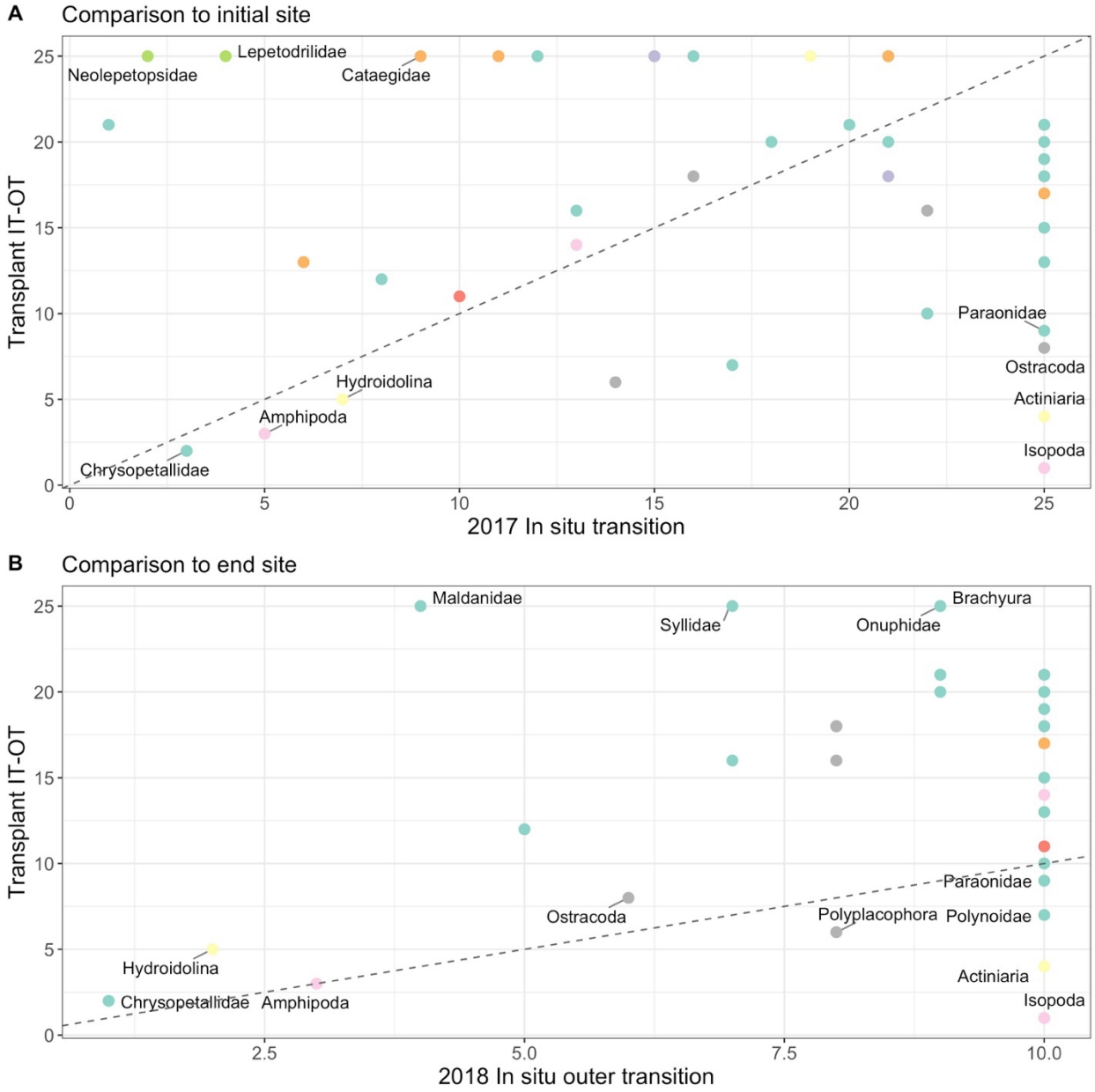

Appendix 4.6: Comparison of rank abundances of macrofaunal invertebrates on experimental carbonate rocks transplanted from active sites to background sites for 17 months and on *in situ* carbonate rocks at active sites collected in 2017.

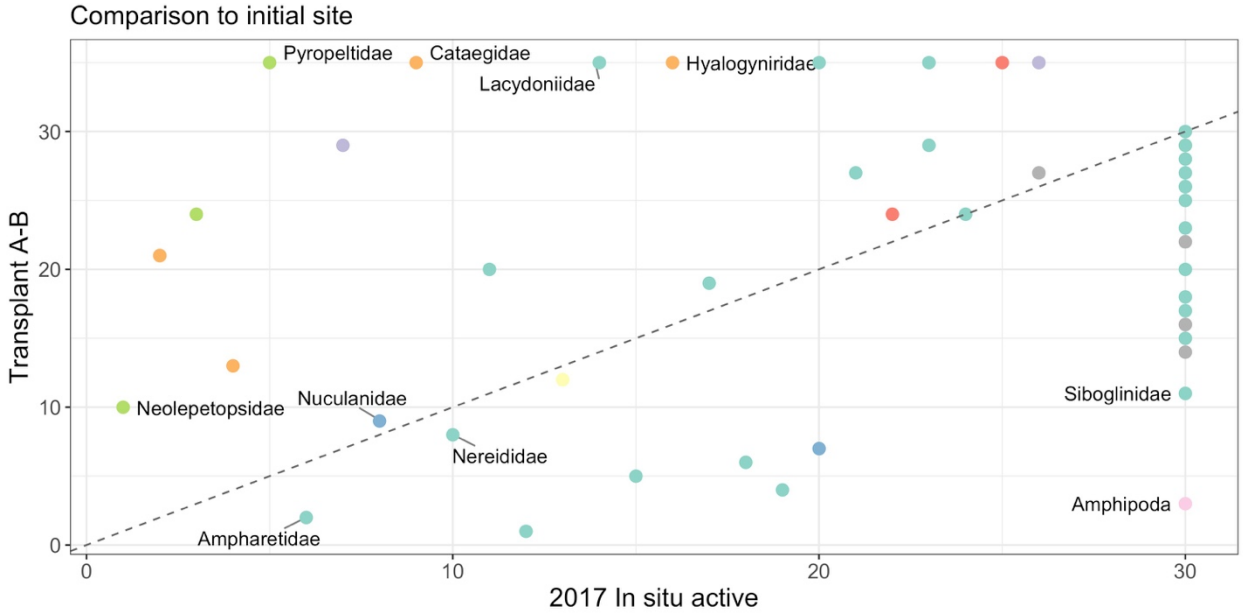

Appendix 4.7: Comparison of rank abundances of macrofaunal invertebrates on experimental carbonate rocks transplanted from inner transition sites to background sites for 17 months and on *in situ* carbonate rocks at transition sites collected in 2017.

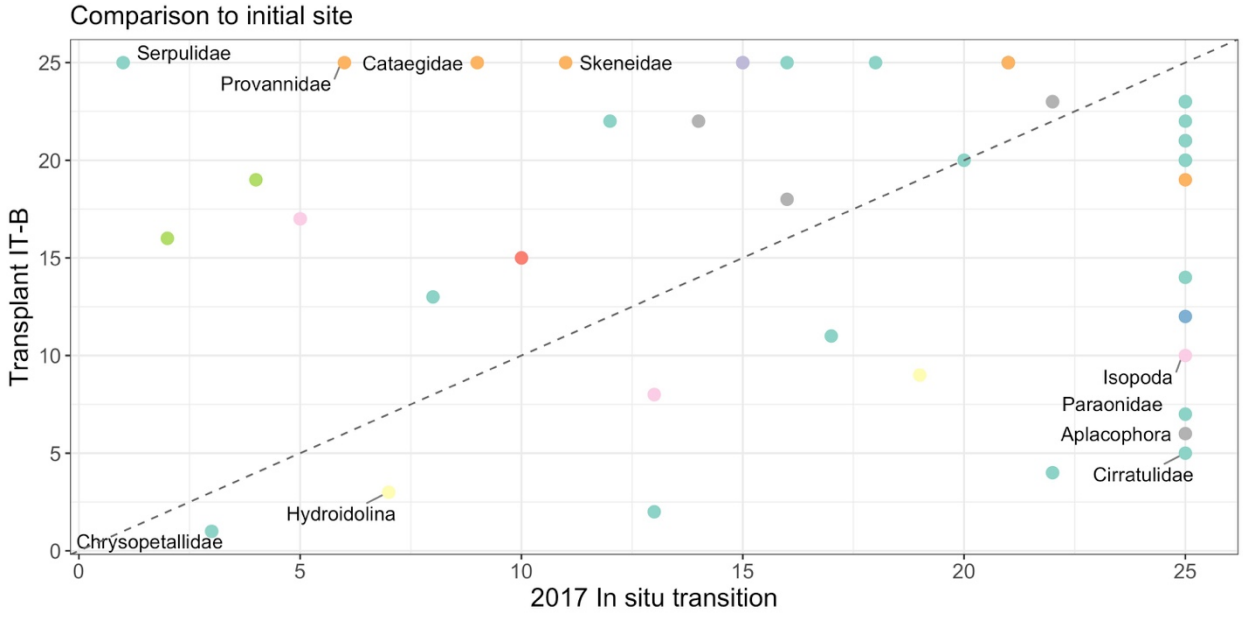

Appendix 4.8: Comparison of rank abundances of macrofaunal invertebrates on experimental carbonate rocks, cow bone and wood deployed for 7 years (2010-2017) at active sites at Mound 12.

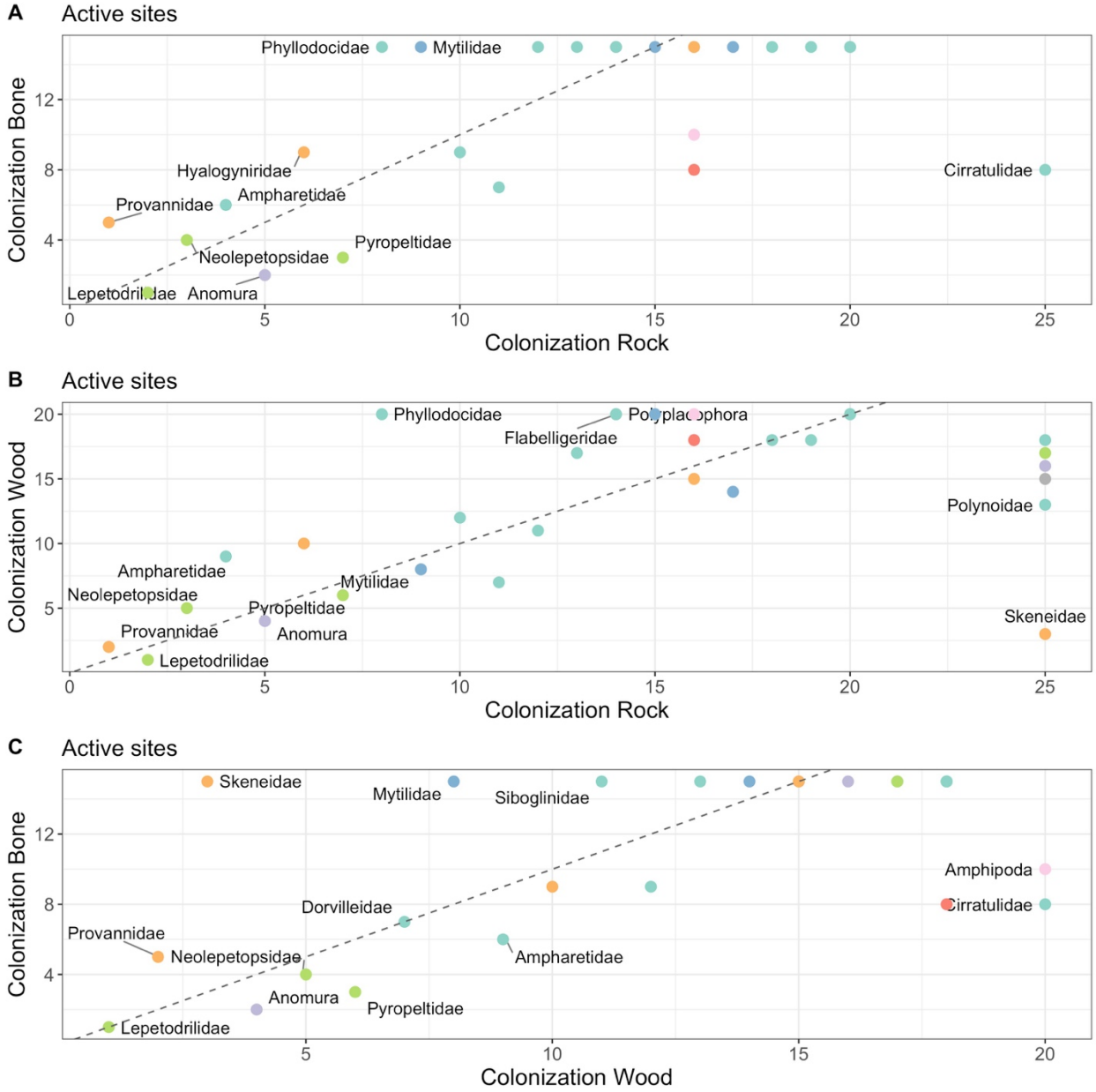

Appendix 4.9: Comparison of rank abundances of macrofaunal invertebrates on experimental carbonate rocks, cow bone and wood deployed for 7 years (2010-2017) at transition sites at Mound 12.

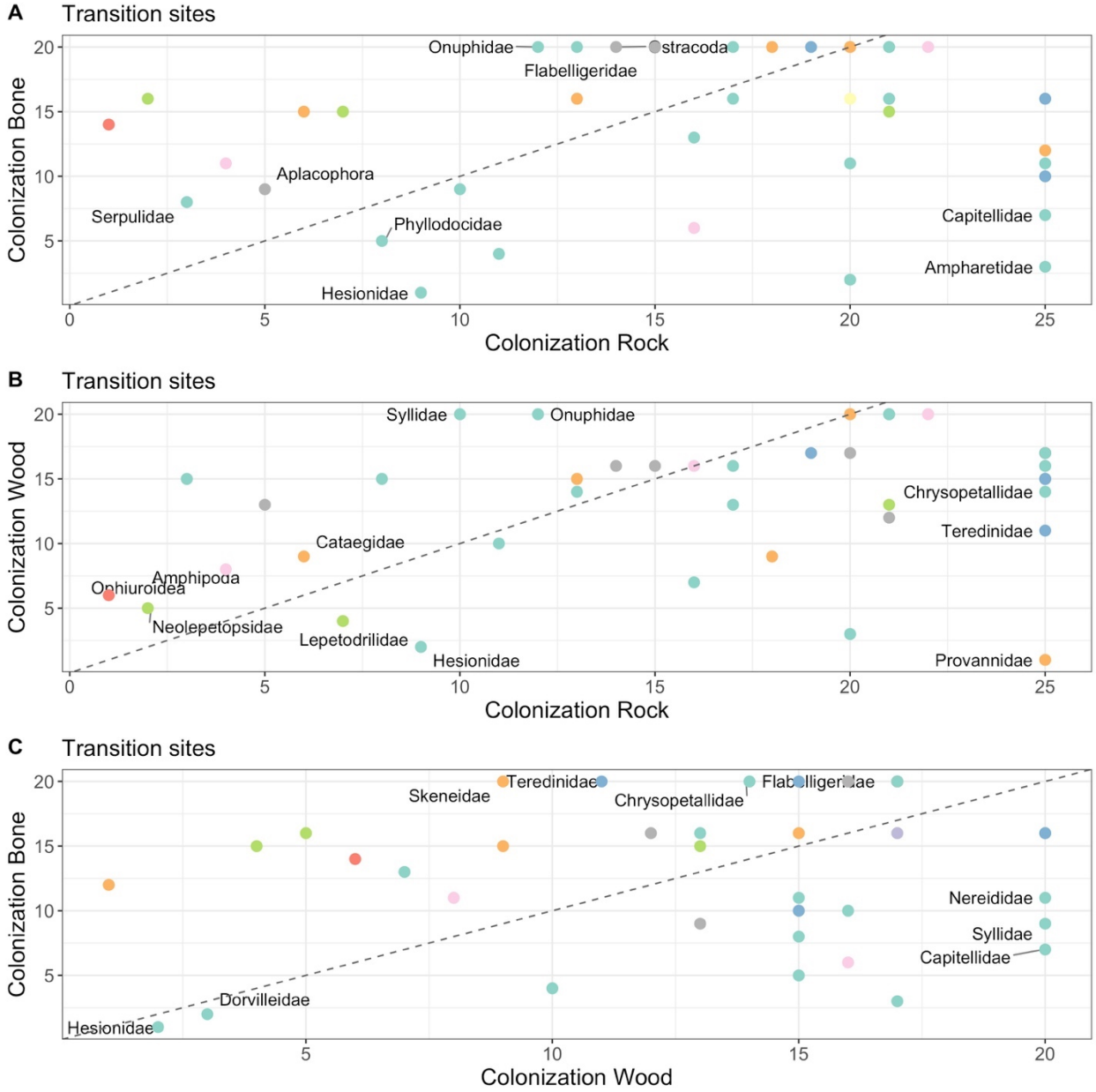

APPENDIX 5: Plots of isotopic composition by taxon of macrofaunal invertebrates at Mound 12

<u>Appendix 5.1:</u> $\delta^{13}C$ and $\delta^{15}N$ values (‰) of macrofaunal invertebrates on *in situ* rocks collected across seepage gradient at Mound 12 in 2017 (A, C) and 2018 (B, D). A: Active, T: Transition, IT: Inner Transition, OT: Outer Transition.

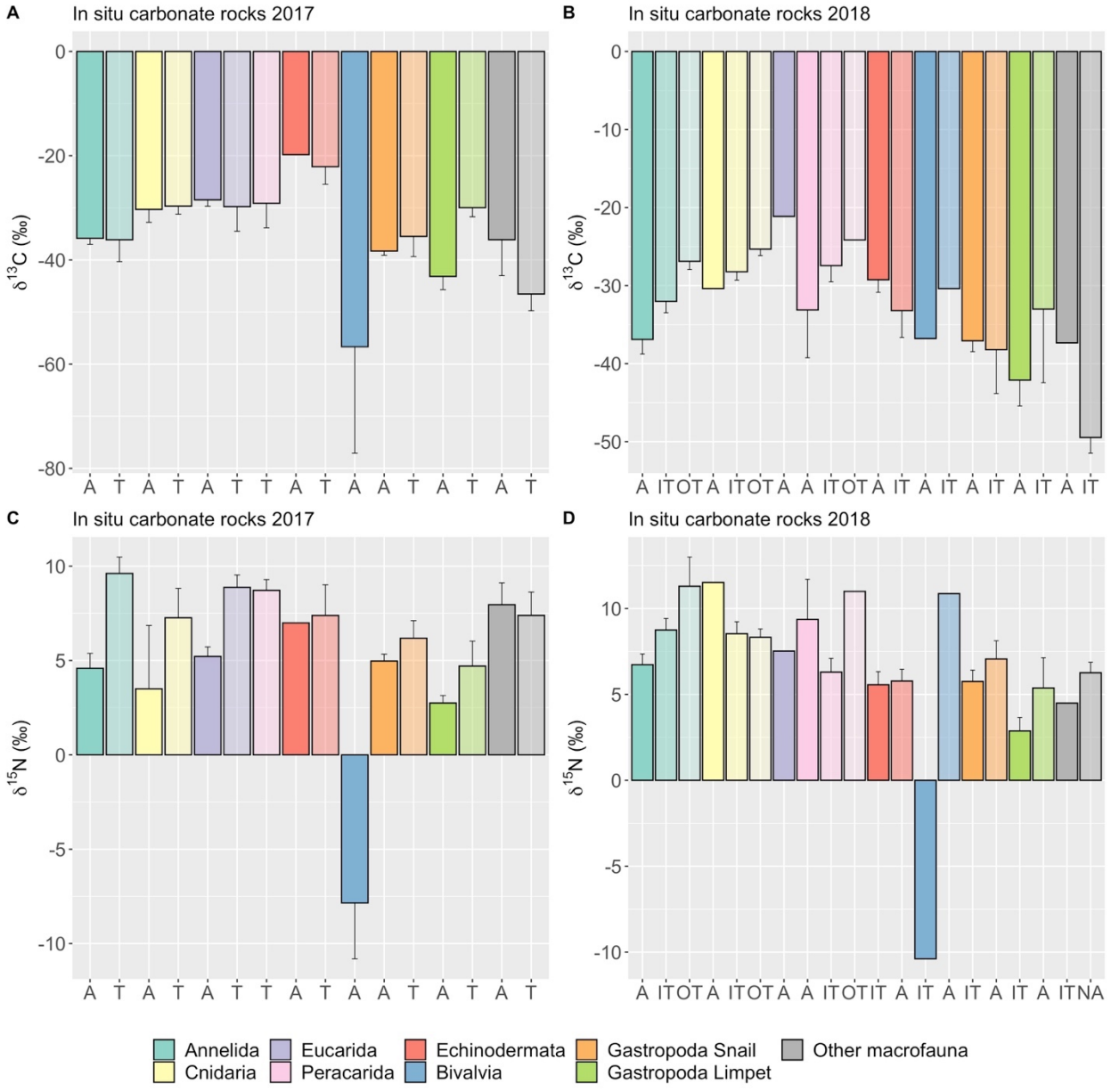

Appendix 5.2: $\delta^{13}C$ and $\delta^{15}N$ values (‰) of macrofaunal invertebrates on experimental carbonate rock, cow bone and wood deployed at active and transition sites for 7 years (2010-2017) at Mound 12. A: Active, T: Transition, IT: Inner Transition, OT: Outer Transition.

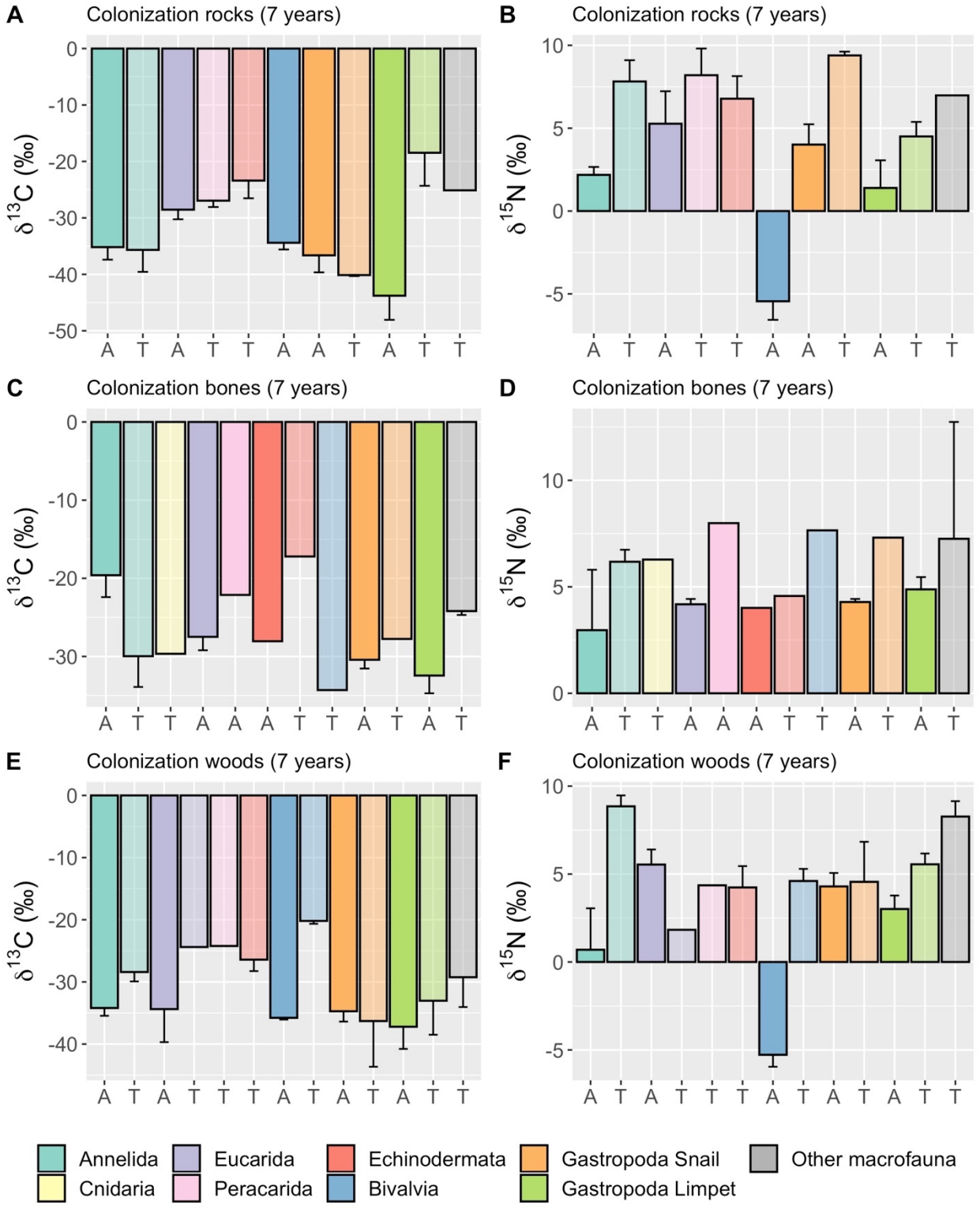

Appendix 5.3: $\delta^{13}C$ and $\delta^{15}N$ values (‰) of annelids on *in situ* carbonate rocks collected at active and transition sites at Mound 12 in 2017 (purple), experimental carbonate rocks transplanted across seepage gradient for 17 months (pink), and *in situ* carbonate rocks collected across seepage gradient in 2018 (orange). A: Active, T: Transition, IT: Inner transition, OT: Outer transition, B: Background.

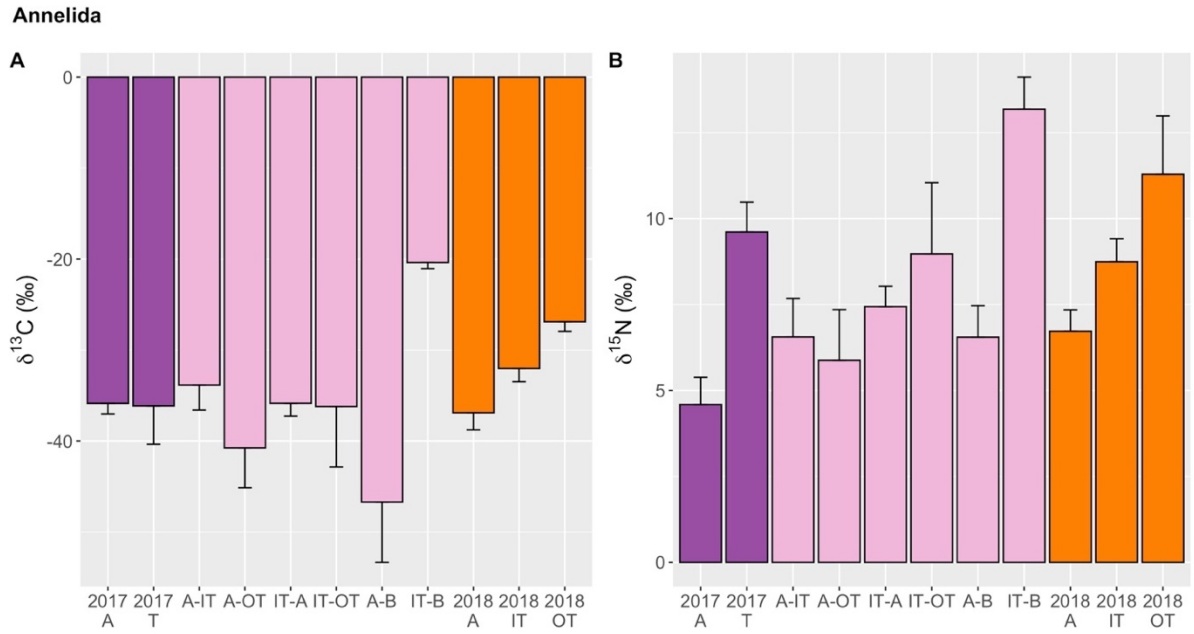

Appendix 5.4: $\delta^{13}C$ and $\delta^{15}N$ values (‰) of cnidarians on *in situ* carbonate rocks collected at active and transition sites at Mound 12 in 2017 (purple), experimental carbonate rocks transplanted across seepage gradient for 17 months (pink), and *in situ* carbonate rocks collected across seepage gradient in 2018 (orange). A: Active, T: Transition, IT: Inner transition, OT: Outer transition, B: Background.

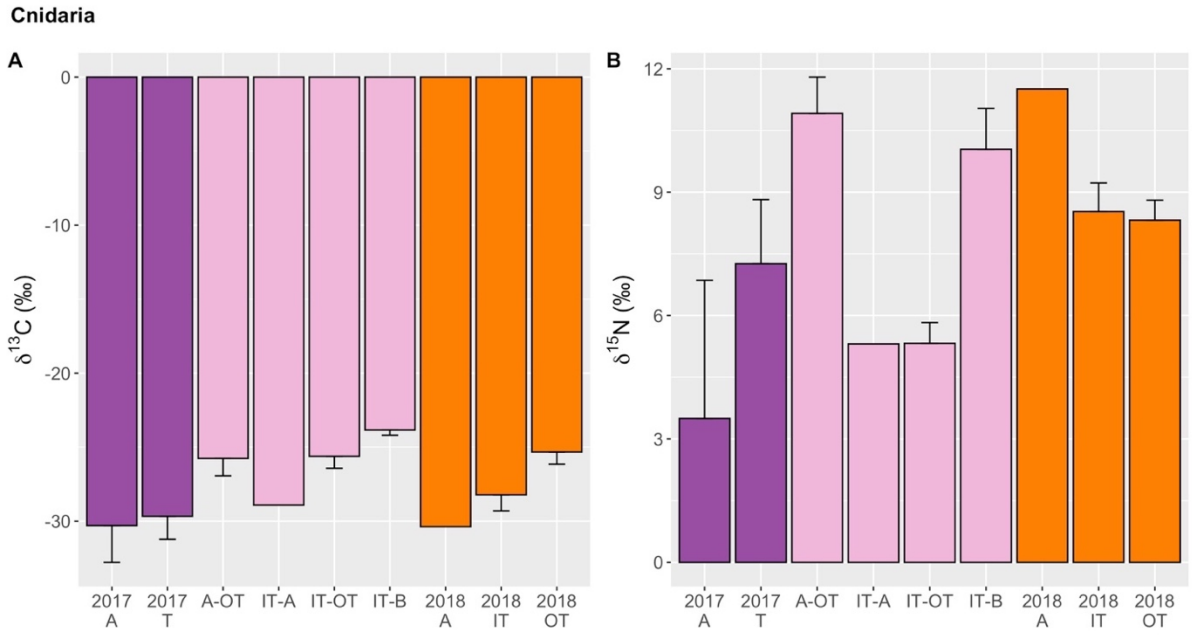

Appendix 5.5: $\delta^{13}C$ and $\delta^{15}N$ values (‰) of eucarids on *in situ* carbonate rocks collected at active and transition sites at Mound 12 in 2017 (purple), experimental carbonate rocks transplanted across seepage gradient for 17 months (pink), and *in situ* carbonate rocks collected at active sites in 2018 (orange). A: Active, T: Transition, IT: Inner transition, OT: Outer transition, B: Background.

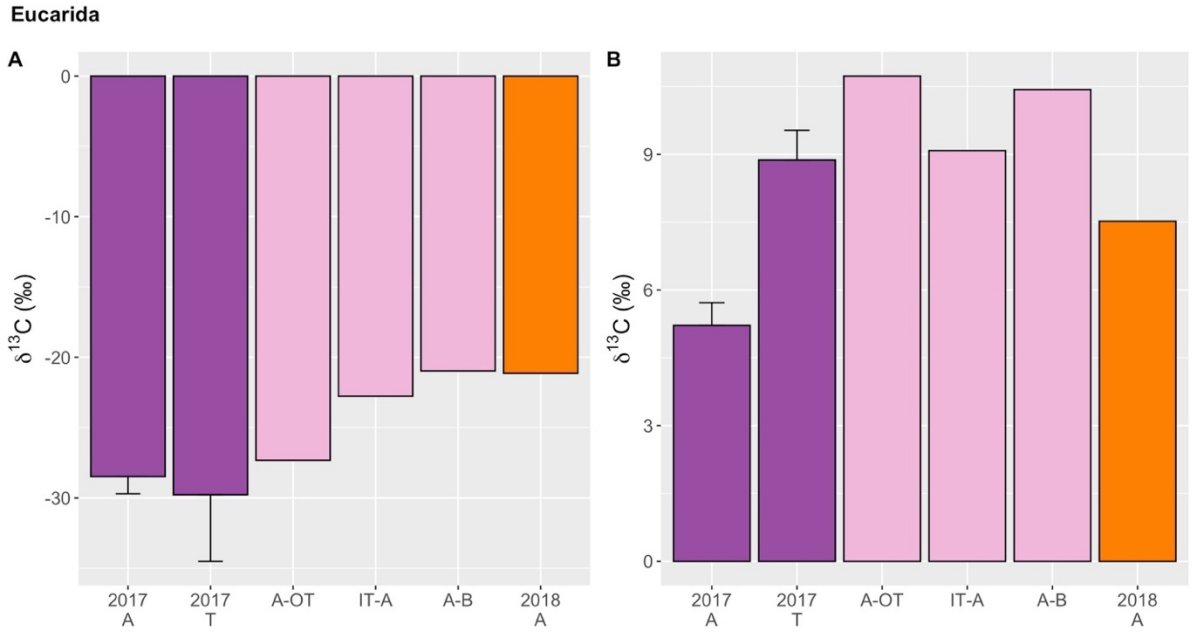

Appendix 5.6: $\delta^{13}C$ and $\delta^{15}N$ values (‰) of peracarids on *in situ* carbonate rocks collected at transition sites at Mound 12 in 2017 (purple), experimental carbonate rocks transplanted across seepage gradient for 17 months (pink), and *in situ* carbonate rocks collected across seepage gradient in 2018 (orange). A: Active, T: Transition, IT: Inner transition, OT: Outer transition, B: Background.

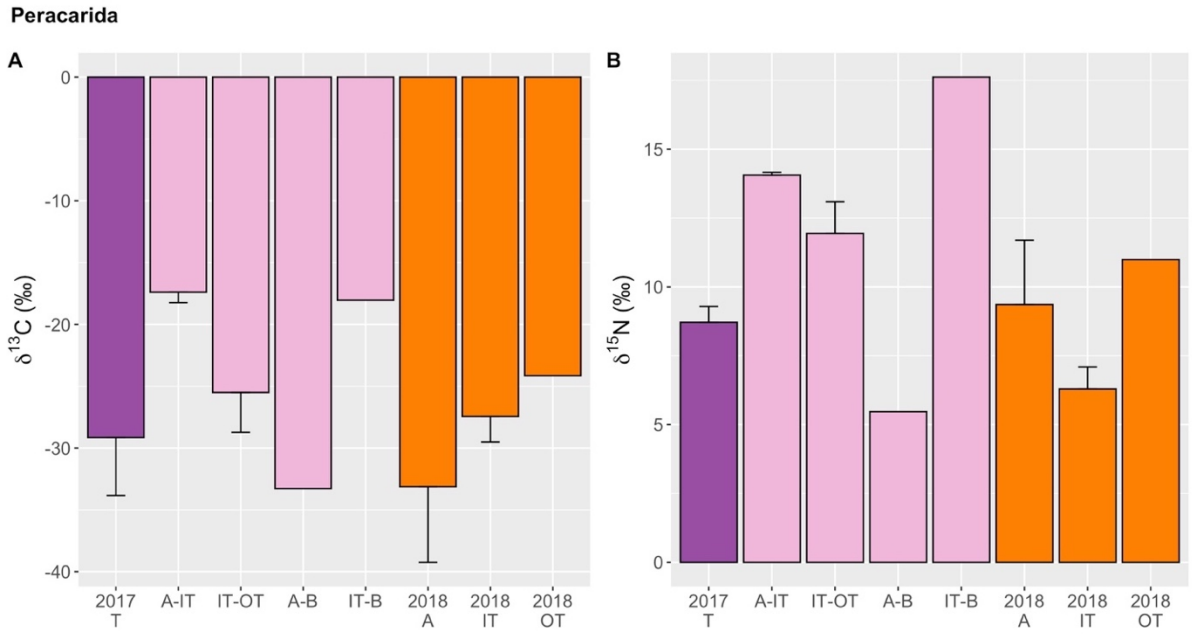

Appendix 5.7: $\delta^{13}C$ and $\delta^{15}N$ values (‰) of echinoderms on *in situ* carbonate rocks collected at active and transition sites at Mound 12 in 2017 (purple), experimental carbonate rocks transplanted across seepage gradient for 17 months (pink), and *in situ* carbonate rocks collected at active and inner transition sites in 2018 (orange). A: Active, T: Transition, IT: Inner transition, OT: Outer transition.

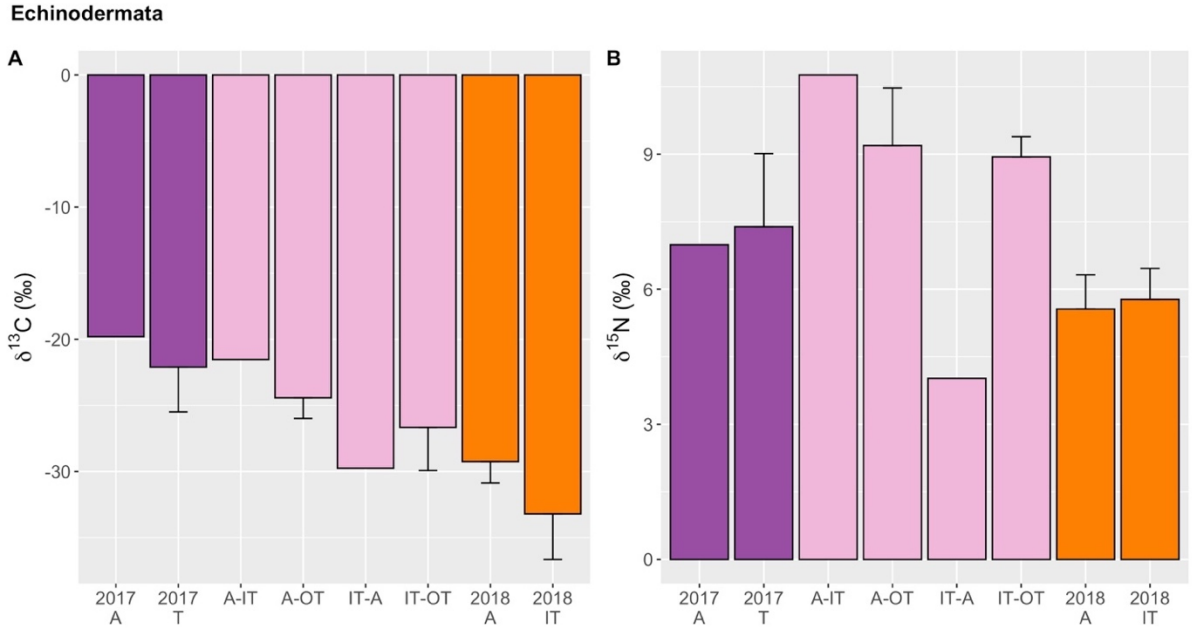

Appendix 5.8: $\delta^{13}C$ and $\delta^{15}N$ values (‰) of bivalves on *in situ* carbonate rocks collected at active sites at Mound 12 in 2017 (purple), experimental carbonate rocks transplanted across seepage gradient for 17 months (pink), and *in situ* carbonate rocks collected at active and inner transition sites in 2018 (orange). A: Active, IT: Inner transition, B: Background.

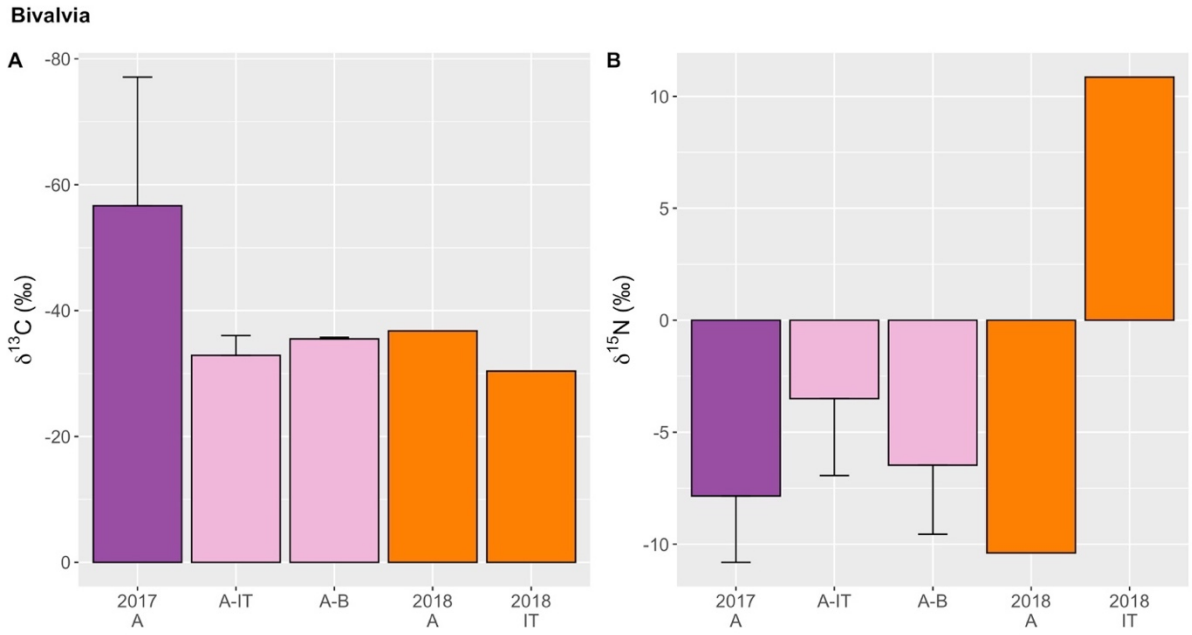

Appendix 5.9: $\delta^{13}C$ and $\delta^{15}N$ values (‰) of snails on *in situ* carbonate rocks collected at active and transition sites at Mound 12 in 2017 (purple), experimental carbonate rocks transplanted across seepage gradient for 17 months (pink), and *in situ* carbonate rocks collected at active and inner transition sites in 2018. A: Active, T: Transition, IT: Inner transition.

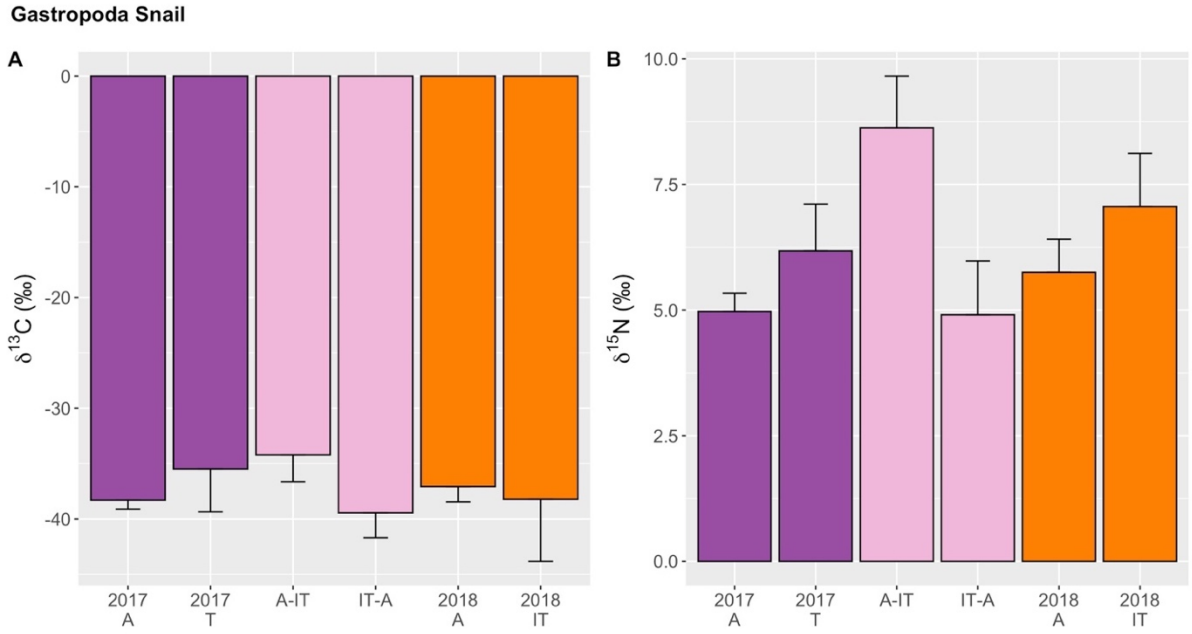

Appendix 5.10: $\delta^{13}C$ and $\delta^{15}N$ values (‰) of cnidarians on *in situ* carbonate rocks collected at active and transition sites at Mound 12 in 2017 (purple), experimental carbonate rocks transplanted across seepage gradient for 17 months (pink), and *in situ* carbonate rocks collected at active and inner transition sites in 2018 (orange). A: Active, T: Transition, IT: Inner transition, OT: Outer transition.

Gastropoda Limpet

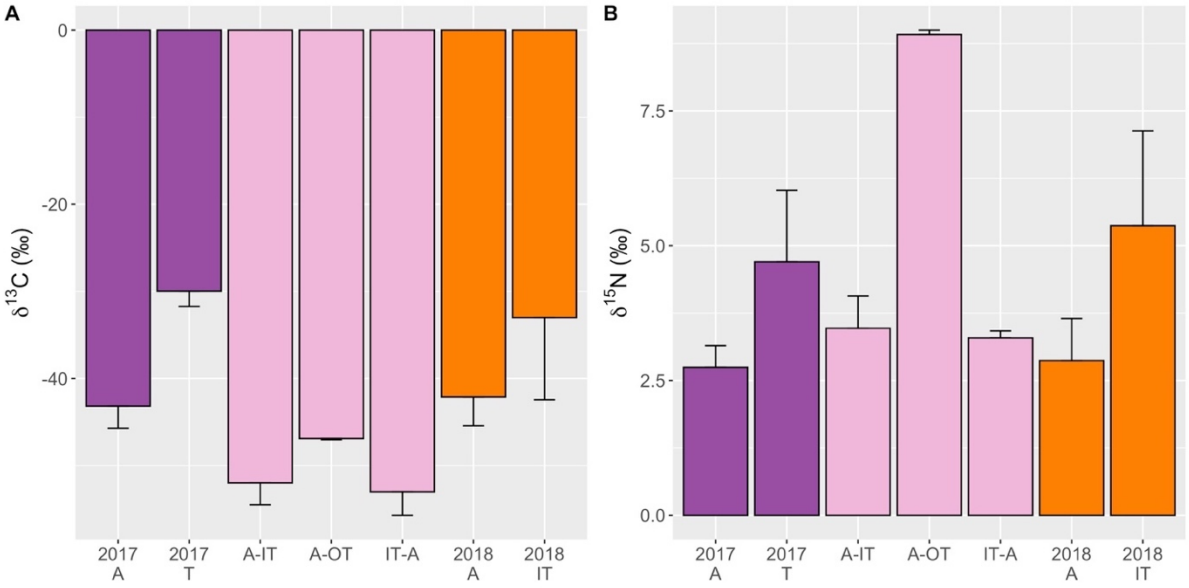

APPENDIX 6: Results of Statistical tests

Appendix 6.1: Wilcox test (W) and Dunn's test (z) for isotopic composition of invertebrate macrofaunal community on *in situ* carbonate rocks collected across seepage gradient in 2017 and 2018 at Mound 12. Below diagonal: tests for $\delta^{13}C$ values; Diagonal: mean $\delta^{13}C$ and $\delta^{15}N$ values; Above diagonal: tests for $\delta^{15}N$ values. Significant values ($p < 0.05$ for Wilcox tests, $p < 0.025$ for Dunn's test) in bold. A: Active, T: Transition, IT: Inner Transition, OT: Outer Transition.

	2017 A	2017 T	2018 A	2018 IT	2018 OT
2017 A	$\delta^{13}C$ = -36.3 ± 1.6‰ $\delta^{15}N$ = 3.5 ± 1.0‰	W = 454.5 p-value < 0.001	**W = 1433.5** **p-value < 0.001**	-	-
2017 T	**W = 825** **p-value = 0.005**	$\delta^{13}C$ = -27.9 ± 2.9‰ $\delta^{15}N$ = 9.2 ± 1.1‰	-	Kruskal-Wallis not significant	Kruskal-Wallis not significant
2018 A	W = 2019.5 p-value = 0.27	-	$\delta^{13}C$ = -36.2 ± 1.3‰ $\delta^{15}N$ = 6.2 ± 0.8‰	**z = -2.4124** **p-value = 0.01**	**z = -3.0117** **p-value = 0.004**
2018 IT[1,2]	-	z = -0.4535 p-value = 0.32	**z = -2.5220** **p-value = 0.006**	$\delta^{13}C$ = -33.7 ± 2.7‰ $\delta^{15}N$ = 7.9 ± 0.6‰	Kruskal-Wallis not significant
2018 OT[1,2]	-	**z = 2.5519** **p-value = 0.008**	**z = -4.0541** **p-value < 0.001**	**z = -2.6428** **p-value = 0.006**	$\delta^{13}C$ = -25.6 ± 0.1‰ $\delta^{15}N$ = 9.4 ± 0.3‰

[1]: Between years at transition sites:
$\delta^{13}C$: Kruskal-Wallis, Chi-squared = 8.2972, df = 2, p-value = 0.01
$\delta^{15}N$: Kruskal-Wallis, Chi-squared = 3.4479, df = 2, p-value = 0.18
[2]: Among seepage activity in 2018:
$\delta^{13}C$: Kruskal-Wallis, Chi-squared = 19.358, df = 2, p-value < 0.001
$\delta^{15}N$: Kruskal-Wallis, Chi-squared = 12.386, df = 2, p-value = 0.002

Appendix 6.2: Wilcox test (W) for isotopic composition of invertebrate macrofaunal community on *in situ* carbonate rocks collected at active and transition sites in 2017 at Mound 12 and on experimental carbonate rocks deployed for 7 years at active and transition sites. Below diagonal: tests for $\delta^{13}C$ values; Diagonal: mean $\delta^{13}C$ and $\delta^{15}N$ values; Above diagonal: tests for $\delta^{15}N$ values. Significant values ($p < 0.05$) in bold.

	In situ Active	*In situ* Transition	Colonization Active	Colonization transition
In situ Active	$\delta^{13}C$ = -36.3 ± 1.6‰ $\delta^{15}N$ = 3.55 ± 1.0‰	W = 454.5 p-value < 0.001	**W = 2139.5** **p-value < 0.001**	-
In situ Transition	**W = 825** **p-value = 0.005**	$\delta^{13}C$ = -27.9 ± 2.9‰ $\delta^{15}N$ = 9.18 ± 1.1‰	-	W = 343 p-value = 0.60
Colonization Active	W = 1299 p-value = 0.18	-	$\delta^{13}C$ = -33.4 ± 2.7‰ $\delta^{15}N$ = 1.3 ± 1.0‰	**W = 79** **p-value < 0.001**
Colonization Transition	-	W = 268 p-value = 0.38	**W = 244** **p-value = 0.02**	$\delta^{13}C$ = -29.8 ± 1.8‰ $\delta^{15}N$ = 7.4 ± 0.6‰

Appendix 6.3: Wilcox test (W) and Dunn's test (z) for isotopic composition of invertebrate macrofaunal community on experimental carbonate rock, bone and wood deployed for 7 years at active and transition sites. Below diagonal: tests for $\delta^{13}C$ values; Diagonal: mean $\delta^{13}C$ and $\delta^{15}N$ values; Above diagonal: tests for $\delta^{15}N$ values. Significant values ($p < 0.05$) in bold.

	Rock A	Rock T	Bone A	Bone T	Wood A	Wood T
Rock A[1]	$\delta^{13}C$ = -33.4 ± 2.7‰ $\delta^{15}N$ = 1.3 ± 1.0‰	**W = 79 p-value < 0.001**	**z = 2.4563 p = 0.007**	-	z = -0.3423 p = 0.37	-
Rock T[2]	**W = 244 p-value = 0.02**	$\delta^{13}C$ = -29.8 ± 1.8‰ $\delta^{15}N$ = 7.4 ± 0.6‰	-	Kruskal-Wallis not significant	-	Kruskal-Wallis not significant
Bone A[1]	**z = 3.2193 p = 0.002**	-	$\delta^{13}C$ = -27.1 ± 0.6‰ $\delta^{15}N$ = 4.5 ± 0.3‰	**W = 41.5 p-value = 0.03**	**z = 2.1756 p = 0.01**	-
Bone T[2]	-	Kruskal-Wallis not significant	W = 74 p-value = 0.68	$\delta^{13}C$ = -28.3 ± 3.1‰ $\delta^{15}N$ = 6.3 ± 0.5‰	-	Kruskal-Wallis not significant
Wood A[1]	z = -0.0166 p = 1.00	-	**z = 3.1359 p = 0.003**	-	$\delta^{13}C$ = -35.0 ± 2.2‰ $\delta^{15}N$ = 2.0 ± 0.5‰	**W = 226 p-value < 0.001**
Wood T[2]	-	Kruskal-Wallis not significant	-	Kruskal-Wallis not significant	**W = 240 p-value < 0.001**	$\delta^{13}C$ = -26.7 ± 2.2‰ $\delta^{15}N$ = 6.2 ± 0.3‰

[1]: Among hard substrates at active sites:
$\delta^{13}C$: Kruskal-Wallis, Chi-squared = 11.371, df = 2, p = 0.003
$\delta^{15}N$: Kruskal-Wallis, Chi-squared = 6.2096, df = 2, p-value = 0.04
[2]: Among hard substrates at transition sites:
$\delta^{13}C$: Kruskal-Wallis, Chi-squared = 0.74631, df = 2, p-value = 0.69
$\delta^{15}N$: Kruskal-Wallis, Chi-squared = 1.9216, df = 2, p-value = 0.38

Appendix 6.4: Statistical tests within taxa between active and transition sites of isotopic composition of invertebrate macrofaunal community on *in situ* carbonate rocks collected in 2017 at Mound 12.

Annelida
$\delta^{13}C$: Wilcox test, W = 122, p-value = 0.985
$\delta^{15}N$: Wilcox test, W = 212, p-value < 0.001*

Cnidaria
$\delta^{13}C$: Wilcox test, W = 8, p-value = 1.00
$\delta^{15}N$: Wilcox test, W = 4, p-value = 0.39

Eucarida
$\delta^{13}C$: Wilcox test, W = 6, p-value = 1.00

$\delta^{15}N$: Wilcox test, W = 0, p-value = 0.07

Peracarida: no data for peracarids at active sites

Echinodermata
$\delta^{13}C$: Wilcox test, W = 4, p-value = 0.67
$\delta^{15}N$: Wilcox test, W = 3, p-value = 1.00

Bivalvia: no data for bivalves at transition sites

Gastropoda: Snail
$\delta^{13}C$: Wilcox test, W = 70, p-value = 0.54
$\delta^{15}N$: Wilcox test, W = 65, p-value = 0.38

Gastropoda: Limpet
$\delta^{13}C$: Wilcox test, W = 5, p-value = 0.02*
$\delta^{15}N$: Wilcox test, W = 14, p-value = 0.19

Appendix 6.5: Statistical tests within taxa among seepage activity of isotopic composition of invertebrate macrofaunal community on *in situ* carbonate rocks collected in 2018 at Mound 12

Annelida
$\delta^{13}C$: Kruskal-Wallis, Chi-squared = 6.4384, df = 2, p-value = 0.04
Active vs Inner transition: Dunn's test, z = -1.9293, p-value = 0.08
Active vs Outer transition: Dunn's test, z = -1.8841, p-value = 0.04
Inner transition vs Outer transition: Dunn's test, z = -1.0912, p-value = 0.14
$\delta^{15}N$: Kruskal-Wallis, Chi-squared = 6.0783, df = 2, p-value = 0.051

Cnidaria
$\delta^{13}C$: Kruskal-Wallis, Chi-squared = 5.7043, df = 2, p-value = 0.06
$\delta^{15}N$: Kruskal-Wallis, Chi-squared = 2.7671, df = 2, p-value = 0.25

Eucarida: no data for eucarids at inner transition and outer transition sites

Peracarida
$\delta^{13}C$: Kruskal-Wallis, Chi-squared = 0.76389, df = 2, p-value = 0.68
$\delta^{15}N$: Kruskal-Wallis, Chi-squared = 3.2222, df = 2, p-value = 0.20

Echinodermata
$\delta^{13}C$: Wilcox test, W = 5, p-value = 0.4
$\delta^{15}N$: Wilcox test, W = 3, p-value = 1

Bivalvia
$\delta^{13}C$: Wilcox test, W = 1, p-value = 1
$\delta^{15}N$: Wilcox test, W = 1, p-value = 1

Gastropoda: Snail
$\delta^{13}C$: Wilcox test, W = 23, p-value = 0.9495
$\delta^{15}N$: Wilcox test, W = 12, p-value = 0.2145

Gastropoda: Limpet
$\delta^{13}C$: Wilcox test, W = 4, p-value = 0.6429
$\delta^{15}N$: Wilcox test, W = 1, p-value = 0.1429

Appendix 6.6: Statistical tests between years (2017 vs 2018) within taxa of isotopic composition of invertebrate macrofaunal community on *in situ* carbonate rocks collected at active sites at Mound 12

Annelida
$\delta^{13}C$: Wilcox test, W = 315.5, p-value = 0.39
$\delta^{15}N$: Wilcox test, W = 248, p-value = 0.01*

Cnidaria
$\delta^{13}C$: Wilcox test, W = 2, p-value = 1.00
$\delta^{15}N$: Wilcox test, W = 0, p-value = 0.50

Eucarida
$\delta^{13}C$: Wilcox test, W = 0, p-value = 0.29
$\delta^{15}N$: Wilcox test, W = 0, p-value = 0.28

Peracarida: no data for peracarids at active sites in 2017

Echinodermata
$\delta^{13}C$: Wilcox test, W = 3, p-value = 0.50
$\delta^{15}N$: Wilcox test, W = 3, p-value = 0.50

Bivalvia
$\delta^{13}C$: Wilcox test, W = 1, p-value = 1.00
$\delta^{15}N$: Wilcox test, W = 1, p-value = 1.00

Gastropoda: Snail
$\delta^{13}C$: Wilcox test, W = 70, p-value = 0.54
$\delta^{15}N$: Wilcox test, W = 65, p-value = 0.38

Gastropoda: Limpet
$\delta^{13}C$: Wilcox test, W = 52, p-value = 0.78
$\delta^{15}N$: Wilcox test, W = 52, p-value = 0.78

Appendix 6.7: Statistical tests between years (2017 vs 2018) within taxa of isotopic composition of invertebrate macrofaunal community on *in situ* carbonate rocks collected at transition sites at Mound 12

Annelida
$\delta^{13}C$: Kruskal-Wallis, Chi-squared = 1.6083, df = 2, p-value = 0.45
$\delta^{15}N$: Kruskal-Wallis, Chi-squared = 1.4164, df = 2, p-value = 0.49

Cnidaria
$\delta^{13}C$: Kruskal-Wallis, Chi-squared = 6.5693, df = 2, p-value = 0.04*
2017 Transition vs 2018 Inner transition: Dunn's test, z = 0.5010, p-value = 0.31
2017 Transition vs 2018 Outer transition: Dunn's test, z = 2.3694, p-value = 0.03
2018 Inner Transition vs 2018 Outer transition: Dunn's test, z = -2.1275, p-value = 0.03
$\delta^{15}N$: Kruskal-Wallis, chi-squared = 1.4746, df = 2, p-value = 0.48

Eucarida: no data for eucarids at transition sites in 2018

Peracarida
$\delta^{13}C$: Kruskal-Wallis, Chi-squared = 1.2857, df = 2, p-value = 0.52
$\delta^{15}N$: Kruskal-Wallis, Chi-squared = 4.8214, df = 2, p-value = 0.09

Echinodermata: 2017 Transition and 2018 Inner transition
$\delta^{13}C$: Wilcox test, W = 10, p-value = 0.09524
$\delta^{15}N$: Wilcox test, W = 7, p-value = 0.5714

Bivalvia: no data for bivalves at transition sites in 2017

Gastropoda: Snail: 2017 Transition vs 2018 Inner Transition
$\delta^{13}C$: Wilcox test, W = 9, p-value = 0.8857
$\delta^{15}N$: Wilcox test, W = 5, p-value = 0.4857

Gastropoda: Limpet: 2017 Transition vs 2018 Inner Transition
$\delta^{13}C$: Wilcox test, W = 3, p-value = 1
$\delta^{15}N$: Wilcox test, W = 2, p-value = 0.8

Appendix 6.8: Statistical tests between active and transition sites within taxa of isotopic composition of invertebrate macrofaunal community on experimental carbonate rocks deployed for 7 years (2010-2017) at Mound 12 within taxa of isotopic composition of invertebrate macrofaunal community on experimental carbonate rocks collected at active sites at Mound 12

Annelida
$\delta^{13}C$: Wilcox test, W = 48, p-value = 1
$\delta^{15}N$: Wilcox test, W W = 0, p-value < 0.001*

Cnidaria: no data for cnidarians on colonization rocks

Eucarida: no data for eucarids on colonization rocks at transition sites

Peracarida: no data for peracarids on colonization rocks at active sites

Bivalvia: no data for bivalves on colonization rocks at transition sites

Gastropoda: Snail
$\delta^{13}C$: Wilcox test, W = 4, p-value = 1.00
$\delta^{15}N$: Wilcox test, W = 0, p-value = 0.13

Gastropoda: Limpet
$\delta^{13}C$: Wilcox test, W = 0, p-value = 0.13
$\delta^{15}N$: Wilcox test, W W = 1, p-value = 0.27

Appendix 6.9: Statistical tests within taxa at active sites between invertebrate macrofauna on *in situ* carbonate rocks collected in 2017 at Mound 12 and on experimental carbonate rocks deployed for 7 years (2010-2017)

Annelida
$\delta^{13}C$: Wilcox test, W = 198, p-value = 0.53
$\delta^{15}N$: Wilcox test, W = 94, p-value = 0.01*

Cnidaria: no data for cnidarians on colonization rocks

Eucarida
$\delta^{13}C$: Wilcox test, W = 20, p-value = 0.82
$\delta^{15}N$: Wilcox test, W = 25, p-value = 0.31

Peracarida: no data for peracarids on colonization rocks at active sites

Bivalvia
$\delta^{13}C$: Wilcox test, W = 20, p-value = 0.20
$\delta^{15}N$: Wilcox test, W = 15, p-value = 0.66

Gastropoda: Limpet
$\delta^{13}C$: Wilcox test, W = 36, p-value = 0.91
$\delta^{15}N$: Wilcox test, W = 29, p-value = 0.50

Gastropoda: Snail
$\delta^{13}C$: Wilcox test, W = 33, p-value = 0.81
$\delta^{15}N$: Wilcox test, W = 20, p-value = 0.34

Appendix 6.10: Statistical tests within taxa at transition sites between invertebrate macrofauna on *in situ* carbonate rocks collected in 2017 at Mound 12 and on experimental carbonate rocks deployed for 7 years (2010-2017)

Annelida
$\delta^{13}C$: Wilcox test, W = 30, p-value = 0.81
$\delta^{15}N$: Wilcox test, W = 21, p-value = 0.26

Cnidaria: no data for cnidarians on colonization rocks

Eucarida: no data for eucarids on colonization rocks at transition sites

Peracarida
$\delta^{13}C$: Wilcox test, W = 3, p-value = 1.00
$\delta^{15}N$: Wilcox test, W = 4, p-value = 0.80

Echinodermata
$\delta^{13}C$: Wilcox test, W = 9, p-value = 0.90
$\delta^{15}N$: Wilcox test, W = 10, p-value = 1.00

Bivalvia: no data for bivalves on colonization rocks at transition sites

Gastropoda: Snail
$\delta^{13}C$: Wilcox test, W = 3, p-value = 0.80
$\delta^{15}N$: Wilcox test, W = 8, p-value = 0.13

Gastropoda: Limpet
$\delta^{13}C$: Wilcox test, W = 6, p-value = 0.20
$\delta^{15}N$: Wilcox test, W = 3, p-value = 1.00

Appendix 6.11: Statistical tests among taxa of invertebrate macrofauna on *in situ* carbonate rocks collected at active and transition sites in 2017 and across seepage gradient in 2018 at Mound 12

2017 Active

$\delta^{13}C$: Kruskal-Wallis, Chi-squared = 24.364, df = 7, p-value < 0.001*

$\delta^{15}N$: Kruskal-Wallis, Chi-squared = 22.849, df = 7, p-value = 0.002*

Dunn's test: Below diagonal: tests or $\delta^{13}C$ values, Above diagonal: tests for $\delta^{15}N$ values. Significant values ($p < 0.025$) in bold.

	Annelida	Bivalvia	Cnidaria	Echinod.	Eucarida	Gastropoda Limpet	Gastropoda Snail
Annelida		**z = 2.4497 p-value = 0.007**	z = 0.3286 p-value = 0.37	z = -1.0974 p-value = 0.13	z = -0.7005 p-value = 0.24	**z = 2.4263 p-value = 0.007**	z = -0.4426 p-value = 0.33
Bivalvia	z = 1.3597 p-value = 0.09		z = -1.7604 p-value = 0.04	**-2.3934 p-value = 0.008**	**z = -2.6110 p-value = 0.004**	-1.4116 p-value = 0.08	**z = -2.6004 p-value = 0.005**
Cnidaria	z = -1.2679 p-value = 0.10	z = -1.9549 p-value = 0.0253		z = -1.1469 p-value = 0.12	z = -0.7423 p-value = 0.23	z = 0.8975 0.18	z = -0.5541 p-value = 0.29
Echinod.	z = -1.4582 p-value = 0.07	**z = -2.0373 p-value = 0.02**	z = -0.6154 p-value = 0.27		z = 0.7402 p-value = 0.23	z = 1.8343 p-value = 0.03	z = 0.9429 p-value = 0.17
Eucarida	**z = -2.3149 p-value = 0.008**	**z = -2.5911 p-value = 0.005**	z = -0.4682 p-value = 0.32	z = 0.3513 p-value = 0.36		**z = 2.3116 p-value = 0.01**	z = 0.3611 p-value = 0.36
Gastropoda: Limpet	**z = 2.1349 p-value = 0.01**	z = -0.3756 p-value = 0.35	**z = 2.4231 p-value = 0.007**	**z = 2.1598 p-value = 0.01**	**z = 3.9215 p-value = 0.0000**		**z = -2.6292 p-value = 0.004**
Gastropoda: Snail	z = 1.2387 p-value = 0.11	z = -0.783 p-value = 0.22	z = 1.8896 p-value = 0.03	z = 1.8452 p-value = 0.03	**z = 3.1594 p-value = 0.001**	z = -0.8982 p-value = 0.184	

2017 Transition

$\delta^{13}C$: Kruskal-Wallis, Chi-squared = 12.322, df = 7, p-value = 0.09

$\delta^{15}N$: Kruskal-Wallis, Chi-squared = 11.562, df = 7, p-value = 0.11

2018 Active

$\delta^{13}C$: Kruskal-Wallis, Chi-squared = 11.339, df = 8, p-value = 0.18

$\delta^{15}N$: Kruskal-Wallis, Chi-squared = 17.668, df = 8, p-value = 0.02*

Dunn's test for $\delta^{15}N$: Significant values ($p < 0.025$) in bold.

	Annelida	Bivalvia	Cnidaria	Echinod.	Eucarida	Gastropoda Limpet	Gastropoda Snail
Bivalvia	z = 1.8785 p-value = 0.03						
Cnidaria	z = -1.3542 p-value = 0.09	**z = -2.3167 p-value = 0.01**					
Echinod.	z = -0.8451 p-value = 0.19	z = -1.2093 p-value = 0.11	z = 1.6280 p-value = 0.05				
Eucarida	z = -0.2943 p-value = 0.38	z = -1.5571 p-value = 0.06	z = 0.7595 p-value = 0.22	z = -0.6977 p-value = 0.24			
Gastropoda: Limpet	**z = 3.0444 p-value = 0.001**	z = -0.5221 p-value = 0.30	**z = 2.5111 p-value = 0.006**	z = 1.1773 p-value = 0.11	z = 1.5167 p-value = 0.06		
Gastropoda: Snail	z = 1.2001 p-value = 0.11	z = -1.428 p-value = 0.08	z = 1.7086 p-value = 0.04	z = -0.1462 p-value = 0.44	z = 0.6802 p-value = 0.25	z = -1.8279 p-value = 0.03	
Peracarida	z = -0.8846 p-value = 0.19	**z = -2.1087 p-value = 0.01**	z = 0.7287 p-value = 0.23	z = 1.2718 p-value = 0.10	z = -0.2016 p-value = 0.42	**z = -2.6458 p-value = 0.004**	z = -1.4480 p-value = 0.07

2018 Inner transition

$\delta^{13}C$: Kruskal-Wallis, Chi-squared = 12.745, df = 7, p-value = 0.08

$\delta^{15}N$: Kruskal-Wallis, Chi-squared = 10.432, df = 7, p-value = 0.16

2018 Outer transition

$\delta^{13}C$: Kruskal-Wallis, Chi-squared = 2.7857, df = 2, p-value = 0.25

$\delta^{15}N$: Kruskal-Wallis, Chi-squared = 4.5, df = 2, p-value = 0.10

Appendix 6.12: Statistical tests among taxa of invertebrate macrofauna on experimental carbonate rocks deployed for 7 years (2010-2017) at active and transition sites at Mound 12

Active sites

$\delta^{13}C$: Kruskal-Wallis, Chi-squared = 11.849, df = 4, p-value = 0.02*

$\delta^{15}N$: Kruskal-Wallis Chi-squared = 22.402, df = 4, p-value < 0.001*

Dunn's test: Below diagonal: tests for $\delta^{13}C$ values, Above diagonal: tests for $\delta^{15}N$ values. Significant values ($p < 0.025$) in bold.

	Annelida	Bivalvia	Eucarida	Gastropoda Limpet	Gastropoda Snail
Annelida		**z = 3.3041 p-value = 0.002**	z = -1.7489 p-value = 0.08	z = 0.2278 p-value = 0.41	z = -0.8293 p-value = 0.25
Bivalvia	z = 0.4135 p-value = 0.38		**z = -4.1980 p-value = 0.0001**	z = -1.9648 p-value = 0.06	**z = -2.9884 p-value = 0.004**
Eucarida	z = -2.1107 p-value = 0.06	z = -2.3367 p-value = 0.05		z = 1.4943 p-value = 0.11	z = 0.5788 p-value = 0.31
Gastropoda: Limpet	z = 2.0323 p-value = 0.05	z = 1.6942 p-value = 0.07	**z = 3.3254 p-value = 0.004**		z = -0.8358 p-value = 0.28
Gastropoda: Snail	z = 0.5012 p-value = 0.36	z = 0.2118 p-value = 0.42	z = 1.9994 p-value = 0.04	z = -1.2104 p-value = 0.16	

Transition sites

$\delta^{13}C$: Kruskal-Wallis, Chi-squared = 8.7778, df = 5, p-value = 0.12

$\delta^{15}N$: Kruskal-Wallis, Chi-squared = 4.2368, df = 5, p-value = 0.51

Appendix 6.13: Statistical tests within taxa of invertebrate macrofauna isotopic composition among experimental carbonate rock, bone and wood deployed at active sites for 7 years (2010-2017) at Mound 12

Annelida
$\delta^{13}C$: Kruskal-Wallis, Chi-squared = 4.2762, df = 2, p-value = 0.12
$\delta^{15}N$: Kruskal-Wallis, Chi-squared = 0.26087, df = 2, p-value = 0.88

Cnidaria: no data for cnidarians on rock and bone

Eucarida
$\delta^{13}C$: Kruskal-Wallis, chi-squared = 0.17262, df = 2, p-value = 0.92
$\delta^{15}N$: Kruskal-Wallis, Chi-squared = 1.6333, df = 2, p-value = 0.44
Peracarida: no data for peracarids on rock and wood

Echinodermata: no data for echinoderms on rock and wood

Bivalvia: rock vs wood
$\delta^{13}C$: Wilcox test, W = 65.5, p-value = 1.00
$\delta^{15}N$: Wilcox test, W = 52, p-value = 0.41

Gastropoda: Snail
$\delta^{13}C$: Kruskal-Wallis, chi-squared = 2.2227, df = 2, p-value = 0.32
$\delta^{15}N$: Kruskal-Wallis, chi-squared = 0.32273, df = 2, p-value = 0.85

Gastropoda: Limpet
$\delta^{13}C$: Kruskal-Wallis, Chi-squared = 1.95, df = 2, p-value = 0.38
$\delta^{15}N$: Kruskal-Wallis, Chi-squared = 2.6854, df = 2, p-value = 0.26

Appendix 6.14: Statistical tests within taxa of invertebrate macrofauna isotopic composition among experimental carbonate rock, bone and wood deployed at transition sites for 7 years (2010-2017) at Mound 12

Annelida
$\delta^{13}C$: Kruskal-Wallis, chi-squared = 2.0509, df = 2, p-value = 0.36
$\delta^{15}N$: Kruskal-Wallis, chi-squared = 7.293, df = 2, p-value = 0.03*
Rock vs Bone: Dunn's test, z = -1.1025, p-value = 0.13
Rock vs Wood: Dunn's test, z = -1.2412, p-value = 0.16
Bone vs Wood: Dunn's test, z = -2.6944, p-value = 0.01*

Cnidaria: no data for cnidarians on rock and bone at transition sites

Eucarida: no data for cnidarians on rock and bone at transition sites

Peracarida: rock vs wood
$\delta^{13}C$: Wilcox test, W = 3, p-value = 0.50
$\delta^{15}N$: Wilcox test, W = 0, p-value = 0.50

Echinodermata
$\delta^{13}C$: Kruskal-Wallis, chi-squared = 1.7667, df = 2, p-value = 0.41
$\delta^{15}N$: Kruskal-Wallis, chi-squared = 1.6667, df = 2, p-value = 0.43

Bivalvia: bone vs wood
$\delta^{13}C$: Wilcox test, W = 4, p-value = 0.40
$\delta^{15}N$: Wilcox test, W = 0, p-value = 0.40

Gastropoda: Snail: rock vs wood
$\delta^{13}C$: Wilcox test, W = 4, p-value = 0.80
$\delta^{15}N$: Wilcox test, W = 0, p-value = 0.20

Gastropoda: Limpet: rock vs wood
$\delta^{13}C$: Wilcox test, W = 0, p-value = 0.13
$\delta^{15}N$: Wilcox test, W = 6, p-value = 0.53

Appendix 6.15: Statistical tests within taxa of invertebrate macrofauna isotopic composition among experimental carbonate rocks transplanted across seepage gradients for 17 months (2017-2018) at Mound 12

Annelida
$\delta^{13}C$: Kruskal-Wallis, Chi-squared = 7.8252, df = 5, p-value = 0.17
$\delta^{15}N$: Kruskal-Wallis chi-squared = 7.202, df = 5, p-value = 0.21

Cnidaria
$\delta^{13}C$: Kruskal-Wallis, chi-squared = 4.3933, df = 3, p-value = 0.22
$\delta^{15}N$: Kruskal-Wallis chi-squared = 8.725, df = 3, p-value = 0.03*
Dunn's test for $\delta^{15}N$ values: Significant values ($p < 0.025$) in bold.

	A-OT	IT-A	IT-F
IT-A	z = 1.6216 p-value = 0.10		
IT-F	z = 0.6770 p-value = 0.30	z = -1.2247 p-value = 0.16	
IT-OT	**z = 2.6879** **p-value = 0.021**	z = 0.1291 p-value = 0.45	z = 2.0412 p-value = 0.06

Eucarida
$\delta^{13}C$: Kruskal-Wallis, Chi-squared = 2, df = 2, p-value = 0.37
$\delta^{15}N$: Kruskal-Wallis, Chi-squared = 2, df = 2, p-value = 0.37

Peracarida
$\delta^{13}C$: Kruskal-Wallis, chi-squared = 5.1429, df = 3, p-value = 0.16
$\delta^{15}N$: Kruskal-Wallis, Chi-squared = 4.0357, df = 3, p-value = 0.26

Echinodermata
$\delta^{13}C$: Kruskal-Wallis, chi-squared = 3.1429, df = 3, p-value = 0.37
$\delta^{15}N$: Kruskal-Wallis chi-squared = 3.5714, df = 3, p-value = 0.31

Bivalvia: A-IT vs IT-A
$\delta^{13}C$: Wilcox test, W = 12, p-value = 0.66
$\delta^{15}N$: Wilcox test, W = 26, p-value = 0.052

Gastropoda: Snail: A-IT vs IT-A
$\delta^{13}C$: Wilcox test, W = 26, p-value = 0.20
$\delta^{15}N$: Wilcox test, W = 30, p-value = 0.05*

Gastropoda: Limpet
$\delta^{13}C$: Kruskal-Wallis, chi-squared = 1.5974, df = 2, p-value = 0.45
$\delta^{15}N$: Kruskal-Wallis, Chi-squared = 5.026, df = 2, p-value = 0.08

Appendix 6.16: Statistical tests of isotopic composition among annelids on experimental carbonate rocks transplanted across seepage gradients for 17 months (2017-2018) at Mound 12 and on *in situ* rock at the initial site collected in 2017 and end site collected in 2018

Active to Inner transition (A-IT)
A-IT vs 2017 Active:
$\delta^{13}C$: Wilcox test, W = 122, p-value = 0.64
$\delta^{15}N$: Wilcox test, W = 143, p-value = 0.19
A-IT vs 2018 Inner transition:
$\delta^{13}C$: Wilcox test, W = 72, p-value = 0.41
$\delta^{15}N$: Wilcox test, W = 56, p-value = 0.11

Active to Outer Transition (A-OT)
A-OT vs 2017 Active:
$\delta^{13}C$: Wilcox test, W = 20, p-value = 0.31
$\delta^{15}N$: Wilcox test, W = 42, p-value = 0.50
A-OT vs 2018 Outer transition:
$\delta^{13}C$: Wilcox test, W = 0, p-value = 0.20
$\delta^{15}N$: Wilcox test, W = 0, p-value = 0.20

Inner transition to Active (IT-A)
IT-A vs 2017 Transition:
$\delta^{13}C$: Wilcox test, W = 84, p-value = 0.96
$\delta^{15}N$: Wilcox test, W = 47, p-value = 0.07
IT-A vs 2018 Active:
$\delta^{13}C$: Wilcox test, W = 271, p-value = 0.90
$\delta^{15}N$: Wilcox test, W = 308, p-value = 0.55

Inner transition to Outer transition (IT-OT)
IT-OT vs 2017 Transition:
$\delta^{13}C$: Wilcox test, W = 13, p-value = 0.66
$\delta^{15}N$: Wilcox test, W = 15, p-value = 0.88
IT-OT vs 2018 Outer transition:
$\delta^{13}C$: Wilcox test, W = 2, p-value = 0.80
$\delta^{15}N$: Wilcox test, W = 2, p-value = 0.80

Active to Background (A-B)
A-B vs 2017 Active:
$\delta^{13}C$: Wilcox test, W = 91, p-value = 0.26
$\delta^{15}N$: Wilcox test, W = 168, p-value = 0.07

Inner transition to Background (IT-B)
IT-B vs 2017 Transition:
$\delta^{13}C$: Wilcox test, W = 21, p-value = 0.051
$\delta^{15}N$: Wilcox test, W = 19, p-value = 0.15

Appendix 6.17: Statistical tests of isotopic composition among cnidarians on experimental carbonate rocks transplanted across seepage gradients for 17 months (2017-2018) at Mound 12 and on *in situ* rock at the initial site collected in 2017 and end site collected in 2018

Active to Inner transition (A-IT): no data for cnidarians on A-IT rocks

Active to Outer Transition (A-OT)
A-OT vs 2017 Active:
$\delta^{13}C$: Wilcox test, W = 15, p-value = 0.17
$\delta^{15}N$: Wilcox test, W = 17, p-value = 0.05*
A-OT vs 2018 Outer transition:
$\delta^{13}C$: Wilcox test, W = 11, p-value = 0.91
$\delta^{15}N$: Wilcox test, W = 21, p-value = 0.07

Inner transition to Active (IT-A)
IT-A vs 2017 Transition:
$\delta^{13}C$: Wilcox test, W = 3, p-value = 1.00
$\delta^{15}N$: Wilcox test, W = 2, p-value = 1.00
IT-A vs 2018 Active:
$\delta^{13}C$: Wilcox test, W = 1, p-value = 1.00
$\delta^{15}N$: Wilcox test, W = 0, p-value = 1.00

Inner transition to Outer transition (IT-OT)
IT-OT vs 2017 Transition:
$\delta^{13}C$: Wilcox test, W = 14, p-value = 0.07
$\delta^{15}N$: Wilcox test, W = 6, p-value = 0.78
IT-OT vs 2018 Outer transition:
$\delta^{13}C$: Wilcox test, W = 6, p-value = 1.00
$\delta^{15}N$: Wilcox test, W = 0, p-value = 0.06

Active to Background (A-B): no data for cnidarians on A-B rocks

Inner transition to Background (IT-B)
IT-B vs 2017 Transition:
$\delta^{13}C$: Wilcox test, W = 25, p-value = 0.008*
$\delta^{15}N$: Wilcox test, W = 20, p-value = 0.15

Appendix 6.18: Statistical tests of isotopic composition among eucarid crustaceans on experimental carbonate rocks transplanted across seepage gradients for 17 months (2017-2018) at Mound 12 and on *in situ* rock at the initial site collected in 2017 and end site collected in 2018

Active to Inner transition (A-IT): no data for eucarids on A-IT rocks

Active to Outer Transition (A-OT)
A-OT vs 2017 Active:
$\delta^{13}C$: Wilcox test, W = 3, p-value = 1.00
$\delta^{15}N$: Wilcox test, W = 6, p-value = 0.28
A-OT vs 2018 Outer transition: no data for eucarids on 2018 *in situ* outer transition rocks

Inner transition to Active (IT-A)
IT-A vs 2017 Transition:
$\delta^{13}C$: Wilcox test, W = 2, p-value = 0.67
$\delta^{15}N$: Wilcox test, W = 1, p-value = 1.00
IT-A vs 2018 Active:
$\delta^{13}C$: Wilcox test, W = 0, p-value = 1.00
$\delta^{15}N$: Wilcox test, W = 1, p-value = 1.00

Inner transition to Outer transition (IT-OT): no data for eucarids on IT-OT rocks

Active to Background (A-B)
A-B vs 2017 Active:
$\delta^{13}C$: Wilcox test, W = 6, p-value = 0.28
$\delta^{15}N$: Wilcox test, W = 6, p-value = 0.28

Inner transition to Background (IT-B): no data for eucarids on IT-B rocks

Appendix 6.19: Statistical tests of isotopic composition among peracarid crustaceans on experimental carbonate rocks transplanted across seepage gradients for 17 months (2017-2018) at Mound 12 and on *in situ* rock at the initial site collected in 2017 and end site collected in 2018

Active to Inner transition (A-IT)
A-IT vs 2017 Active: no data for peracarids on 2017 Active *in situ* rocks
A-IT vs 2018 Inner transition:
$\delta^{13}C$: Wilcox test, W = 8, p-value = 0.13
$\delta^{15}N$: Wilcox test, W = 8, p-value = 0.13

Active to Outer Transition (A-OT): no data for peracarids on A-OT rocks

Inner transition to Active (IT-A): no data for peracarids on IT-A rocks

Inner transition to Outer transition (IT-OT)
IT-OT vs 2017 Transition:
$\delta^{13}C$: Wilcox test, W = 4, p-value = 0.80
$\delta^{15}N$: Wilcox test, W = 6, p-value = 0.20
IT-OT vs 2018 Outer transition:
$\delta^{13}C$: Wilcox test, W = 1, p-value = 1.00
$\delta^{15}N$: Wilcox test, W = 2, p-value = 1.00

Active to Background (A-B): no data for peracarids on 2017 *in situ* active rocks

Inner transition to Background (IT-B)
IT-B vs 2017 Transition:
$\delta^{13}C$: Wilcox test, W = 2, p-value = 0.67
$\delta^{15}N$: Wilcox test, W = 2, p-value = 0.67

Appendix 6.20: Statistical tests of isotopic composition among echinoderms on experimental carbonate rocks transplanted across seepage gradients for 17 months (2017-2018) at Mound 12 and on *in situ* rock at the initial site collected in 2017 and end site collected in 2018

Active to Inner transition (A-IT)
A-IT vs 2017 Active:
$\delta^{13}C$: Wilcox test, W = 0, p-value = 1.00
$\delta^{15}N$: Wilcox test, W = 1, p-value = 1.00
A-IT vs 2018 Inner transition:
$\delta^{13}C$: Wilcox test, W = 2, p-value = 0.67
$\delta^{15}N$: Wilcox test, W = 2, p-value = 0.67

Active to Outer Transition (A-OT)
A-OT vs 2017 Active:
$\delta^{13}C$: Wilcox test, W = 0, p-value = 0.67
$\delta^{15}N$: Wilcox test, W = 2, p-value = 0.67
A-OT vs 2018 Outer transition: no data for echinoderms on 2018 *in situ* outer transition rocks

Inner transition to Active (IT-A)
IT-A vs 2017 Transition:
$\delta^{13}C$: Wilcox test, W = 0, p-value = 0.33
$\delta^{15}N$: Wilcox test, W = 1, p-value = 0.67
IT-A vs 2018 Active:
$\delta^{13}C$: Wilcox test, W = 1, p-value = 1.00
$\delta^{15}N$: Wilcox test, W = 0, p-value = 0.50

Inner transition to Outer transition (IT-OT)
IT-OT vs 2017 Transition:
$\delta^{13}C$: Wilcox test, W = 2, p-value = 0.38
$\delta^{15}N$: Wilcox test, W = 8, p-value = 0.38
IT-OT vs 2018 Outer transition: no echinoderms on 2018 *in situ* outer transition rocks

Active to Background (A-B): no data for echinoderms on A-B rocks

Inner transition to Background (IT-B): no data for echinoderms on IT-B rocks

Appendix 6.21: Statistical tests of isotopic composition among bivalves on experimental carbonate rocks transplanted across seepage gradients for 17 months (2017-2018) at Mound 12 and on *in situ* rock at the initial site collected in 2017 and end site collected in 2018

Active to Inner transition (A-IT)
A-IT vs 2017 Active:
$\delta^{13}C$: Wilcox test, W = 8, p-value = 0.38
$\delta^{15}N$: Wilcox test, W = 6, p-value = 0.86
A-IT vs 2018 Inner transition:
$\delta^{13}C$: Wilcox test, W = 1, p-value = 0.67
$\delta^{15}N$: Wilcox test, W = 0, p-value = 0.33

Active to Outer Transition (A-OT): no data for bivalves on A-OT rocks

Inner transition to Active (IT-A): no data for bivalves on IT-A rocks

Inner transition to Outer transition (IT-OT): no data for bivalves on IT-OT rocks

Active to Background (A-B)
A-B vs 2017 Active:
$\delta^{13}C$: Wilcox test, W = 12, p-value = 0.07
$\delta^{15}N$: Wilcox test, W = 5, p-value = 0.86

Inner transition to Background (IT-B): no data for bivalves on IT-B rocks

Appendix 6.22: Statistical tests of isotopic composition among snails on experimental carbonate rocks transplanted across seepage gradients for 17 months (2017-2018) at Mound 12 and on *in situ* rock at the initial site collected in 2017 and end site collected in 2018

Active to Inner transition (A-IT)
A-IT vs 2017 Active:
$\delta^{13}C$: Wilcox test, W = 72, p-value = 0.1851
$\delta^{15}N$: Wilcox test, W = 87, p-value = 0.01651
A-IT vs 2018 Inner transition:
$\delta^{13}C$: Wilcox test, W = 17, p-value = 0.6485
$\delta^{15}N$: Wilcox test, W = 18, p-value = 0.5273

Active to Outer Transition (A-OT): no data for snails on A-OT rocks

Inner transition to Active (IT-A)
IT-A vs 2017 Transition:
$\delta^{13}C$: Wilcox test, W = 7, p-value = 0.55
$\delta^{15}N$: Wilcox test, W = 5, p-value = 0.28
IT-A vs 2018 Active:
$\delta^{13}C$: Wilcox test, W = 18, p-value = 0.32
$\delta^{15}N$: Wilcox test, W = 24, p-value = 0.73

Inner transition to Outer transition (IT-OT): no data for snails on IT-OT rocks

Active to Background (A-B): no data for snails on A-B rocks

Inner transition to Background (IT-B): no data for snails on IT-B rocks

Appendix 6.23: Statistical tests of isotopic composition among limpets on experimental carbonate rocks transplanted across seepage gradients for 17 months (2017-2018) at Mound 12 and on *in situ* rock at the initial site collected in 2017 and end site collected in 2018

Active to Inner transition (A-IT)
A-IT vs 2017 Active:
$\delta^{13}C$: Wilcox test, W = 39, p-value = 0.12
$\delta^{15}N$: Wilcox test, W = 82, p-value = 0.39
A-IT vs 2018 Inner transition:
$\delta^{13}C$: Wilcox test, W = 0, p-value = 0.06
$\delta^{15}N$: Wilcox test, W = 2, p-value = 0.22

Active to Outer Transition (A-OT)
A-OT vs 2017 Active:
$\delta^{13}C$: Wilcox test, W = 16, p-value = 0.77
$\delta^{15}N$: Wilcox test, W = 38, p-value = 0.009*
A-OT vs 2018 Outer transition: no data for limpet on 2018 *in situ* outer transition rocks

Inner transition to Active (IT-A)
IT-A vs 2017 Transition:
$\delta^{13}C$: Wilcox test, W = 2, p-value = 0.20
$\delta^{15}N$: Wilcox test, W = 2, p-value = 0.80
IT-A vs 2018 Active:
$\delta^{13}C$: Wilcox test, W = 1, p-value = 0.14
$\delta^{15}N$: Wilcox test, W = 7.5, p-value = 0.74

Inner transition to Outer transition (IT-OT)
IT-OT vs 2017 Transition:
$\delta^{13}C$: Wilcox test,
$\delta^{15}N$: Wilcox test,
IT-OT vs 2018 Outer transition:
$\delta^{13}C$: Wilcox test,
$\delta^{15}N$: Wilcox test,

Active to Background (A-B): no data for limpets on A-B rocks

Inner transition to Background (IT-B): no data for limpets on IT-B rocks

APPENDIX 7: Raw isotope data of invertebrate macrofauna at Mound 12

Appendix 7.1: Mean $\delta^{13}C$ and $\delta^{15}N$ values (Avg. ‰) and standard error (SE. ‰) of invertebrate macrofauna on *in situ* carbonate rocks collected across seepage gradients at Mound 12 in 2017 and 2018. Raw data used for biplots. A: Active, T: Transition, IT: Inner Transition, OT: Outer transition.

***In situ* carbonate rocks**						
Cruise	**Seepage activity**	**ID**	**Avg.$\delta^{13}C$ (‰)**	**Avg.$\delta^{15}N$ (‰)**	**SE. $\delta^{13}C$ (‰)**	**SE.$\delta^{15}N$ (‰)**
2017	A	Ampharetidae	-34.7	0.5	-	-
2017	A	*Archinome levinae*	-37.7	3.2	3.0	4.1
2017	A	*Amphisamytha* sp.	-39.0	4.5	-	-
2017	A	Anemone	-35.2	4.0	-	-
2017	A	*Bathymodiolus* sp.	-36.3	-4.9	-	-
2017	A	*Bathymodiolus earlougheri*	-77.1	-10.8	-	-
2017	A	Polyplacophora	-48.9	6.4	-	-
2017	A	Cocculinidae	-44.6	4.4	-	-
2017	A	Folliculinidae	-35.0	-3.7	-	-
2017	A	Hesionidae	-35.4	6.6	0.7	1.8
2017	A	*Kanoia* sp.	-39.4	5.6	0.8	0.5
2017	A	*Kiwa puravida*	-28.5	5.2	1.2	0.5
2017	A	*Laminatubus* sp.	-47.4	4.2	-	-
2017	A	*Lepetodrilus* sp.	-30.6	2.9	2.9	0.3
2017	A	*Lepetodrilus georgeschneideri*	-40.5	5.7	-	-
2017	A	Maldanidae	-44.2	6.3	-	-
2017	A	Nemertea	-29.8	8.8	4.5	1.4
2017	A	*Neoamphitrite* sp.	-39.7	5.7	0.7	0.2
2017	A	*Neoamphitrite* sp.	-34.9	7.8	0.3	0.4
2017	A	*Neolepetopsis* sp.	-55.3	1.2	2.0	0.8
2017	A	Nereidae	-36.6	0.1	-	-
2017	A	Ophiuroidea	-19.8	7.0	-	-
2017	A	*Ophryotrocha* sp.	-31.9	6.8	-	-
2017	A	*Paralepetopsis* sp.	-54.3	5.2	0.5	0.0
2017	A	Paraonidae	-34.6	5.4	-	-
2017	A	Polynoidae	-35.9	0.7	1.4	1.3
2017	A	*Provanna laevis*	-37.6	4.6	1.2	0.5
2017	A	*Pyropelta* sp.	-44.3	1.9	2.1	0.7
2017	A	*Swiftia* sp.	-27.9	3.3	0.7	5.8
2017	A	Syllidae	-28.0	14.8	-	-
2017	A	Terebellidae	-34.7	3.0	2.2	1.4

Appendix 7.1 continued.

***In situ* carbonate rocks**						
Cruise	**Seepage activity**	**ID**	**Avg.$\delta^{13}C$ (‰)**	**Avg.$\delta^{15}N$ (‰)**	**SE. $\delta^{13}C$ (‰)**	**SE.$\delta^{15}N$ (‰)**
2017	T	Amphipoda	-24.5	9.3	NA	NA
2017	T	Aplacophora	-40.8	9.7	NA	NA
2017	T	Polyplacophora	-49.4	6.3	2.5	0.8
2017	T	Galatheidae	-34.5	8.2	NA	NA
2017	T	Gammaridae	-33.8	8.1	NA	NA
2017	T	Hesionidae	-22.5	10.3	0.0	0.2
2017	T	Hydroid	-31.5	5.1	1.9	1.0
2017	T	*Kanoia* sp.	-40.2	9.0	NA	NA
2017	T	*Laminatubus* sp.	-45.4	5.6	NA	NA
2017	T	*Lepetodrilus* sp.	-30.0	4.7	1.7	1.3
2017	T	Maldanidae	-36.9	10.4	14.4	4.6
2017	T	*Neoamphitrite* sp.	-37.6	10.4	NA	NA
2017	T	Ophiuroidea	-22.1	7.4	3.4	1.6
2017	T	Paraonidae	-65.0	10.0	NA	NA
2017	T	Polynoidae	-30.4	10.4	4.8	1.6
2017	T	*Provanna laevis*	-33.9	5.3	5.0	0.1
2017	T	Shrimp	-25.1	9.5	NA	NA
2017	T	*Swiftia* sp.	-27.0	10.4	1.1	2.2
2017	T	Terebellidae	-39.3	7.2	NA	NA
2018	A	*Alvinocaris* sp.	-21.1	7.5	NA	NA
2018	A	*Amphiduropsis axialensis*	-33.5	5.9	0.5	2.9
2018	A	*Archinome levinae*	-32.7	-0.1	0.6	6.8
2018	A	*Aonides* sp.	-38.7	6.0	4.8	0.5
2018	A	*Bathykurila sp.*	-26.0	5.2	6.3	4.6
2018	A	*Bathymodiolus earlougheri*	-36.8	-10.4	NA	NA
2018	A	*Branchinotoglanda* sp.	-31.8	3.7	NA	NA
2018	A	Polyplacophora sp. 1	-37.3	4.5	NA	NA
2018	A	Cirratulidae	-28.0	8.5	NA	NA
2018	A	*Eulepetopsis* sp.	-40.6	2.1	NA	NA
2018	A	*Eunice* sp.	-22.9	11.5	NA	NA
2018	A	*Eupolymnia amphiduropsis*	-36.1	5.3	NA	NA
2018	A	*Eupolymnia heterobranchia*	-35.2	4.1	NA	NA
2018	A	*Eupolymnia* sp.	-38.0	8.2	NA	NA
2018	A	*Gyptis robertscrippsii*	-33.7	7.0	2.0	1.0
2018	A	*Harpinae* sp.	-42.5	8.3	NA	NA

Appendix 7.1 continued.

***In situ* carbonate rocks**						
Cruise	**Seepage activity**	**ID**	**Avg.$\delta^{13}C$ (‰)**	**Avg.$\delta^{15}N$ (‰)**	**SE. $\delta^{13}C$ (‰)**	**SE.$\delta^{15}N$ (‰)**
2018	A	Hesionidae	-33.6	7.2	2.3	0.1
2018	A	Hesionidae	-34.5	6.1	NA	NA
2018	A	Hydroid	-30.4	11.5	NA	NA
2018	A	*Kanoia* sp.	-39.3	6.2	2.1	0.7
2018	A	*Kanoia myronfeinergi*	-43.3	8.1	NA	NA
2018	A	*Lacydonia* sp.	-35.5	9.0	2.9	1.2
2018	A	Lacydonidae	-25.8	10.9	NA	NA
2018	A	*Laminatubus* sp.	-45.4	2.3	NA	NA
2018	A	*Laminatubus* sp. 2	-39.2	4.0	NA	NA
2018	A	*Lepetodrilus* sp.	-35.5	5.7	NA	NA
2018	A	Leptognathiidae	-35.3	5.9	NA	NA
2018	A	Lumbrineridae	-25.6	14.3	NA	NA
2018	A	Maldanidae sp. 1	-61.5	7.8	4.1	0.3
2018	A	Maldanidae sp. 2	-56.2	6.5	NA	NA
2018	A	*Neolepetopsis* sp.	-34.0	-0.1	NA	NA
2018	A	*Nicomache* sp.	-59.9	7.8	2.5	0.9
2018	A	Ophiuroidea sp. 1	-29.2	5.6	NA	NA
2018	A	Ophiuroidea	-29.3	5.5	2.8	1.3
2018	A	*Paralepetopsis* sp.	-55.7	3.5	NA	NA
2018	A	Paraonidae	-46.5	10.7	NA	NA
2018	A	*Parougia cerulibohnorum*	-27.3	3.1	NA	NA
2018	A	*Parougia sulleyi*	-16.4	10.9	NA	NA
2018	A	*Protis* sp.	-37.7	6.4	7.2	4.7
2018	A	*Provanna laevis*	-34.5	5.0	1.4	1.1
2018	A	*Pyropelta* sp.	-43.5	3.0	3.8	0.2
2018	A	*Raricirrus maculatus*	-32.1	8.5	NA	NA
2018	A	*Stenula* sp.	-21.6	13.8	NA	NA
2018	IT	*Amphiduropsis axialensis*	-27.6	7.0	3.7	0.7
2018	IT	Anemone	-26.7	11.2	NA	NA
2018	IT	*Brada* sp.	-47.2	4.5	NA	NA
2018	IT	Capitellidae	-31.0	9.7	NA	NA
2018	IT	Polyplacophora	-51.0	7.2	NA	NA
2018	IT	Polyplacophora sp. 1	-48.7	5.8	3.2	0.7
2018	IT	Cirratulidae	-29.3	12.3	NA	NA
2018	IT	Cnidaria	-29.6	7.5	NA	NA

Appendix 7.1 continued.

***In situ* carbonate rocks**						
Cruise	**Seepage activity**	**ID**	**Avg.δ^{13}C (‰)**	**Avg.δ^{15}N (‰)**	**SE. δ^{13}C (‰)**	**SE.δ^{15}N (‰)**
2018	IT	*Cuspidaria* sp.	-30.4	10.9	NA	NA
2018	IT	*Eugerda* sp.	-23.0	4.5	NA	NA
2018	IT	*Eupolymnia heterobranchia*	-28.6	12.3	NA	NA
2018	IT	*Eupolymnia* sp.	-30.8	9.8	NA	NA
2018	IT	Hesionidae	-35.5	5.9	NA	NA
2018	IT	Hydroid	-28.3	8.2	1.4	0.8
2018	IT	*Kanoia* sp.	-43.8	10.1	NA	NA
2018	IT	*Kanoia myronfeinergi*	-38.2	6.5	12.6	0.2
2018	IT	*Lacydonia* sp.	-39.3	8.6	NA	NA
2018	IT	*Laminatubus paulbrooksi*	-26.7	13.0	NA	NA
2018	IT	*Lepetodrilus* sp.	-23.6	7.1	NA	NA
2018	IT	Maldanidae	-30.9	10.4	NA	NA
2018	IT	Maldanidae sp. 1	-31.9	10.1	NA	NA
2018	IT	Nereidae	-43.2	4.7	NA	NA
2018	IT	Ophiuroidea	-33.2	5.8	3.4	0.7
2018	IT	*Paralepetopsis* sp.	-42.4	3.6	NA	NA
2018	IT	*Parougia* sp.	-26.5	6.0	NA	NA
2018	IT	*Protis* sp.	-26.9	11.3	NA	NA
2018	IT	*Provanna laevis*	-32.7	5.2	NA	NA
2018	IT	Sabellidae	-26.2	11.2	NA	NA
2018	IT	Stenothoidae	-25.9	7.5	NA	NA
2018	IT	Syllidae	-36.3	4.5	NA	NA
2018	IT	Tryphosinidae	-30.4	6.6	2.4	1.2
2018	OT	*Amphiduropsis axialensis*	-27.9	9.6	NA	NA
2018	OT	*Bonierella* sp.	-24.2	11.0	NA	NA
2018	OT	Cnidaria	-27.3	6.9	NA	NA
2018	OT	Hydroids (white)	-24.8	8.7	NA	NA
2018	OT	Hydroids (yellow)	-24.6	8.9	1.2	0.3
2018	OT	Phyllodocidae	-25.9	13.0	NA	NA

Appendix 7.2: Mean $\delta^{13}C$ and $\delta^{15}N$ values (Avg. ‰) and standard error (SE. ‰) of invertebrate macrofauna on experimental carbonate rock, bone and wood deployed for 7 years (2010-2017) at active and transition sites at Mound 12. Raw data used for biplots.

Colonization experiment (7 years)						
Substrate	**Seepage activity**	**Taxa**	**Avg.$\delta^{13}C$ (‰)**	**Avg.$\delta^{15}N$ (‰)**	**SE.$\delta^{13}C$ (‰)**	**SE.$\delta^{15}N$ (‰)**
Carbonate rock	A	*Archinome levinae*	-37.0	2.6	3.1	1.8
Carbonate rock	A	*Amphisamytha* sp.	-45.0	1.6	9.8	0.6
Carbonate rock	A	*Bathymodiolus earlougheri*	-35.1	-7.4	1.1	0.7
Carbonate rock	A	*Bathymodiolus nancyschneideri*	-36.1	-5.6	0.2	0.6
Carbonate rock	A	*Brada* sp.	-35.9	1.8	NA	NA
Carbonate rock	A	Polyplacophora	-38.0	3.0	NA	NA
Carbonate rock	A	Cirratulidae	-32.1	3.7	NA	NA
Carbonate rock	A	Cocculinidae	-52.0	0.0	NA	NA
Carbonate rock	A	*Gyptis robertscrippsii*	-31.6	1.3	NA	NA
Carbonate rock	A	Hesionidae	-27.9	3.3	7.0	0.4
Carbonate rock	A	*Idas* sp.	-28.8	0.8	6.1	4.8
Carbonate rock	A	*Kiwa puravida*	-29.7	4.4	1.6	2.1
Carbonate rock	A	*Lacydonia* sp.	-32.2	3.2	NA	NA
Carbonate rock	A	*Laminatubus* sp.	-48.9	-1.3	NA	NA
Carbonate rock	A	*Lepetodrilus* sp.	-36.4	2.6	NA	NA
Carbonate rock	A	*Neoamphitrite* sp.	-34.3	5.2	NA	NA
Carbonate rock	A	*Neoamphitrite* sp.	-38.0	3.7	NA	NA
Carbonate rock	A	*Neolepetopsis* sp.	-50.3	5.4	NA	NA
Carbonate rock	A	Polynoidae	-35.1	-1.3	NA	NA
Carbonate rock	A	*Provanna laevis*	-36.6	4.0	3.0	1.2
Carbonate rock	A	*Pyropelta* sp.	-36.4	-2.4	NA	NA
Carbonate rock	A	Shrimp	-23.0	9.6	NA	NA
Bone	A	Amphipoda	-22.1	8.0	NA	NA
Bone	A	Cirratulidae	-16.8	0.1	NA	NA
Bone	A	*Kiwa puravida*	-27.5	4.2	1.7	0.3
Bone	A	*Lepetodrilus* sp.	-28.9	3.9	NA	NA
Bone	A	Ophiuroidea	-28.1	4.0	NA	NA
Bone	A	*Ophryotrocha* sp.	-22.4	5.8	NA	NA
Bone	A	*Provanna laevis*	-30.4	4.3	1.1	0.1
Bone	A	*Pyropelta* sp.	-34.2	5.4	2.4	0.5
Wood	A	*Archinome levinae*	-37.1	1.5	NA	NA
Wood	A	*Bathymodiolus earlougheri*	-35.7	-6.5	0.2	0.8
Wood	A	*Bathymodiolus nancyschneideri*	-35.8	-3.8	0.6	0.8
Wood	A	*Kanoia* sp.	-38.8	6.6	NA	NA

Appendix 7.2 continued.

Colonization experiment (7 years)						
Substrate	**Seepage activity**	**Taxa**	**Avg.δ^{13}C (‰)**	**Avg.δ^{15}N (‰)**	**SE.δ^{13}C (‰)**	**SE.δ^{15}N (‰)**
Wood	A	*Kiwa puravida*	-31.0	5.1	2.6	1.1
Wood	A	*Lepetodrilus* sp.	-30.0	4.3	0.8	0.7
Wood	A	*Lepetodrilus shannonae*	-25.9	6.1	NA	NA
Wood	A	*Neoamphitrite* sp.	-32.7	1.7	NA	NA
Wood	A	*Neolepetopsis* sp.	-50.2	1.6	4.9	0.6
Wood	A	Polynoidae	-35.3	-5.8	NA	NA
Wood	A	*Provanna laevis*	-33.7	3.7	1.7	0.7
Wood	A	*Pyropelta* sp.	-40.7	1.0	2.6	1.1
Wood	A	Shrimp	-42.9	6.6	20.5	1.0
Wood	A	Terebellidae	-31.6	5.4	NA	NA
Carbonate rock	T	*Archinome levinae*	-22.7	8.5	NA	NA
Carbonate rock	T	Amphipoda	-25.4	9.7	NA	NA
Carbonate rock	T	Cirratulidae	-44.4	5.9	NA	NA
Carbonate rock	T	*Eulepetopsis* sp.	-24.3	3.6	NA	NA
Carbonate rock	T	*Flabellligeria* sp.	-31.1	7.9	NA	NA
Carbonate rock	T	Gammaridae	-26.3	9.9	NA	NA
Carbonate rock	T	Isopoda	-29.2	5.0	NA	NA
Carbonate rock	T	*Kanoia* sp.	-40.1	9.4	0.2	0.2
Carbonate rock	T	Nemertea	-25.1	7.0	NA	NA
Carbonate rock	T	Ophiuroidea	-23.4	6.8	3.1	1.4
Carbonate rock	T	Phyllodocidae	-28.2	13.7	NA	NA
Carbonate rock	T	*Pyropelta* sp.	-12.6	5.4	NA	NA
Carbonate rock	T	Serpulidae	-43.8	5.5	1.3	0.2
Bone	T	*Archinome levinae*	-41.9	7.6	NA	NA
Bone	T	Aplacophora	-24.2	7.3	0.5	5.5
Bone	T	Hydroid	-29.7	6.3	NA	NA
Bone	T	*Neoamphitrite* sp.	-21.2	5.4	NA	NA
Bone	T	Nereidae	-18.6	3.8	NA	NA
Bone	T	*Nicomache* sp.	-21.1	7.0	NA	NA
Bone	T	Ophiuroidea	-17.2	4.6	NA	NA
Bone	T	*Pliocardia kurplovata*	-34.3	7.7	NA	NA
Bone	T	*Provanna laevis*	-27.8	7.3	NA	NA
Bone	T	Sabellidae	-27.4	9.5	NA	NA
Bone	T	Serpulidae	-46.8	5.1	0.6	0.1
Bone	T	Terebellidae	-19.9	5.8	NA	NA

Appendix 7.2 continued.

Colonization experiment (7 years)						
Substrate	**Seepage activity**	**Taxa**	**Avg.δ^{13}C (‰)**	**Avg.δ^{15}N (‰)**	**SE.δ^{13}C (‰)**	**SE.δ^{15}N (‰)**
Bone	T	Trichobranchidae	-26.1	6.3	NA	NA
Wood	T	*Archinome levinae*	-27.3	9.4	3.4	0.7
Wood	T	Amphipoda	-24.2	4.4	NA	NA
Wood	T	Aplacophora	-22.4	9.0	NA	NA
Wood	T	Polyplacophora	-36.8	6.9	4.9	0.7
Wood	T	*Gyptis robertscrippsii*	-31.8	9.4	NA	NA
Wood	T	Hesionidae	-21.3	8.4	0.7	0.2
Wood	T	Hyalogyriniridae	-22.2	2.2	NA	NA
Wood	T	*Kanoia* sp.	-39.6	9.1	NA	NA
Wood	T	*Kiwa puravida*	-24.4	1.8	NA	NA
Wood	T	*Lacydonia* sp.	-31.0	4.2	NA	NA
Wood	T	*Lepetodrilus* sp.	-27.7	5.4	1.8	0.8
Wood	T	Maldanidae	-34.0	9.5	NA	NA
Wood	T	Nemertea	-20.9	10.3	NA	NA
Wood	T	*Neoamphitrite* sp.	-31.4	7.3	NA	NA
Wood	T	*Neolepetopsis* sp.	-49.0	5.9	NA	NA
Wood	T	Ophiuroidea	-26.4	4.2	1.8	1.2
Wood	T	Platyhelminthes	-20.0	2.8	0.6	1.5
Wood	T	Polynoidae	-27.3	12.3	NA	NA
Wood	T	*Provanna laevis*	-47.1	2.3	NA	NA
Wood	T	Terebellidae	-32.5	9.5	NA	NA
Wood	T	Teredo	-20.2	4.6	0.5	0.7

Appendix 7.3: Mean $\delta^{13}C$ and $\delta^{15}N$ values (Avg. ‰) and standard error (SE. ‰) of invertebrate macrofauna on experimental carbonate rocks transplanted across seepage gradients for 17 months. Rocks were transplanted from: active to inner transition (A-IT), active to outer transition (A-OT), inner transition to active (IT-A), inner transition to outer transition (IT-OT), active to background (A-B), and inner transition to background (IT-B). Raw data used for biplots.

Transplant experiment (17 months)					
Treatment	**Taxa**	**Avg.$\delta^{13}C$ (‰)**	**Avg.$\delta^{15}N$ (‰)**	**SE.$\delta^{13}C$ (‰)**	**SE.$\delta^{15}N$ (‰)**
A-IT	*Archinome levinae*	-34.6	7.4	NA	NA
A-IT	*Bathykurila sp.*	-35.3	1.6	NA	NA
A-IT	*Bathymodiolus earlougheri*	-36.0	-6.9	0.2	0.2
A-IT	Polyplacophora sp. 1	-52.3	6.2	NA	NA
A-IT	*Eupolymnia* sp.	-34.9	6.3	NA	NA
A-IT	Eusiridae	-16.6	14.2	NA	NA
A-IT	Gnathidae	-18.2	14.0	NA	NA
A-IT	*Gyptis robertscrippsii*	-35.5	3.6	NA	NA
A-IT	*Gyptis* sp.	-21.2	11.0	NA	NA
A-IT	Heterobranchia	-25.7	10.7	NA	NA
A-IT	*Kanoia* sp.	-35.4	9.4	3.4	1.4
A-IT	*Kanoia myronfeinergi*	-35.9	8.6	4.9	1.9
A-IT	*Lacydonia* sp.	-28.9	9.5	NA	NA
A-IT	*Laminatubus* sp.	-45.1	3.3	3.1	0.1
A-IT	Nemertea, white	-30.3	11.4	NA	NA
A-IT	*Neolepetopsis* sp.	-63.0	2.5	NA	NA
A-IT	Ophiuroidea	-21.5	10.8	NA	NA
A-IT	*Paralepetopsis* sp.	-53.8	3.7	0.7	1.2
A-IT	Paraonidae	-19.8	11.7	NA	NA
A-IT	*Provanna laevis*	-35.3	5.1	NA	NA
A-IT	*Pyropelta* sp. 1	-44.9	2.9	NA	NA
A-IT	Pyropelta sp. 2	-43.0	5.6	NA	NA
A-IT	Solemyidae	-20.3	10.2	NA	NA
A-IT	Trichobranchidae	-38.1	8.1	NA	NA
A-OT	*Archinome levinae*	-32.7	7.4	NA	NA
A-OT	Anemone	-25.9	11.4	1.7	1.0
A-OT	Brachyura	-27.3	10.7	NA	NA
A-OT	Polyplacophora	-51.3	6.2	1.7	0.6
A-OT	*Cirratulus* sp.	-41.9	7.4	NA	NA
A-OT	Hydroid	-25.5	10.0	2.1	2.1
A-OT	*Laminatubus* sp. 2	-47.7	2.9	NA	NA
A-OT	Nemertea	-30.4	7.9	NA	NA
A-OT	Ophiuroidea	-24.4	9.2	1.6	1.3

Appendix 7.3 continued.

Transplant experiment (17 months)					
Treatment	**Taxa**	**Avg.δ^{13}C (‰)**	**Avg.δ^{15}N (‰)**	**SE.δ^{13}C (‰)**	**SE.δ^{15}N (‰)**
A-OT	*Paralepetopsis* sp.	-46.9	8.9	0.1	0.1
IT-A	*Amphiduropsis axialensis*	-33.1	7.8	0.4	1.2
IT-A	*Archinome levinae*	-35.7	5.8	NA	NA
IT-A	*Amphisamytha* sp.	-38.3	4.8	NA	NA
IT-A	*Aonides* sp.	-28.9	8.4	NA	NA
IT-A	*Bathykurila sp.*	-34.1	9.1	NA	NA
IT-A	*Branchypolynoe* sp.	-47.4	8.9	NA	NA
IT-A	Polyplacophora	-46.2	6.0	1.7	0.3
IT-A	*Eupolymnia heterobranchia*	-33.6	7.1	NA	NA
IT-A	*Gyptis robertscrippsii*	-37.4	8.0	NA	NA
IT-A	Hydroid	-28.9	5.3	NA	NA
IT-A	*Kanoia* sp.	-37.7	8.2	NA	NA
IT-A	*Kanoia myronfeinergi*	-41.4	4.5	NA	NA
IT-A	*Laminatubus* sp.	-42.6	3.8	NA	NA
IT-A	*Laminatubus paulbrooksi*	-44.5	3.4	NA	NA
IT-A	Maldanidae	-30.9	10.2	NA	NA
IT-A	Ophiuroidea	-29.8	4.0	NA	NA
IT-A	*Ophryotrocha* sp.	-30.2	6.3	NA	NA
IT-A	*Paralepetopsis* sp.	-55.7	3.2	NA	NA
IT-A	*Provanna laevis*	-39.4	3.9	4.0	1.2
IT-A	*Pyropelta* sp.	-50.3	3.4	NA	NA
IT-A	Shrimp sp. 1	-22.8	9.1	NA	NA
IT-A	*Sirsoe dalilamai*	-36.5	9.0	NA	NA
IT-A	*Tubulanus* sp.	-33.7	9.4	0.1	0.5
IT-OT	Amphipoda	-20.5	14.2	NA	NA
IT-OT	Polyplacophora	-45.7	9.1	2.7	0.6
IT-OT	Crysopetalidae	-23.0	13.1	NA	NA
IT-OT	Gnathidae	-31.5	11.2	NA	NA
IT-OT	Hydroid	-25.6	5.3	0.8	0.5
IT-OT	Nemertea	-21.6	11.6	2.0	1.6
IT-OT	Ophiuroidea sp. 1	-29.9	8.5	NA	NA
IT-OT	Ophiuroidea	-23.4	9.4	NA	NA
IT-OT	Serpulidae	-42.8	6.9	1.6	0.6
IT-OT	*Stenula* sp.	-24.5	10.4	NA	NA
A-B	*Bathymodiolus nancyschneideri*	-35.5	-6.5	0.2	3.1
A-B	*Capitella* sp.	-64.3	8.7	6.6	1.1

Appendix 7.3 continued.

Transplant experiment (17 months)					
Treatment	**Taxa**	**Avg.δ^{13}C (‰)**	**Avg.δ^{15}N (‰)**	**SE.δ^{13}C (‰)**	**SE.δ^{15}N (‰)**
A-B	Polyplacophora	-42.4	2.6	NA	NA
A-B	*Lamellibranchia* sp.	-22.5	4.6	0.2	1.8
A-B	*Munidopsis lanensis*	-21.0	10.4	NA	NA
A-B	Nereidae	-38.2	3.2	NA	NA
A-B	*Ophryotrocha* sp.	-22.7	10.7	NA	NA
A-B	*Phyllochaetopterus* sp.	-52.9	7.6	0.1	0.5
A-B	*Raricirrus maculatus*	-72.8	7.6	15.8	0.9
A-B	Thoracica	-21.8	9.9	NA	NA
A-B	*Tubularis* sp.	-27.5	6.8	NA	NA
A-B	Vestimentifera	-27.8	1.1	NA	NA
IT-B	Aegiddae	-18.0	17.6	NA	NA
IT-B	Aplacophora	-29.5	9.3	5.1	3.2
IT-B	Cirripedia	-22.0	7.2	NA	NA
IT-B	Hydroid	-23.8	10.0	0.4	1.0
IT-B	Phyllodocidae	-21.1	14.1	NA	NA
IT-B	*Spiophanes* sp.	-19.7	12.3	NA	NA
IT-B	*Tubularis* sp.	-19.7	-2.5	NA	NA

REFERENCES

Alfaro-Lucas, J.M., Shimabukuro, M., Ogata, I.V., Fujiwara, Y., & Sumida, P.Y.G. (2018). Trophic structure and chemosynthesis contributions to heterotrophic fauna inhabiting an abyssal whale carcass. *Marine Ecology Progress Series, 596*, 1-12. doi:10.3354/meps12617

Aloisi, G., Pierre, C., Rouchy, J.-M., Foucher, J.-P., & Woodside, J. (2000). Methane-related authigenic carbonates of eastern Mediterranean Sea mud volcanoes and their possible relation to gas hydrate destabilisation. *Earth and Planetary Science Letters*, *184*, 321–338.

Baco, A. R., Rowden, A. A., Levin, L. A., Smith, C. R., & Bowden, D. A. (2010). Initial characterization of cold seep faunal communities on the New Zealand Hikurangi margin. *Marine Geology*, 272, 251-259.

Baco, A.R., & Smith, C.R. (2003). High species richness in deep-sea chemoautotrophic whale skeleton communities. *Marine Ecology Progress Series, 260*, 109-114. doi:10.3354/meps260109

Bahr, A., Pape, T., Bohrmann, G., Mazzini, A., Haeckel, M., Reitz, & Ivanov, M. (2009). Authigenic carbonate precipitates from the NE Black Sea: A mineralogical, geochemical, and lipid biomarker study. *Int J Earth Sci (Geol Rundsch), 98*, 677-695.

Baumberger, T., Embley, R. W., Merle, S. G., Lilley, M. D., Raineault, N. A., & Lupton, J. E. (2018). Mantle-derived helium and multiple methane sources in gas bubbles of cold seeps along the Cascadia continental margin. *Geochemistry, Geophysics, Geosystems, 19*, 4476-4486. https://doi.org/ 10.1029/2018GC007859

Benjamini, Y., & Hochberg, Y. (1995). Controlling the False Discovery Rate: A Practical and Powerful Approach to Multiple Testing. *Journal of the Royal Statistical Society, Series B (Methodological)*, *57*, 289-300.

Bergquist, D. C., Eckner, J. T., Urcuyo, I. A., Cordes, E. E., Hourdez, S., Macko, S. A., & Fisher, C. R. (2007). Using stable isotopes and quantitative community characteristics to determine a local hydrothermal vent food web. *Marine Ecology Progress Series, 330*, 49-65.

Bernardino, A. F., Levin, L., Thurber, A., & Smith, C. (2012). Comparative composition, diversity and trophic ecology of sediment macrofauna at vents, seeps and organic falls. *PLoS ONE*, *7*:e33515. doi:10.1371/journal.pone.0033515

Bernardino, A. F., Smith, C. R., Baco, A., Altamira, I., & Sumida, P. Y. G. (2010). Macrofaunal succession in sediments around kelp and wood falls in the deep NE Pacific and community overlap with other reducing habitats. *Deep-Sea Research Part I, 57*, 708-723.

Boetius, A., & Wenzhoefer, F. (2013) Seafloor oxygen consumption fuelled by methane from cold seeps. *Nature Geoscience*, *6*, 725-734. doi: 10.1038/ngeo1926

Boetius, A., Ravenschlag, K., Schubert, C. J., Rickert, D., Widdel, F., Gleseke, A., Amann, R., Jørgenses, B. B., Witte, U., & Pfannkuche, O. (2000). A marine microbial consortium apparently mediating anaerobic oxidation of methane. *Nature, 407*, 623-626.

Boggeman, M. (2009). Polychaetes (Annelida) of the abyssal SE Atlantic. *Org. Divers. Evol., 9*, 251-428.

Bowden, D. A., Rowden, A. A., Thurber, A. R., Baco, A. R., Levin, L. A., & Smith, C. R. (2013) Cold seep epifaunal communities on the Hikurangi Margin, New Zealand: composition, succession, and vulnerability to human activities. *PLoS ONE, 8*:e76869. doi:10.1371/journal.pone.0076869

Case, D. H., Pasulka, A. L., Marlow, J. J., Grupe, B. M., Levin, L. A., & Orphan, V. J. (2015). Methane seep carbonates host distinct, diverse, and dynamic microbial assemblages. *mBio, 6*(6), e01348-01315.

Clarke, K. R., & Gorley, R. N. (2015). Primer7 v7: User manual/tutorial. PRIMER-EPlymouth.

Cordes, E. E., Bergquist, D. C., & Fisher, C. R. (2009). Macro-ecology of Gulf of Mexico cold seeps. *Annual Review of Marine Science, 1*, 143-168. doi:10.1146/annurev.marine.010908.163912

Dattaguppta, S., Bergquist, D. C., Szalai, E. B., Macko, S. A., & Fisher, C. R. (2004). Tissue carbon, nitrogen, and sulfur stable isotope turnover in transplanted *Bathymodiolus childressi* mussels: Relation to growth and physiological condition. *Limnol. Oceanogr., 49*(4), 1144-1151.

Dekas, A. E., Poretsky, R. S., & Orphan, V. J. (2009). Deep-sea archaea fix and share nitrogen in methane-consuming microbial consortia. *Science, 326*(5951), 422-426. doi:10.1126/science.1178223

DeNiro, M. J., & Epstien, S. (1978). Influence of diet on the distribution of nitrogen isotopes in animals. *Geochimica et Cosmochimica Acta, 45*, 341-351.

Desbruyères, D., Almeida, A., Biscoito, M., Comtet, T., Khripounoff, A., Le Bris, N., Sarradin, P.M., & Segonzac, M., 2000. A review of the distribution of hydrothermal vent communities along the northern Mid-Atlantic Ridge: Dispersal vs. environmental controls. *Hydrobiologia, 440*, 201-216

Dubilier, N., Bergin, C., & Lott, C. (2008). Symbiotic diversity in marine animals: the art of harnessing chemosynthesis. *Nature Reviews Microbiology, 6*, 725–740.

Duperron, S., Nadalig, T., Caprais, J.-C., Sibuet, M., Fiala-Médioni, A., Amann, R., & Dubilier, N. (2005). Dual symbiosis in a Bathymodiolus sp. mussel from a methane seep on the Gabon continental margin (Southeast Atlantic): 16S rRNA phylogeny and distribution of the symbionts in gills. *Applied and Environmental Microbiology, 71*(4), 1694-1700. doi:10.1128/AEM.71.4.1694-1700.2005

Fox, M., Juniper, S. K., & Vali, H. (2002). Chemoautotrophy as a possible nutritional source in the hydrothermal vent limpet *Lepetodrilus fucensis*. *Cah Biol Mar, 43*, 371-376.

Fry, B., & Sherr, E. B. (1984). δ13C measurements as indicators of carbon flow in marine and freshwater ecosystems. *Contribution in Marine Science, 27*, 13-47.

Fujikura, K., Kojima, S., Tamaki, K., Maki, Y., Hunt, J., & Okutani, T. (1999). The deepest chemosynthetis-based community yet discovered from the hadal zone, 7326 m deep, in the Japan Trench. *Marine Ecology Progress Series, 190*, 17-26.

Gage, J. D. (2004). Diversity in deep-sea benthic macrofauna: The importance of local ecology, the larger scale, history and the Antarctic. *Deep-Sea Research II, 51*, 1689-1708. doi:10.1016/j.dsr2.2004.07.013

Godet, L., Zelnio, K. A., & Van Dover, C. L. (2001) Scientists as stakeholders in conservation of hydrothermal vents. *Conservation Biology, 25*, 214-222. doi:10.1111/j.1523- 1739.2010.01642.x

Goffredi, S. K., Tilic, E., Mullin, S. W., Dawson, K. S., Keller, A., Lee, R. W., Wu, F., Levin, L. A., Rouse, G. W., Cordes, E. E., & Orphan, V. J. (in press). Methanotrophic bacterial symbionts fuel dense populations of deep-sea feather duster worms (Sabellida, Annelida) and extend the spatial influence of methane seepage.

Govenar, B., Le Bris, N., Gollner, S., Glanville, J., Aperghis, A. B., Hourdez, S., & Fisher, C R. (2005). Epifaunal community structure associated with *Riftia pachyptila* aggregations in chemically different hydrothermal vent habitats. *Marine Ecology Progress Series, 305*, 67-77.

Grémare, A., Amouroux, J. M., Charles, F., Dinet, A., Riaux-Gobin, C., Baudart, J., Medernach, L., Bodiou, J. Y., Vétion, G., Colomines, J. C., & Albert, P. (1997). Temporal changes in the biochemical composition and nutritional value of the particulate organic matter available to surface deposit-feeders: A two year study. *Marine Ecology Progress Series, 150*, 195-206.

Grupe, B. M. (2014). Implications of environmental heterogeneity for community structure, colonization, and trophic dynamics at Eastern Pacific Methane Seeps. Dissertation (PhD in Oceanography) – Scripps Institution of Oceanography, UC San Diego.

Han, Z., Suess, E., Sahling, H., & Wallmann, K. (2004). Fluid venting activity on the Costa Rica margin: New results from authigenic carbonates. *Int. J. Earth Sci. (Geol. Rundsch), 93*, 596-611. doi:10.1007/s00531-004-0402-y

Hansman, R. L., Thurber, A. R., Levin, L. A., & Aluwihare, L. I. (2017). Methane fates in the benthos and water column at cold seep sites along the continental margin of Central and North America. *Deep-Sea Research Part I, 120*, 122-131.

House, C. H., Orphan, V. J., Turk, K. A., Thomas, B., Pernthaler, A., Vrentas, J. M., & Joye, S. B. (2009). Extensive carbon isotopic heterogeneity among methane seep microbiota. *Environ Microbiol, 11*(9), 2207-2215. doi:10.1111/j.1462-2920.2009.01934.x

InterRidge. (2006). *Statement of Commitment of Responsible Research Practices at Deep-Sea Hydrothermal Vents*. Kiel: Underwater Mining Institute.

IPCC, 2019: Technical Summary [H.-O. Pörtner, D.C. Roberts, V. Masson-Delmotte, P. Zhai, E. Poloczanska, K. Mintenbeck, M. Tignor, A. Alegría, M. Nicolai, A. Okem, J. Petzold, B. Rama, N.M. Weyer (eds.)]. In: Pörtner, H.-O., Roberts, D. C., Masson-Delmotte, V., Zhai, P., Tignor, M., Poloczanska, E., Mintenbeck, K., Alegría, A., Nicolai, M., Okem, A., Petzold, J., Rama, B., & Weyer, N. M. (eds.). *IPCC Special Report on the Ocean and Cryosphere in a Changing Climate*. In press.

Jackson, A. L., Inger, R., Parnell, A. C., & Bearhop, S. (2011). Comparing isotopic niche widths among and within communities: SIBER-Stable Isotope Bayesian Ellipses. R. *Journal of Animal Ecology, 80*, 595-602. doi:10.1111/j.1365-2656.2011.01806

Jumars, P. A., Dorgan, K. M., & Lindsay, S. R. (2015). Diet of Worms emended: An update of Polychaete feeding guilds. *Annual Review in Marine Science, 7*, 497-520. doi:10.1146/annurev-marine-010814-020007

Kędra, M., Kuliński, K., Walkusz, W., & Legeżyńska, J. (2012). The shallow benthic food web structure in the high Arctic does not follow seasonal changes in the surrounding environment. *Estuar Coast Shelf Sci, 114*, 183-191.

Kiel, S. (2016). A biogeographic network reveals evolutionary links between deep-sea hydrothermal vent and methane seep faunas. *Proceedings of the Royal Society B, 283*, 20162337. doi:10.1098/rspb.2016.2337

Kimura, G., Silver, E. A., Blum, P., & the Shipboard Scientific Party Leg 170. (1997). *Proceedings of the Ocean Drilling Program, Initial Reports, 170*, 458pp., Ocean Drilling Program, College Station, Tex.

Klaucke, I., Masson, D. G., Petersen, C. J., Weinrebe, W., & Ranero, C. R. (2008). Multifrequency geoacoustic imaging of fluid escaoe structures offshore Costa Rica: Implications for the quantification of seep processes. *Geochemistry, Geophysics, Geosystems, 9*, Q04010. doi:10.1029/2007GC001708

Layman, C. A., Arrington, D. A., Montaña, C. G., & Post, D. M. (2007). Can stable isotope ratios provide for community-wide measures of trophic structure? *Ecology, 88*, 42-48. doi:10.1890/0012-9658(2007)88[42:csirpfj2.0.co;2

Leibold, M. A., Holyoak, M., Mouquet, N., Amarasekare, P., Chase, J. M., Hoopes, M. F., Holt, R. D., Shurin, J. B., Law, R., Tilman, D., Loreau, M., & Gonzalez, A. (2004). The metacommunity concept: A framework for multi-scale community ecology. *Ecology Letters, 7*, 601-613.

Levin, L. A. (2005). Ecology of cold seep sediments: Interactions of fauna with flow, chemistry and microbes. *Oceanography and Marine Biology: An Annual Review, 43*, 1-46.

Levin, L. A., & Mendoza, G. (2007). Community structure and nutrition of deep methane seep macroinfauna from the Aleutian Margin and Florida Escarpment, Gulf of Mexico. *Marine Ecology, 28*, 131-151. doi:10.1111/j.1439-0485.2006.00131.x

Levin, L. A., & Sibuet, M. (2012). Understanding continental margin biodiversity: A new imperative. *Annual Review in Marine Science, 4*, 79-112. doi:10.1146/annurev-marine-120709-142714

Levin, L. A., Baco, A. R., Bowden, D. A., Colaço, A., Cordes, E. E., Cunha, M. R., Demopoulos, A. W. J., Gobin, J., Grupe, B. M., Le, J., Metaxas, A., Netburn, A., Rouse, G. W., Thurber, A. R., Tunnicliffe, W., Van Dover, C. L., Vanreusel, A., & Watling, L. (2016).

Hydrothermal vents and methane seeps: rethinking the sphere of influence. *Frontiers in Marine Science*, *3*:72. doi:10.3389/fmars.2016.00072

Levin, L. A., Blair, N. E., Martin, C. M., DeMaster, D. J., Plaia, G., & Thomas, C. J. (1999). Macrofaunal processing of phytodetritus at two sites on the Carolina margin: *in situ* experiments using ^{13}C-labeled diatoms. *Marine Ecology Progress Series, 182*, 37-54.

Levin, L. A., Mendoza, G. F., & Grupe, B. M. (2017). Methane seepage effects on biodiversity and biological traits of macrofauna inhabiting authigenic carbonates. *Deep-Sea Research Part II, 137*, 26-41. doi:10.1016/j.dsr2.2016.05.021

Levin, L. A., Mendoza, G. F., Grupe, B.M., Gonzalez, J. P., Jellison, B., Rouse, G. W., Thurber, A. R., & Waren, A. (2015). Biodiversity on the rocks: Macrofauna inhabiting authigenic carbonate at Costa Rica methane seeps. *PLoS ONE, 10*(7), e0131080. doi:10.1371/journal.pone.0131080

Levin, L. A., Mendoza, G. F., Konotchick, T., & Lee, R. (2009). Community structure and trophic relationships in Pacific hydrothermal sediments. *Deep Sea Research Part II*, *56,* 1632-1648. doi:10.1016/j.dsr2.2009. 05.010

Levin, L. A., Orphan, V. J., Rouse, G. R., Rathburn, A. E., Ussler III, W., Cook, G. S., Goffredi, S. K., Perez, E. M., Waren, A., Grupe, B. M., Chadwick, G., & Strickrott, B. (2012). A hydrothermal seep on Costa Rica margin: middle ground in a continuum of reducing ecosystems. *Proceedings of The Royal Society B-Biological Sciences, 279*, 2580-2588. doi:10.1098/rspb.2012.0205

Levin, L.A., & Michener, R.H. (2002). Isotopic evidence for chemosynthetic-based nutrition of macrobenthos: The lightness of being at Pacific methane seeps. *Limnol. Oceanogr., 47*(5), 1336-1345. doi:10.4319/lo.2002.47.5.1336

MacAvoy, S. E., Fisher, C. R., Carney, R. S., & Macko, S. A. (2005). Nutritional associations among fauna at hydrocarbon seep communities in the Gulf of Mexico. *Marine Ecology Progress Series, 292*, 51-60.

Marlow, J. J., Steele, J. A., Case, D. H., Connon, S. A., Levin, L. A., & Orphan, V. J. (2014a). Microbial abundance and diversity patterns associated with sediments and carbonates from the methane seep environments of Hydrate Ridge, OR. *Frontiers in Marine Science Aquatic Microbiology, 1*:44. doi: 10.3389/fmars.2014.00044

Marlow, J. J., Steele, J. A., Ziebis, W., Thurber, A., Levin, L. A., & Orphan, V. J. (2014b). Carbonate-hosted methanotrophy represents and unrecognized methane sink in the deep sea. *Nature Communications*, *5*:5094. doi: 10/1038/ncomms6094

Mau, S., Rehder, G., Sahling, H., Schleicher, T., & Linke, P. (2014). Seepage of methane at Jaco Scar, a slide caused by seamount subduction offshore Costa Rica. *International Journal of Earth Sciences, 103*, 1801-1815. doi:10.1007/s00531-012-0822-z

Mau, S., Sahling, H., Rehder, G., Suess, E., Linke, P., & Soeding, E. (2006). Estimates of methane output from mud extrusions at the erosive convergent margin off Costa Rica. *Marine Geology*, *225*, 129-144. doi:10.1016/j.margeo.2005.09.007

McAdoo, B. G., Orange, D. L., Silver, E. A., McIntosh, K., Abbott, L., Galewsky, J., Kahn, L., & Protti, M. (1996). Seafloor structural observations, Costa Rica accretionary prism. *Geophysical Research Letters, 23*, 883-886. doi:10.1029/96GL00731

McCutchan, J. H., Lewis, W. M., Kendall, C., & McGrath, C. (2003). Variation in trophic shift for stable isotope ratios of carbon, nitrogen, and sulfur. *Oikos, 102*, 378-390.

McLeod, R. J., Wing, S. R., & Skilton, J. E. (2010). High inicidence of invertebrate-chemoautotroph symbioses in benthic communities of the New Zealand fjords. *Limnology. Oceanogr., 55*, 2097-2106.

Mengerink, K. J., Van Dover, C. L., Ardron, J., Baker, M., Escobar-Briones, E., Gjerde, K., Koslow, J. A., Ramirez-Llodra, E., Lara-Lopez, A., Squires, D., Sutton, T., Sweetman, A. K., & Levin, L. A. (2014). A call for Deep-Ocean Stewardship. *Science, 344*(6185), 696-698. doi:10.1126/science.1251458.

Metaxas, A., & Kelly, N. E. (2010). Do larval supply and recruitment vary among chemosynthetic environments of the deep sea? *PLoS ONE, 5*, e11646.

Michaelis, W., Seifert, R., Nauhaus, K., Treude, T., Thiel, V., Blumenberg, M., Knittel, K., Gieseke, A., Peterknecht, K., Pape, T., Boetius, A., Amann, R., Jørgensen, B. B., Widdel, F., Peckmann, J., Pimenov, N. V., & Gulin, M. B. (2002). Microbial reefs in the Black Sea fueled by anaerobic oxidation of methane. *Science, 297*(5583), 1013-1015. doi:10.1126/science.1072502

Minagawa, M., & Wada, W. (1974). Stepwise enrichment of 15N along food chains: Future evidence and the relation between δ15N and animal age. *Geochimica et Cosmochimica Acta, 48*, 1135-1140.

Moerz, T., Fekete, N., Kopf, A., Brueckmann, W., Kreiter, S., Huehnerbach, V., Masson, D. G., Hepp, D. A., Schmidt, M., Kutterolf, S., Sahling, H., Abegg, F., Spiess, V., Suess, E., & Ranero, C. R. (2005). Styles and productivity of mud diapirism along the Middle American margin, Part II: Mound Culebra and Mounds 11 and 12. In: Martinelli, G., & Panahi, B. (eds.). Mud Volcanoes, Geodynamics and Seismicity. NATO Science Series, Springer, Dordrecht, 49-76.

Niemann, H., Linke, P., Knittel, K., MacPherson, E., Boetius, A., Brückmann, W., Larvik, G., Wallmann, K., Schacht, U., Omoregie, E., Hilton, D., Brown, K., & Rehder, G. (2013). Methane-carbon flow into the benthic food web at colds seeps: A case study from the Costa Rica subduction zone. *PLoS ONE, 8*(10), e74894. doi:10.1371/journal.pone.0074894

NOAA. (2019). Groundfish FMP Amendment 28: Essential fish habitat. *Federal Register*, 84, 223.

Orphan, V. J., Hinrichs, K. U., Ussler, W>, Paull, C. K., Taylor, L. T., Sylva, S. O., Hayes, J. M., & Delong, E. F. (2001). Comparative analysis of methane-oxidizing archaea and sulfate-reducing bacteria in anoxic marine sediments. *Appl. Environ Microbiol, 67*, 1922-1934.

Orphan, V. J., House, C. H., Hinrichs, K. U., McKeegan, K. D., & DeLong, E. F. (2002). Multiple archaeal groups mediate methane oxidation in anoxic cold seep sediments. *Proc Natl Acad Sci USA, 99*, 7663-7668.

Petersen, J. M., & Dubilier, N. (2009). Methanotrophic symbioses in marine invertebrates. *Environmental Microbiology Reports, 1*(5), 319-335. doi:10.1111/j.1758-2229.2009.00081.x

Petersen, J. M., Kemper, A., Gruber-Vodicka, H., Cardini, U., van der Geest, M., Kleiner, M., Bulgheresi, S., MuBmann, M., Herbold, C., Seah, B. K. B., Antony, C. P., Liu, D., Belitz, A., & Weber, M. (2016). Chemosynthetic symbionts of marine invertebrate animals are capable of nitrogen fixation. *Nature Microbiology, 2*, 16195. doi:10.1038/nmicrobiol.2016.195

Peterson, B. J., & Fry, B. (1987). Stable isotopes in ecosystem studies. *An. Rev. Ecol. Syst., 18*, 293-320.

Post, D. M. (2002). Using stable isotopes to estimate trophic position: models, methods, and assumptions. *Ecology, 83*, 703-718.

Ramirez-Llodra, E., Brandt, A., Danovaro, R., De Mol, B., Escobar, E., German, C. R., Levin, L. A., Arbizu, P. M., Menot, L., Buhl-Mortensen, P., Narayanaswamy, B. E., Smith, C. R., Tittensor, D. P., Tyler, P. A., Vanreusel, A., & Vecchione, M. (2010). Deep, diverse and

definitely different: Unique attributes of the world's largest ecosystem. *Biogeosciences, 7*, 2851-2899. doi:10.5194/bg-7-2851-2010

Ramirez-Llodra, E., Tyler, P. A., Baker, M. C., Bergstad, O. A., Clark, M. R., Escobar, E., Levin, L. A., Menot, L., Rowden, A. A., Smith, C. R., & Van Dover, C. L. (2011). Man and the last great wilderness: human impact on the deep sea. *PLoS ONE*, *6*:e22588. doi:10.1371/journal.pone.00 22588

Reeburg, W. S. (2007). Oceanic methane biogeochemistry. *Chem. Rev, 107*, 486-513.

Riekeneber, P. M., Carney, R. S., & Fry, B. (2016). Trophic plasticity of the methanotrophic mussel *Bathymodiolus childressi* in the Gulf of Mexico. *Marine Ecology Progress Series, 547*, 91-106. doi:10.3354/meps11645

Ritt, B., Sarrazin, J., Caprais, J.-C., Noël, P., Gauthier, O., Pierre, C., Henry, P., & Desbruyères, D. (2010). First insights into the structure and environmental setting of cold-seep communities in the Marmara Sea. *Deep-Sea Research Part I, 57*, 1120-1136. doi:10.1016/j.dsr.2010.05.011

Sahling, H., Masson, D. G., Ranero, C. R., Hühnerbach, V., Weinrebe, W., Klaucke, I., Bürk, D., Brückmann, W., & Suess, E. (2008). Fluid seepage at the continental margin offshore Costa Rica and southern Nicaragua. *Geochemistry, Geophysics, Geosystems, 9*, Q05S05, doi:10.1029/2008GC001978

Sasaki, T., Warén, A., Kano, Y., Okutani, T., & Fujikura, K. (2010). Gastropods from recent hot vents and cold seeps: Systematics, diversity and life strategies. *Topics in Geobiology*, *33*, 169-254.

Seabrook, S., De Leo, F. C., & Thurber, A. R. (2019). Flipping for food: the use of a methane seep by tanner crabs (*Chionoecetes tanneri*). *Frontiers in Marine Science*, 6:43. doi:10.3389/fmars.2019.00043

Shank, T. M., Fornari, D. J., Von Damm, K. L., Lilley, M. D., Haymon, R. M., & Lutz, R. A. (1998). Temporal and spatial patterns of biological community development at nascent deep-sea hydrothermal vents (9º50'N, East Pacific Rise). *Deep-Sea Research Part II*, 45, 465.

Sibuet, M., & Olu, K. (1998). Biogeography, biodiversity and fluid dependence of deep- sea cold-seep communities at active and passive margins. *Deep Sea Research Part II, 45*, 517-567. doi:10.1016/S0967-0645(97)00074-X

Skarke, A., Ruppel, C., Kodis, D., & Lobecker, E. (2014). Widespread methane leekage from sea floor on the northern US Atlantic margin. *Nature Geoscience, 7*, 657-661.

Smith, C. R., & Baco, A. R. (2003). Ecology of whale falls at the deep-sea floor. *Oceanography and Marine Biology*, *41*, 311-354.

Smith, C. R., Bernardino, A. F., Baco, A., Hannides, A., & Altamira, I. (2014). Seven-year enrichment: Macrofaunal succession in deep-sea sediments around a 30 tonne whale fall in the Northeast Pacific. *Marine Ecology Progress Series, 515*, 133-149. doi:10.3354/meps10955

Smith, C. R., Glover, A. G., Treude, T., Higgs, N. D., & Amon, D. J., (2015). Whale-fall ecosystems: Recent insights into ecology, paleoecology, and evolution. *Annu. Rev. Mar. Sci., 7*, 571-596. doi:10.1146/annurev-marine-010213-135144

Sommer, S., Pfannkucke, O., Linke, P., Luff, R., Greinert, J., Drews, M., Gubsch, S., Pieper, M., Poser, M., & Viergutz, T. (2006). Efficiency of the benthic filter: Biological control of the emission of dissolved methane from sediments containing shallow gas hydrates at Hydrate Ridge. *Global Biogeochemical Cycles, 20*, GB2019. doi:10.1029/2004GB002389

Stewart, J. D., Rohner, C. A., Araujo, G., Avila, J., Fernando, D., Forsberg, K., Ponzo, A., Rambahiniarison, J. M., Kurle, C. M., & Semmens, B. X. (2017). Trophic overlap in mobulid rays: Insights from stable isotope analysis. *Marine Ecology Progress Series, 580*, 131-151. doi:10.3354/meps12304

Thiel, M. (1999). Duration of extended parental care in marine amphipods. *Journal of Crustacean Biology, 19*(1), 60-71.

Thiel, M., Sampson, S., & Watling, L. (1996). Extended parental care in two endobenthic amphipods. *Journal of Natural History, 31*(5): 713-725. doi:10.1080/00222939700770351

Thurber, A. R. (2014). Diet-dependent incorporation of biomarkers: Implications for food-web studies using stable isotope and fatty acid analyses with special application to chemosynthetic environments. *Marine Ecology*, 1-17. doi:10.1111/maec.12192

Thurber, A. R., Jones, W. J., & Schnabel, K. (2011). Dancing for food in the deep sea: Bacterial farming by a new species of yeti crab. *PLoS ONE, 6*(11), e26243. doi:10.1371/journal.pone.0026243

Thurber, A. R., Levin, L. A., Orphan, V. J., & Marlow, J. J. (2012). Archaea in metazoan diets: Implications for food webs and biogeochemical cycling. *The ISME Journal*, 1-12.

Thurber, A. R., Levin, L. A., Rowden, A., Sommer, S., Linke, P., & Kroger, K. (2013). Microbes, macrofaunal and methane: a novel seep community fueled by aerobic methanotrophy. *Limnology & Oceanography, 58*, 1640-1656. doi:10.4319/lo.2013.58.5.1640

Tunnicliffe, V., Juniper, S. K., & Sibuet, M. (2003). Reducing environments of the deep-sea floor. Ecosystems of the World, 81-110.

Turner, P. J., Ball, B., Diana, Z., Fariñas-Bermeko, A., Grace, I., McVeigh, D., Powers, M. M., Audenhaege, L. V., Maslakova, S., Young, C. Y., & Van Dover, C. L. (2020). Methane seeps on the US Atlantic margin and their potential importance to populations of the commercially valuable deep-sea red crab, *Chaceon quinquedens*. *Frontiers in Marine Science*, 7:75, doi:10.3389/fmars.2020.00075

Van Dover, C. L., 2000. The Ecology of Deep-Sea Hydrothermal Vents. Princeton University Press, Princeton. (424 pp.).

Van Dover, C. L., Smith, C. R., Ardron, J., Dunn, D., Gjerde, K., Levin, L. A., Smith, S., & Contributors, T. D. W. (2012). Designating networks of chemosynthetic ecosystem reserves in the deep sea. *Marine Policy, 36*, 378-381.

Vinn, O., Hryniewicz, K., & Little, C. T. S. (2014). A Boreal serpulid fauna from Volgian-Ryazanian (latest Jurassic-earliest Cretaceous) shelf sediments and hydrocarbon seeps from Svalbard. *Geodiversitas, 36*(4), 527-540. doi:10.5252/g2014n4a2

Vinn, O., Kupriyanova, E. K., & Kiel, S. (2013). Serpulids (Annelida, Polychaeta) at Cretaceous to modern hydrocarbon seeps: Ecological and evolutionary patterns. *Palaeogeography, Palaeoclimatology, Palaeoecology, 390*, 35-41.

Vrijenhoek, R. C. (2010). Genetic diversity and connectivity of deep-sea hydrothermal vent metapopulations. *Molecular Ecology, 19*, 4391-4411. doi:10.1111/j.1365-294X.2010.04789.x

Warén, A., & Bouchet, P. (2001). Gastropoda and Monoplacophora from hydrothermal vents and seeps: New taxa and records. *Veliger, 44*, 116-231.

Warén, A., & Bouchet, P. (2009). New gastropods from deep-sea hydrocarbon seeps off West Africa. *Deep Sea Research Part II: Tropical Studies in Oceanography, 56*(23), 2326-2349.

Warén, A., Bouchet, P., & von Cosel, R. (2006). Gastropoda. In: Desbruyères, D., Segonzac, M., & Bright, M. (eds). Handbook of deep-sea hydrothermal vent gauna. Denisia, 18, 82-140. Biologiezentrum des Oberösterreichischen Landesmuseums, Linz, Austria.

Wiklund, W., Glover, A. G., Johannessen, P. J., & Dahlgren T. G. (2009). Cryptic speciation at organic-rich marine habitats: a new bacteriovore annelid from whale-fall and fish farms in the north-east Atlantic. *Zool. J. Linn. Soc., 155*, 774-785.

Würzberg, L., Peters, J., & Brandt, J. (2011). Fatty acid patterns of Southern Ocean shelf and deep sea peracarid crustaceans and a possible food source, foraminiferans. *Deep-Sea Research Part II: Tropical Studies in Oceanography, 58*(19-20), 2027-2035.

Zapata-Hérnandez, G., Sellanes, J., Thurber, A. R., Levin, L. A., Frédéric Chazalon, & Linke, P. (2013). New insights on the trophic ecology of bathyal communities from the methane seep area off Concepción Chile (~36ºS). *Marine Ecology, 35*, 1-21. doi: 10.1111/maec.12051